UNIVERSITÉ LAVAL

INVERSE MODELLING OF DESORPTION TESTS TO ESTABLISH THE HYDRAULIC CONDUCTIVITY OF UNSATURATED SANDS

Mémoire

Seyed Mohammad Javad Hosseini Siahdashti

Maîtrise en génie civil
Maître ès sciences (M.Sc.)

Québec, Canada

Résumé

Conductivité hydraulique non saturée est un paramètre important pour caractériser le comportement des sols non saturés. Ce paramètre peut être utilisé pour modéliser l'écoulement de l'eau dans les sols. Le défaut de mesure ou d'estimation de ce paramètre avec une précision fiable peut causer des incidents catastrophiques.

La mesure de la conductivité hydraulique des sols non saturés peut être longue et coûteuse. Des méthodes directes et indirectes peuvent être utilisées pour établir ce paramètre. Dans cette étude, en vue de réduire le temps et le coût de la mesure de la conductivité hydraulique des sols non saturés nécessaires par les méthodes directes, la modélisation inverse a été utilisée comme une méthode indirecte pour estimer ce paramètre. Des essais de laboratoire ont été effectués pour trouver la courbe de rétention d'eau des différents échantillons de sol étudié. Les résultats expérimentaux obtenus ont été utilisés pour effectuer la modélisation inverse, et la conductivité hydraulique non saturée de chaque échantillon a été estimé.

Abstract

Unsaturated hydraulic conductivity is an important parameter to characterize unsaturated soils behaviour. This parameter can be used to model flow of water in soils. Failure in measuring or estimating this parameter with a reliable precision can cause catastrophic incidents.

Measuring unsaturated hydraulic conductivity can be expensive and time consuming. Direct and indirect methods can be used to determine this parameter. In this study, in order to decrease the time and the expense of measuring unsaturated hydraulic conductivity by direct methods, inverse modelling was used as an indirect method to estimate this parameter. Some laboratory tests were performed to find water retention curve of different samples of the studied soil. Obtained experimental results were used to perform inverse modelling, and unsaturated hydraulic conductivity of each sample was estimated.

Table of Contents

List of Tables

List of Figures

List of Abbreviations

AEV	*AIR-ENTRY VALUE*
BC	*BROOKS AND COREY*
EDS	*ENERGY DISPERSIVE SPECTROSCOPY*
IPM	*INSTANTANEOUS PROFILE METHOD*
MSO	*MULTI-STEP OUTFLOW*
OSO	*ONE-STEP OUTFLOW*
SWCC	*SOIL WATER CHARACTERISTIC CURVE*
SWRC	*SOIL WATER RETENTION CURVE*
VG	*VAN GENUCHTEN*

Acknowledgements

First and foremost I wish to thank my advisor Dr. Jean Côté, the Associate Chairholder of the NSERC-Hydro-Québec Industrial Research Chair in life cycle optimization for embankment dams. He has been supportive since I began my master studies.

I would like to thank Dr. Jean-Marie Konrad and Dr. Jean-Pascal Bilodeau, whose detailed remarks and comments improved the quality of this manuscript, and François Gilbert, Christian Juneau, Luc Boisvert, and Marc Lebeau for their help during my experiments.

For financial support for my studies, I am grateful to Laval University, Hydro-Quebec, and other partners of the NSERC-Hydro-Québec Industrial Research Chair in life cycle optimization for embankment dams.

I want to thank my friends and fellow graduate students for being supportive through these recent years.

Finally, I am grateful to my dear parents, my brother and my lovely sister. They always supported me, and they were always there for me. Thank you.

1 Introduction

This research aims to find ways to decrease the required time and expense of measuring hydraulic properties of soils directly by laboratory tests. Numerical models have been developed to simulate water movement in porous media. These models can be used to estimate hydraulic conductivity of unsaturated soils by using water retention data. There are different methods to determine water retention data. For the purpose of this study, transient outflow method was used to determine water retention data in laboratory.

This research attempts to characterize the retention and hydraulic properties of sandy materials in an unsaturated state. Some transient flow tests have been performed to measure soils water retention values. These values were then used to simulate water movement and estimate unsaturated hydraulic conductivity by inverse modelling. This reduced the time and expenses of the tests. To achieve this goal, an experimental procedure had been developed to simulate seepage in transient flow to measure hydraulic conductivity.

Laboratory tests were performed under controlled conditions with well-defined initial and boundary conditions. The flow variables were measured in each test. The water flow was written with mathematical relations. A numerical model was used and inverse modelling was performed by minimizing the difference between observed laboratory results and estimated flow variables.

To understand hydraulic functions of unsaturated soils, it is necessary to understand different phases of unsaturated soils. Chapter 2 deals with definition of unsaturated soils and capillary mechanism. This chapter also describes soil water retention curve and its components (water content and soil suction) and different methods of measuring or estimating these values. There are different methods that have been used to model soil water retention curve in literatures such as Brooks & Corey (1964), Fredlund & Xing (1994) and van Genuchten (1980). These methods are also reviewed in this chapter.

In chapter 3 the theory of inverse methods is discussed. Richards' equation is used to express water flow in unsaturated soils. Then the parameter optimization is reviewed.

Chapter 4 focuses on the performed experiments in the scope of this study and the specification of the materials that was tested to find its unsaturated hydraulic conductivity. In this chapter multi-step outflow experiment is discussed and different steps of experimental protocol is reviewed.

In chapter 5 experimental results of the performed multi-step outflow method experiments is summarized. These results include soil pressures in three different elevations of soil samples and amount of extracted water for each pressure step. By using our laboratory results, soil water retention curve is determined for each material. Soil water retention curve of each sample is discussed based on its grain size distribution and the coefficient of uniformity.

Chapter 6 reviews unsaturated hydraulic conductivity results for each sample. Different methods are used to determine unsaturated hydraulic conductivity of each material. These methods includes van Genuchten (1980) and Fredlund et al. (1994) models. These results are then compared with inverse modelling results.

2 Unsaturated Soils

2.1 Unsaturated Soil Definition

Most geotechnical engineering projects that include water flow in soil are related to the unsaturated soils. For example, during the construction of an earth fill dam, the soil is normally compacted with a degree of saturation about 80%. After construction and during the filling period, the dam will face different unsaturated zones. When the dam's reservoir is fully filled with water, some regions in dam structure remain unsaturated.

As another application, road pavements are constructed with compacted unsaturated soils with degree of saturation between 75-90 %. Pavement's stiffness and strength are significantly influenced by soil suction due to the presence of water between soil particles.

About a century ago, Buckingham (1907) was one of the pioneers who worked on multiphase flow. This was the basis of studies on unsaturated soils. An unsaturated soil is a system that contains three different phases, namely as soil particles, water, and gas. Each phase has its own specified volume and mass fraction. Fredlund & Rahardjo (1993) proposed the air-water interface as the fourth phase of unsaturated soils. This phase was called contractile skin.

Unsaturated soils behave differently in comparison with the saturated soils. These differences are mainly related to the mechanical and hydraulic properties. Therefore, knowing these differences and their effects are essential in designing a geotechnical structure.

Generally, the geotechnical problems of unsaturated soils are related to volume changes, shear strength and hydraulic flow in the soil.

Shear strength is one of the most important parameter in unsaturated soils that has to be considered during soil analysis. Many reported failures in dams, embankments and slopes during past decades were related to miscalculation of the shear strength in unsaturated soils.

Classical soil mechanics cannot be used to determine the mechanical properties of unsaturated soils, and they are proper to determine the mechanical properties of saturated soils. Tarantino (2007), Sun et al. (2003) and Alonso et al. (1990) proposed several failure criteria that can be used to predict shear strength of unsaturated soils.

Volume change can cause settlements leading to damages in structures like embankments. Fredlund et al. (2000) conducted some experiments to estimate volume change functions for unsaturated soils. Fredlund et al. (2000) provided a series of postulates based on saturated volume change and using soil water characteristic curve information.

Soil is composed of particles that are in contact with each another. These particles have different shapes and sizes. These differences lead to different pore sizes in soil. These pores act like tubes with different radii. Due to capillary forces in a narrow tube, water tends to move upward. Capillary forces have inverse relation with the tube diameter.

2.1.1 Water Content

The ratio between different phases of soil gives different properties to the system. Therefore, having a good knowledge on these ratios will be useful to predict the soil properties. "Degree of saturation" is one of the definitions that is normally used while studying unsaturated soils. This parameter is shown by "S_r" and defines the percentage of voids filled with water.

$$S_r\ (\%) = \frac{V_w}{V_v} \times 100 \qquad \textit{Equation 1}$$

where V_w is the water volume and V_v is the total void volume (Figure 1). The lower and upper limits for S_r are 0% and 100% for utterly dried and fully saturated soils, respectively.

To quantify the amount of water in porous materials such as soil, "water content" parameter, θ can be expressed as:

$$\theta(\%) = \frac{V_w}{V_{total}} \times 100$$ *Equation 2*

where V_{total} is the total volume and is equal to the sum of volumes of soil, water and air. Water content is also known as moisture content and varies between 0% to 100%.

There are direct and indirect methods to measure or estimate soil water content. Direct methods are based on extracting water from the soil sample. Leaching and evaporation, for example, are the methods that can be used to directly measure the water content of the soil.

In direct methods, water removed from the sample is directly measured by weight. Besides the direct methods, some indirect methods can also be used to find soil water content. In these methods, another material like an absorber is normally used. By placing these materials in soil and measuring its properties, water content can be measured.

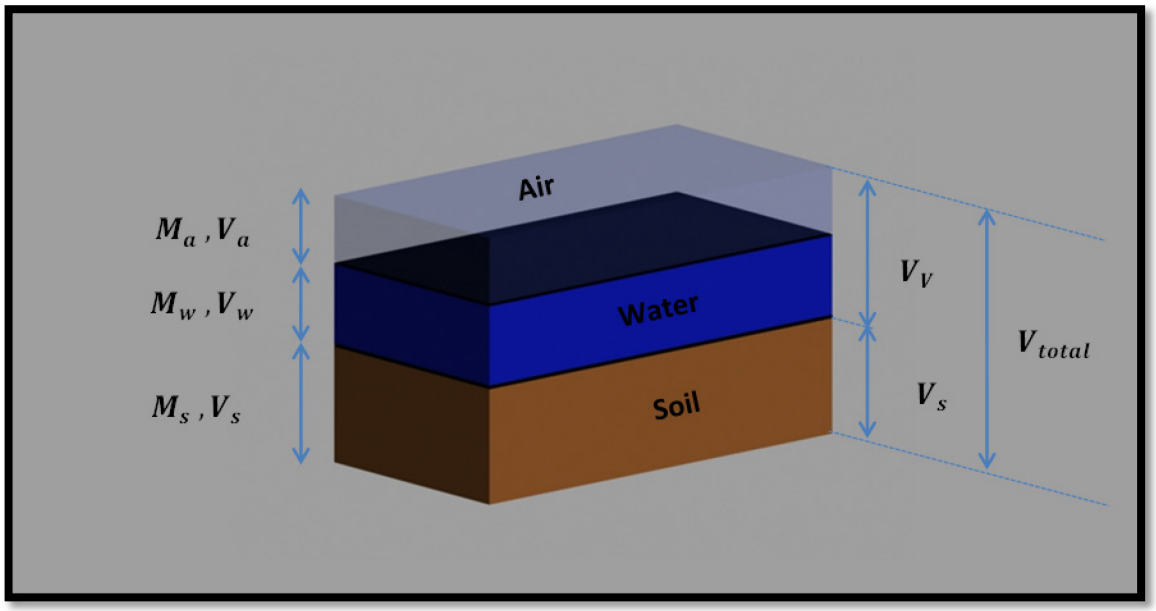

Figure 1: Distribution of different phases in soil

2.1.2 Soil Suction

Soil suction (total suction), which is defined in term of the energy state of the soil water system, has two different components; matric component and osmotic component. Soil suction can be written as:

$$\psi = (u_a - u_w) + \pi \qquad \textit{Equation 3}$$

where ψ is the soil suction, $(u_a - u_w)$ is the matric suction which is also known as capillary pressure, π is the osmotic suction, u_a and u_w are the pore air and pore water pressure, respectively. All are measured in *kPa*.

As shown in Figure 2 (Inspired from Fredlund & Rahardjo, 1993), the level of the water in a tube connected to a water container rises because of the capillary phenomenon. This phenomenon happens because of surface tension in the contractile skin. These forces cause a curved surface at the top of the water level in the tube. The height of the water in the tube can be found by using capillary equation:

$$2\pi r T_s \cos\alpha = \pi r^2 h \rho_w g \qquad \textit{Equation 4}$$

where r is the radius of the capillary tube, T_s is the surface tension of water, α is the contact angle, ρ_w is the density of water, g is the gravitational acceleration and h is the capillary height. Solving the Equation 4 for h gives the height of raised water in the capillary tube:

$$h = 2T_s \cos\alpha / r\rho_w g \qquad \textit{Equation 5}$$

Considering an equilibrium condition and applying the Pascal's law between the points A and B, one can write:

$$u_w = -\rho_w g h \qquad \textit{Equation 6}$$

where u_w is the hydrostatic pressure at point A. At this point, the value of air pressure is set to zero. Therefore:

$$(u_a - u_w) = \rho_w g h = 2T_s \cos\alpha / r$$ *Equation 7*

Based on the Equation 7, when radius of the tube decreases, matric suction $(u_a - u_w)$ increases.

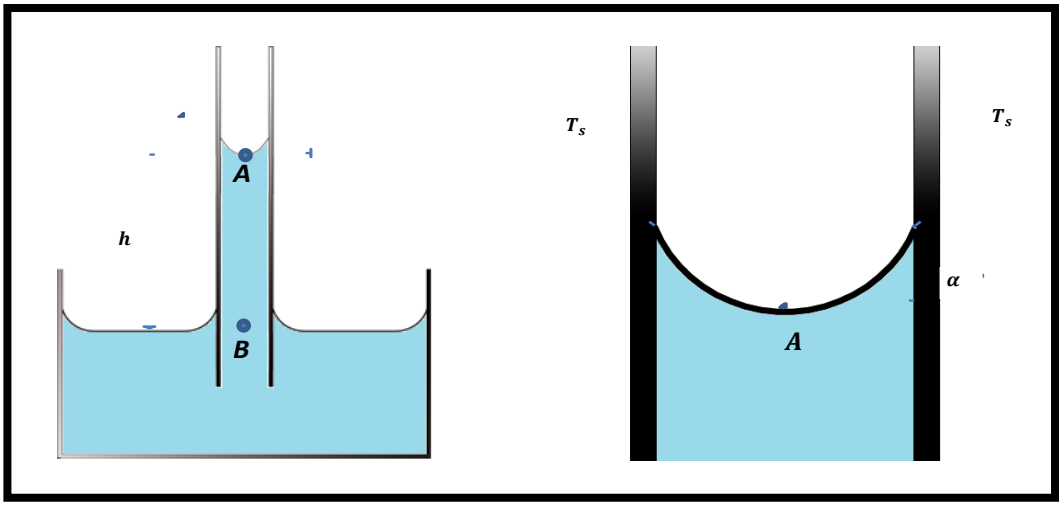

Figure 2: Rising water in a capillary tube
(Inspired from Fredlund & Rahardjo, 1993)

As it was mentioned earlier, soil is composed of particles of different shapes and sizes. Because of these differences, pores between these particles have irregular shapes and sizes. These pores can be simplified as tubes with different sizes. These tubes could either be fully or partially filled with water, or empty. As is seen in Figure 3-b when the soil is partially saturated an air- water interface is formed between soil's particles. This interface has a curved meniscus. Capillary pressure is the pressure difference between ambient air and water phase in their interface (Karkare & Fort, 1993).

Capillary pressure is an inter-granular pressure between soil particles. In Figure 3 (Inspired from Farouk et al. 2004) water in soil pores and tensions between water and soil particles surface from a saturated state to a dry state is illustrated. In this figure, "a" shows two soil particles in a saturated state, while "b" and "c" illustrate these particles in an state between fully saturated and dried conditions. Tensions on soil particles due to the presence of water

between these particles are illustrated by the black vectors. In Figure 3, “d” shows a fully dried soil.

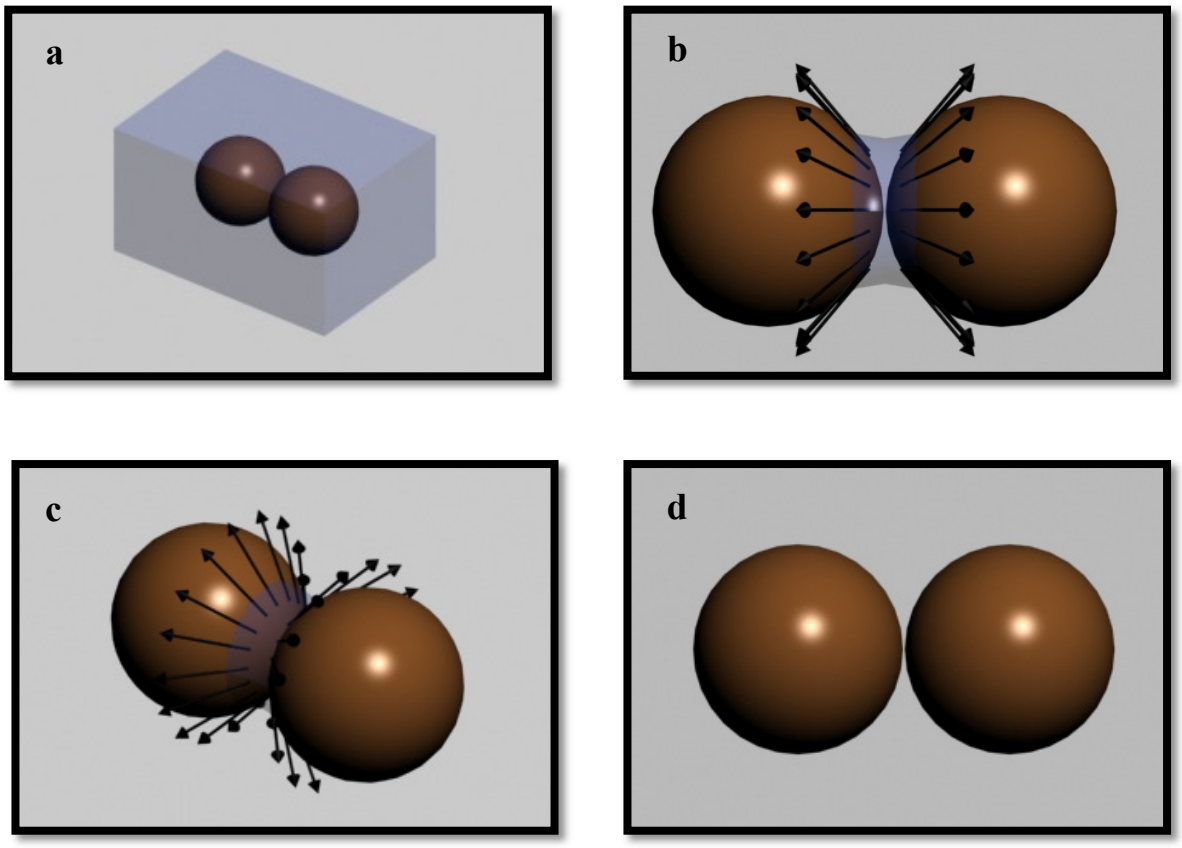

Figure 3: Water in soil pores and tensions between water and soil particles surface from a saturated state to a dry state (Inspired from Farouk et al. 2004)

a) Saturated b and c) Unsaturated d) Dry

Figure 4 (adapted from Tuller & Or 2003) illustrates a conceptual sketch of relationship between pore sizes and capillary rise in tube. As it can be seen, in smaller pores capillary rises are greater. The dark blue color shows the rising water in each tube with a certain diameter due to capillary phenomenon. Soil water content at each elevation will be the accumulated volume of water in all tubes from $z=0$ to that certain elevation.

Due to the capillarity phenomenon, the degree of saturation above the water surface (capillary zone) is less than 100 percent. In capillary zone, pressure is negative and less than atmospheric pressure.

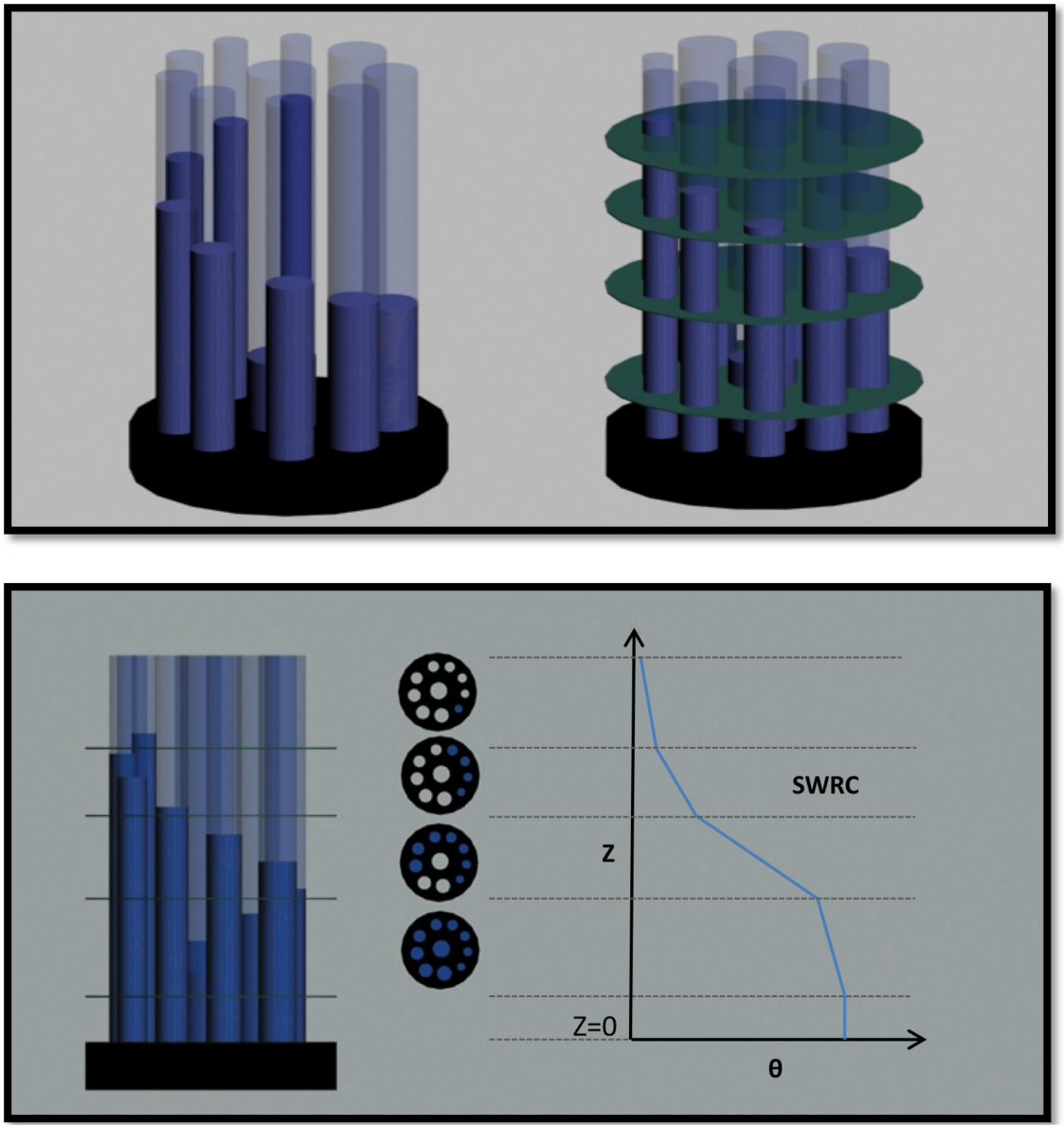

Figure 4: Conceptual sketch showing the relationship between pore sizes, capillary rise in tube and the SWRC (Adapted from Tuller and Or 2003)

As it was mentioned earlier, total suction has two components, osmotic suction and matric suction. Measuring matric suction in soil, particularly in high pressures is not easy. Since the osmotic suction does not have a great influence on water content of the soils, the total suction can be used as a representative for soil suction (Fredlund & Rahardjo, 1993). There are different instruments, that can be used to measure soil matric or total suction. These

instruments are designed to measure soil suction in field or laboratory. These methods can be divided into two major groups, Direct methods and Indirect methods.

2.1.2.1 Direct Methods for Measuring Soil Suction

There are different instruments and techniques, which were developed during the past decades to measure soil matric or total suction. Tensiometers and null type pressure plates are examples of equipment that are used to measure matric suction. To measure soil total suction directly, the chilled mirror dew-point apparatus and psychrometer can be used.

2.1.2.1.1 Tensiometer

Tensiometer is an instrument to measure soil matric suction directly. Richards & Gardner (1936) and Richards (1941) were among the firsts who designed and used the tensiometer.

As it can be seen in Figure 5-a (Soilmoisture Corp.), this instrument consists of a porous cup (normally ceramic) which is connected to a vacuum gauge through a rigid body tube. To measure soil suction, tensiometer should be saturated. Tensiometer's cup is inserted in the soil with a good contact to the soil particles. Water moves through the cup and after a while tensiometer equilibrate with water in the soil. These types of tensiometers are called vacuum gauge tensiometers. Presence of air in the water column will reduce accuracy of the tensiometer and increases measurement's time (Smajstrla & Harrison, 1998). Some models of tensiometers include a transducer. These transducers are connected to data loggers and can continuously record pressure values. Due to the cavitation problem, tensiometers can be used for low pressure ranges, normally lower than 90 (*kPa*) (negative pressure). The other problem is related to the air diffusion through the ceramic cup. This phenomenon can reduce the accuracy and response of the tensiometers (Fredlund & Rahardjo, 1993). The Jet-fill tensiometer was designed to reduce the air bubbles' negative effect on the tensiometer's results. This tensiometer can remove the accumulated air bubbles. As is shown in Figure 5-b (Soilmoisture Corp.), at the top of the jet-fill tensiometer a water reservoir is placed. This reservoir can be used to jet water into the tube to remove air bubbles.

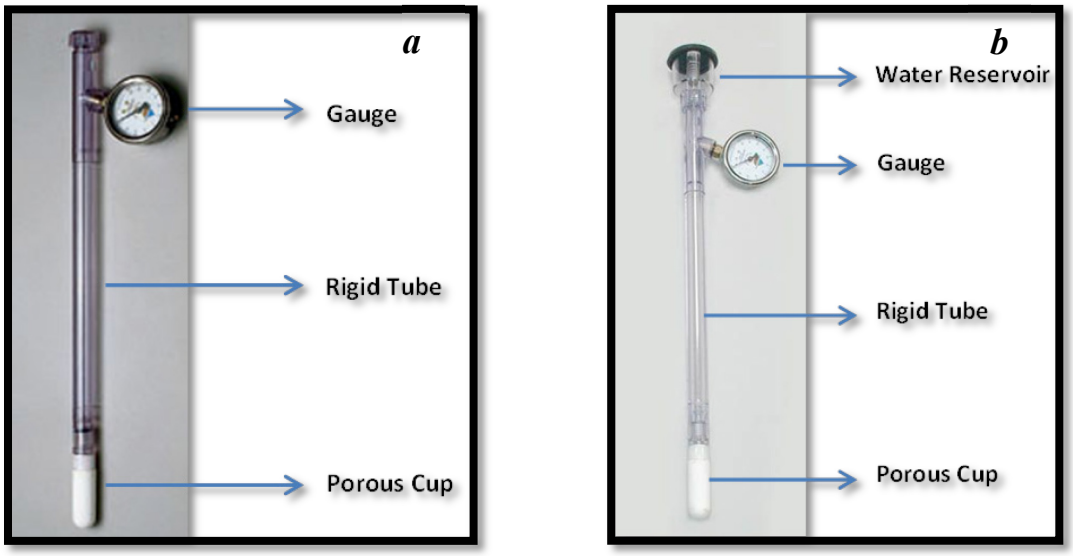

Figure 5: a) Tensiometer, Model: 2710ARL (Soilmoisture Equipment Corp.)

b) Jet fill tensiometer (Eijkelkamp Agrisearch Equipment)

2.1.2.1.2 Null Type Pressure Plate

A null-type pressure plate is one of the instruments for measuring matric suction by direct methods. This instrument can be used to measure matric suction in laboratory for fine-grained unsaturated soil specimens by applying the axis translation technique and is suitable for pressures between 50-500 *kPa*. As seen in Figure 6 (Fredlund & Rahardjo, 1993), a high air-entry disk is inserted under the soil specimen. The soil specimen is placed in a chamber, which is air proof. Air pressure can be applied to get to desired soil suction. Soil suction is measured at each air pressure. The following apparatus was used for the axis translation technique.

2.1.2.1.3 Chilled Mirror Dew Point

There is a relation between the soil total suction and the water vapour pressure, so this property can be measured by devices that are used to measure relative humidity (Tripathy et al. 2003). Instruments and techniques used to measure the soil total suction include, chilled mirror dew-point device, paper method, psychrometer, and relative humidity.

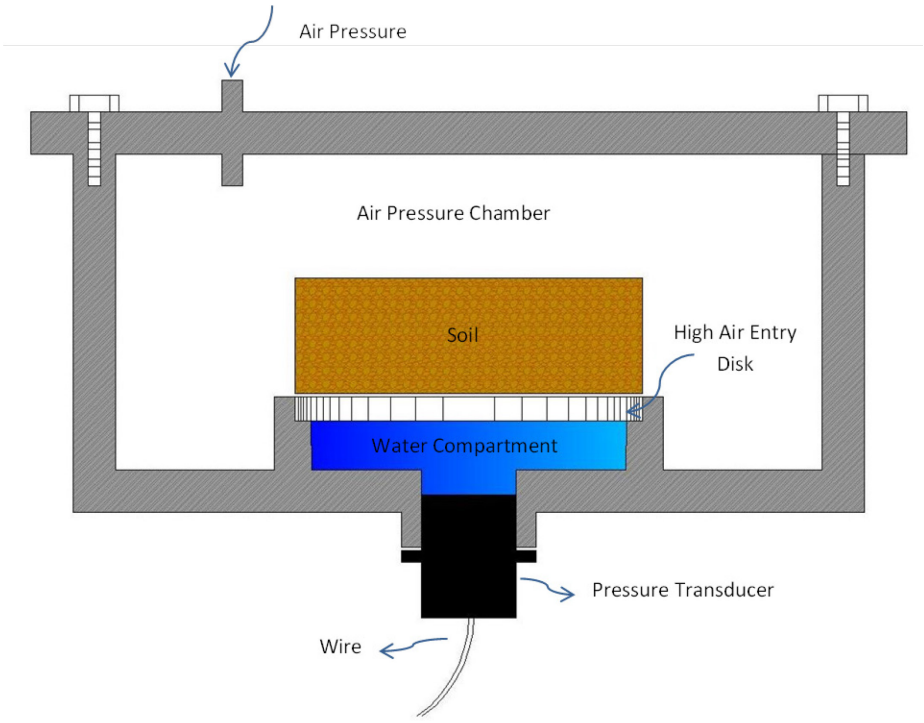

Figure 6: Schematic view of the Null Type Pressure Plate apparatus (Fredlund & Rahardjo, 1993)

The Chilled mirror dew-point device can be used to measure soil total suction in laboratory. Dew-point is the temperature at which the water vapour in a volume of humid air at a constant pressure will condense into liquid water. In other words, at this point there is enough water vapour in the air to fully saturate it. A schematic view of a dew-point chilled mirror is shown in Figure 7 (Tripathy et al. 2003).

To use this device for measuring soil suction, a soil sample is prepared, placed into a container filling it half way and inserted into a sealed chamber. The soil equilibrates with the water vapour in the space around the soil sample. A mirror in the chamber is connected to a thermoelectric cooler. The temperature of the point that condensation happens is recorded by thermocouple attached to the mirror. To measure soil suction for different water contents, a series of specimens are prepared and for each the suction is measured. This method has an accuracy around ±0.1% (Tripathy et al. 2003).

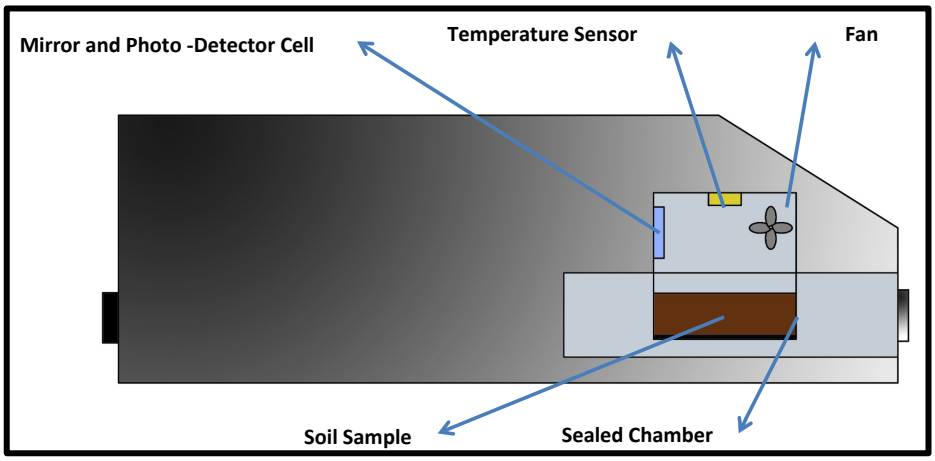

Figure 7: Schematic of chilled-mirror dew-point device (Tripathy et al. 2003)

Figure 8 (ASTM-D6836-02, 2012) is a photograph of a Chilled Mirror Hygrometer and the specimen to be tested.

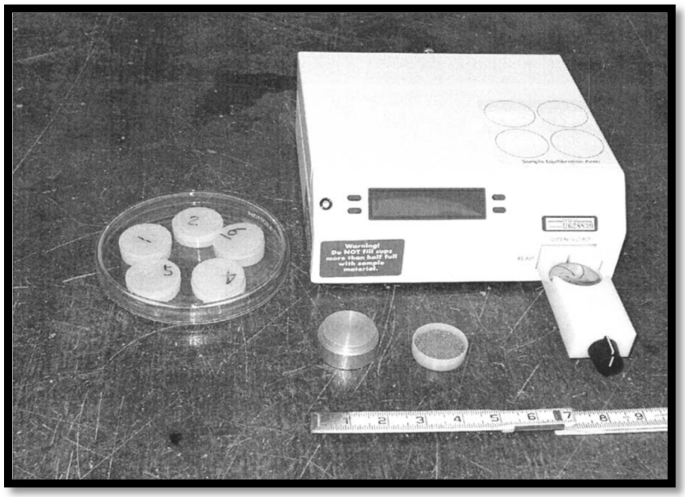

Figure 8: Photograph of a Chilled Mirror Hygrometer (ASTM-D6836-02, 2012)

As it was mentioned earlier, this method was developed for laboratory suction measurement; but recently some attempts were made to use a chilled mirror for field measurement (Richardson et al. 1999).

2.1.2.1.4 Psychrometer

Psychrometer can measure soil total suction by measuring relative humidity in the air phase of soil pores or the region near the soil (Fredlund & Rahardjo, 1993). Psychrometers are generally used in laboratories. This instrument uses Kelvin's Law to measure soil's suction.

This measuring technique has two main problems. The first problem relates to the small amount of relative humidity changes in the soil gas phase. The second problem originates from the fact that temperature differences in the sensor–sample system may cause large errors in water potential determination (Dane & Topp, 2002). There are different types of psychrometers. Most of them consist of two similar thermometers that are installed side by side. Psychrometers are of three major types:

a) Thermistor psychrometer

b) Thermocouple psychrometer

c) Transistor psychrometer

2.1.2.1.4.1 Thermocouple Psychrometer

Spanner (1951) was the first to introduce the thermocouple psychrometer. Spanner's thermocouple psychrometer is limited by the required rigid temperature control (Kay & Low, 1970). Rawlins and Dalton (1967) did some modifications to improve Spanner's psychrometer for in-situ measurements. Rawlins and Dalton used a Peltier cooling system to make a wet junction. The Peltier sensor is one of the two major sensor types that are used in thermocouple psychrometers.

The other type of sensor that is generally used in thermocouple psychrometers is called wet-loop sensor (Dane & Topp, 2002). Tensiometers have upper and lower boundaries for the pressure they can measure, and these limits are highly influenced by the sensor's design and measurement protocol (Dane & Topp, 2002). Thermocouple psychrometers can measure the soil total suction at any point in the soil profile. The soil water potential gradient can be determined by its results (Enfield & Hsieh, 1971).

Figure 9 (Cokca, 2000) shows a schematic view of a ceramic shielded thermocouple psychrometer.

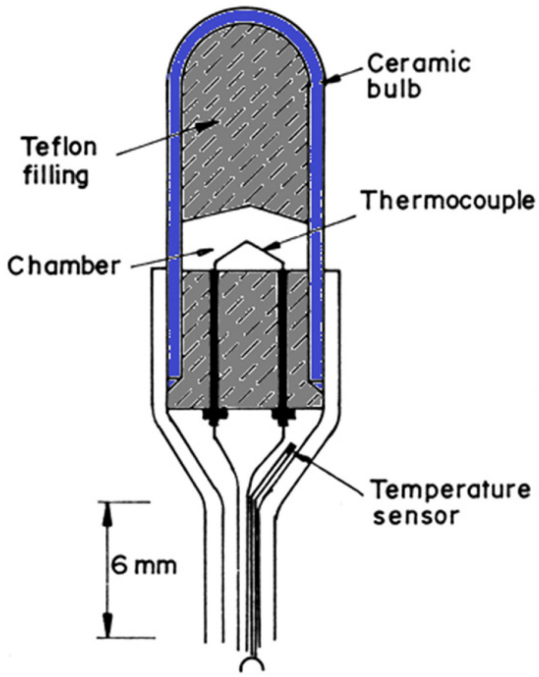

Figure 9: Ceramic shielded thermocouple psychrometer (Cokca, 2000)

2.1.2.1.4.2 Transistor Psychrometers

This type of psychrometers also uses relative humidity to find soil total suction. In this type of psychrometer, the evaporating wet-bulb is wetted by placing a drop of water into a small ring in all the psychrometer's probes. In Figure 10 (Cardoso et al. 2007) a schematic view of an SMI transistor psychrometer is given. These bulbs act as wet and dry thermometers. The difference in temperature between these two bulbs is used to measure relative humidity (Cardoso et al. 2007). The transistor psychrometer can be used to measure total suction in the range of 0.1 *MPa* to 10 *MPa* with good accuracy. Results obtained by Bulut et al. (2000) showed that at low suctions, this method is highly sensitive.

2.1.2.2 Indirect Methods to Measure Soil Suction

Beside direct methods of measuring soil total or matric suction, there are some indirect methods that can be used to find soil suction. These methods are influenced by different

parameters that can affect their accuracy. Isothermal equilibrium between the sensor, and the vapour space in the closed system of measurement media has an effect on the indirect methods' accuracy (Agus & Schanz, 2005).

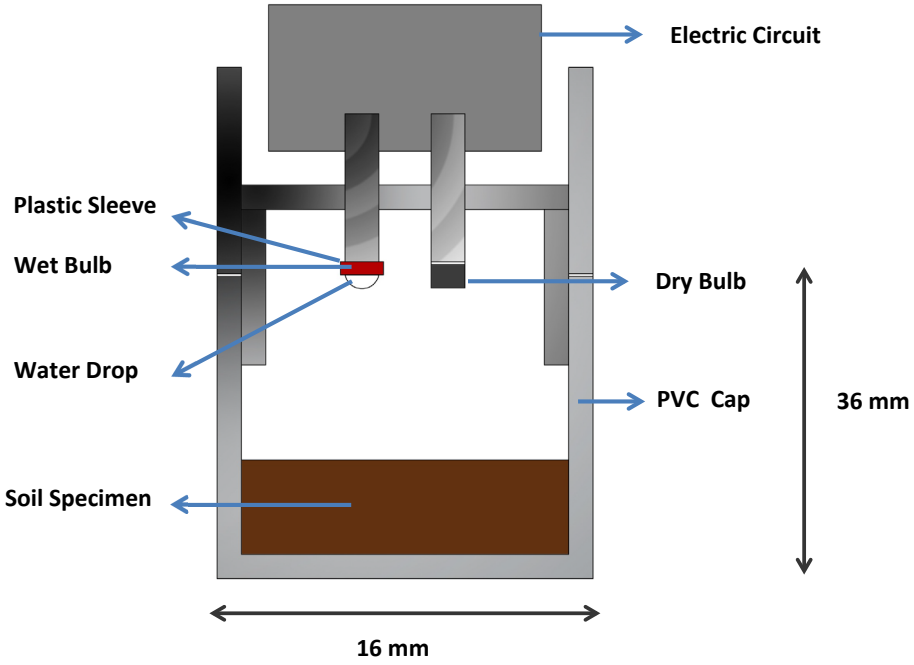

Figure 10: Schematic view of an SMI transistor psychrometer
(Cardoso et al. 2007)

2.1.2.2.1 Filter Paper Method

Gardner (1937) was the first who succeeded in using a filter paper to measure the soil matric and total suction. This method is based on measuring the amount of moisture transferred form an unsaturated soil sample to an initially dry filter to estimate soil suction (Likos & Lu, 1981).

The contact between the soil sample and filter paper plays an important role in the nature of the measured. If the filter paper is in contact with the soil sample, the water absorbed by the filter paper has the same concentration as the soil sample. In this case, the measured suction is matric suction. However, if there is no contact between the soil sample and the filter paper, the measured suction is equal to the soil's total suction (Marinho & Oliveira, 2012).

This method uses Kelvin's Law to find soil's total suction by its relationship with the pore water vapour's relative humidity (Agus & Schanz, 2005).

$$S = \frac{-RT}{M_W(1/\rho_W)} ln(RH) \qquad \textit{Equation 8}$$

where S is the total suction, R is the universal gas constant ($8.32432\ J\ mol^{-1}K^{-1}$), T is the absolute measured temperature (in Kelvin), M_W is the molecular weight of water ($18.016\ kg\ kmol^{-1}$), ρ_W is ythe unit weight of water (998 $kg\ /\ m^3$ at $20^o\ C$), as a function of temperature and RH is the measured relative humidity $[u_v/u_{vo}]$, where u_v is the partial pressure of pore water vapour in the specimen and u_{vo} is the saturation pressure of water vapour over a flat surface of water at the same temperature). At $20°\ C$, Equation 8 becomes:

$$S = -135055\ ln(RH) \qquad [kPa] \qquad \textit{Equation 9}$$

The papers should be calibrated prior to starting each test. To calibrate the filter paper, the relationship between equilibrium water content of the filter paper and the relative humidity of vapour phase is determined (Likos & Lu, 1981). This calibration can be done by using a salt solution that has a known concentration. Pressure membranes (100 *kPa* to 1500 *kPa*) or the ceramic plate (10 *kPa* to 100 *kPa*) can also be used to calibrate filter paper (ASTM-5298-10, 2010).

Likos and Lu (2002) have done two series of tests to evaluate the accuracy of noncontact filter paper technique for total suction testing. Their results shown that the filter paper calibration curves can vary significantly from batch to batch. Based on their studies, they recommended independent calibration from batch to batch. They had also shown that by decreasing total suction, uncertainty in total suction measurement by using the noncontact filter increases dramatically.

2.1.2.2.2 Thermal Conductivity Sensors

Shaw and Baver (1939) introduced a technique to measure soil suction by using thermal properties of water. They used heat conductivity as an index of the changing moisture

condition in-situ. Thermal conductivity method is one of the best instruments of measuring soil matric suction. This method is based on thermal conductivity of air and water. Thermal conductivity of water is better than thermal conductivity of air. When percentage of air in soil decreases, total thermal conductivity will decrease. Thermal conductivity sensors use this difference to measure soil suction. The accuracy measurements of thermal conductivity sensors are influenced by their calibration (Fredlund & Wong, 1989; Leong et al. 2012; Wong et al. 1989). Calibration of thermal conductivity device is the first step in using it for measuring soil suction.

As is shown in Figure 11 (Sattler & Fredlund, 1989), thermal conductivity sensor has a porous ceramic block containing a temperature-sensing element and a miniature heater. To measure soil suction by this method, a hole is drilled in the soil. By putting the sensor in drilled hole, water can flows between the porous block and the soil. After a while, water content of the soil and sensor will equilibrate. Heat dissipation in the block will change by changing amount of water content in porous ceramic block. By measuring this heat dissipation amount of water content can be measured indirectly (Sattler & Fredlund, 1989).

2.1.3 Water Flow in Unsaturated Soil

Generally, a vast knowledge of water flow process in soil is required to study a geotechnical problem. To model water and solute transport in unsaturated soils, it is necessary to hydraulic properties properly. Hydraulic properties are also used for hydraulic classification. This information is necessary for basic understanding of soil hydraulic process.

To select the method for determining soil hydraulic properties, time and expenses are important parameters. Some other parameters like measurement range and accuracy are also concerns to choose the proper technique to find soil hydraulic properties. Regarding these criteria, different methods had been developed to determine or measure soil's hydraulic properties. Direct and indirect methods are two main categories that can be used to find these properties. Direct methods are usually time consuming and need labor that makes it expensive. To decrease the expenses and the required time to measure these parameters,

some methods were developed to predict soil hydraulic parameters instead of direct measurement. Direct methods rely on measuring the desired hydraulic properties in field or in laboratory. In these methods, parameters like water potential, water flux and water content are measured in soil. Generally, these methods take a longer time and need expensive tools to be performed.

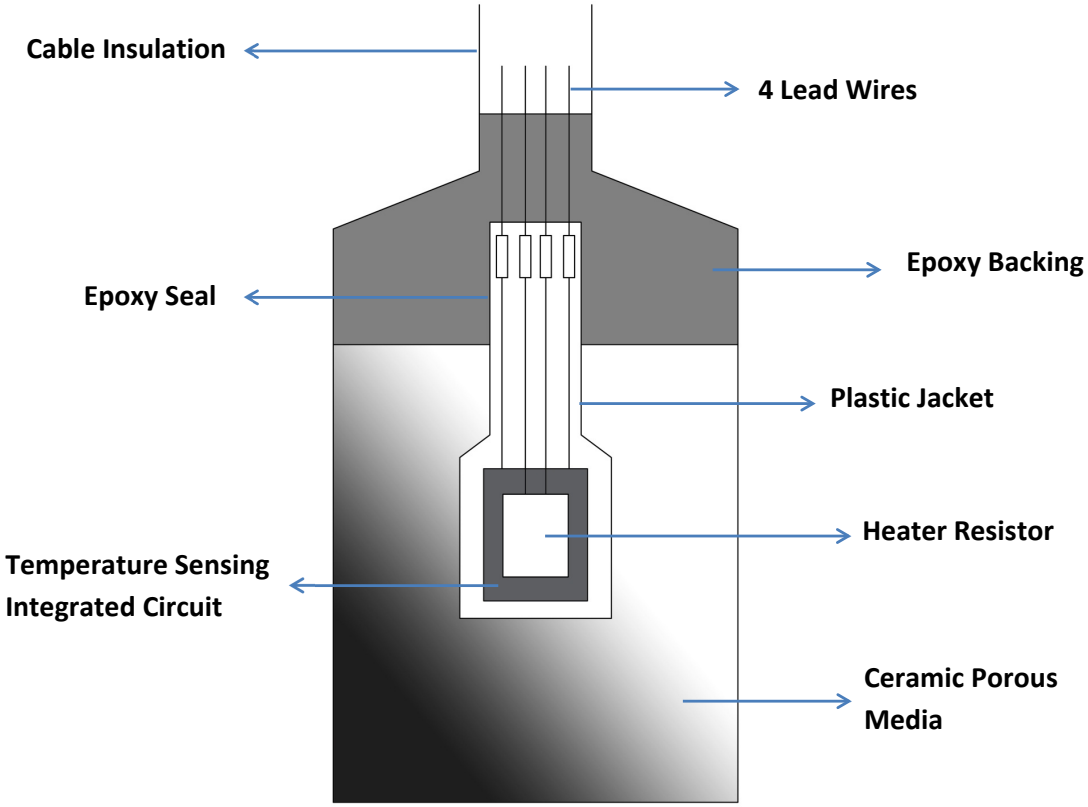

Figure 11: A cross sectional diagram of the thermal conductivity sensor (Sattler & Fredlund, 1989)

Unsaturated flow process is not easy to describe and formulate. Normally, during the flow in unsaturated media, soil water content changes.

Darcy's law is the fundamental equation for describing flow in porous material. This equation was presented by Darcy (1856) and relates the flow velocity (q) to the permeability of the medium (K) and the fluid's inside pressure (ψ).

$$v_w = -k\frac{\partial h_w}{\partial z}$$ *Equation 10*

where v_w is the flow rate of water and k is the coefficient of permeability with respect to the water phase. $\partial h_w/\partial z$ is the hydraulic head gradient in z-direction, where h_w is the total hydraulic head.

By combining Darcy's law with the continuity equation, Richards (1931) proposed an equation to describe water movement in unsaturated soils. Richards' equation for one-dimensional z-direction (vertical) flow is as below:

$$\frac{\partial \theta}{\partial t} = \frac{\partial}{\partial z}\left[K(h)\left(\frac{\partial h}{\partial z} + 1\right)\right]$$ *Equation 11*

where K is the hydraulic conductivity, h is the pressure head, z is the elevation above a vertical datum, θ is the water content, and t is time. Because of the constitutive relationship between h and θ it is possible to write Richards' equation either with pressure head or soil moisture form.

This is the basic equation for flow in unsaturated soils. By analytical or numerical solutions of this equation, the soil water content corresponding to a spatial location and a given time can be found. Richards' equation can be applied to saturated and unsaturated soils. At equilibrium $[\partial h/\partial z]$ is equal to 1.

In Richards' equation the $[\partial \theta/\partial t]$ term can be replaced by $C(h) * [\partial h/\partial t]$ where $C(h)$ is $[d\theta/dh]$. Celia et al. (1990) proposed $C(h_m)$ as water capacity function.

Hydraulic conductivity is one the most important hydraulic properties of the soils that effects flow in soil. By solving Richards' equation using inverse modelling method, hydraulic properties of unsaturated soils can be estimated (Eching et al. 1994; Fujimaki & Inoue 2004; van Dam et al. 1994; Šimůnek et al. 1998). Inverse modelling requires some soil retention data (van Dam et al. 1990). These data can be provided by using experimental

methods. Soil water retention curve which represents relationship between soil suction (ψ) and volumetric water content (θ) can be found by performing some laboratory experiments.

2.2 Hydraulic Properties of Unsaturated Soils

2.2.1 Soil Water Retention Curve

Soil water retention curve (SWRC), which is also called soil water characteristic curve (SWCC) is the relationship between soil suction and soil water content (degree of saturation). Figure 12 (Inspired from Fredlund et al. 1994) illustrates a typical SWRC. In this figure, vertical and horizontal axis show volumetric water content and soil suction, respectively. Air-entry value (AEV), residual water content (θ_r) and saturated water content (θ_s) are shown in this figure. Pore space distribution in soil texture has an important role in properties of SWRC.

As is illustrated in Figure 12 (Inspired from Fredlund et al. 1994), water content in the wetting curve is lower than the drying curve for a given matric potential. This behaviour is called hysteresis and affects the SWRC. Hysteresis is a result of entrapped air, contact angles in soil structure, swelling and shrinking and inkbottle effects in soil.

As it is shown in Figure 13 (Fredlund & Xing, 1994), SWRC changes in a wide range for different types of soils. Generally, soils with higher plasticity values have higher saturated volumetric water content and air-entry values (Fredlund & Xing, 1994). Clay has the highest saturated water content compare to silt and sand.

Maqsoud et al. (1975) did some studies on effects of hysteresis on the water retention curve. They performed some tests to study this phenomenon and compared their experimental results with predictive models. They used different types of sands (fine, coarse and silty sand). Their results showed that hysteresis has more effect on fine sands and silty sands compare to coarse sands. Their results also showed that the "Universal Mualem" model cannot predict SWRC adequately. Normally this hysteresis can be neglected in most practical applications. It is also possible to translate wetting or drying SWRC to another by using some techniques (Fredlund et al. 2011).

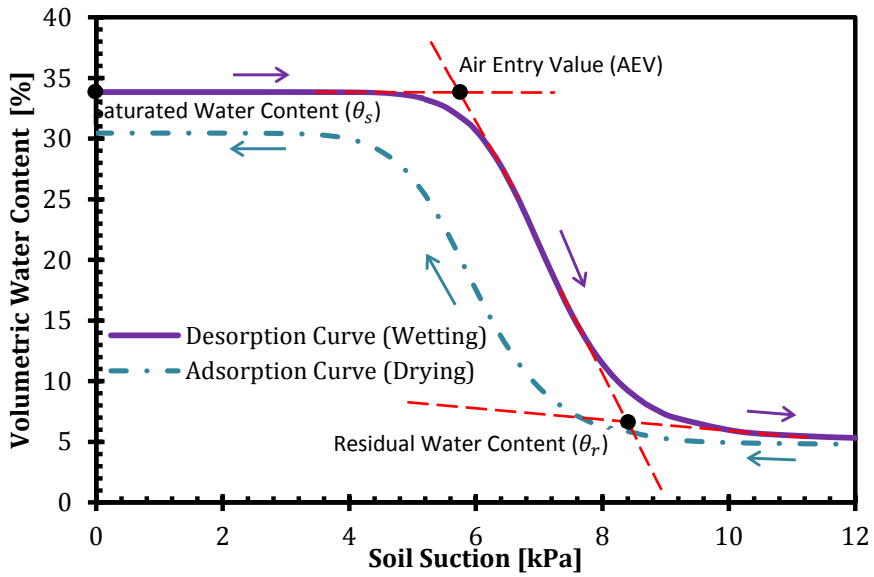

Figure 12: Typical SWRC, wetting and drying curves
(Inspired from Fredlund et al. 1994)

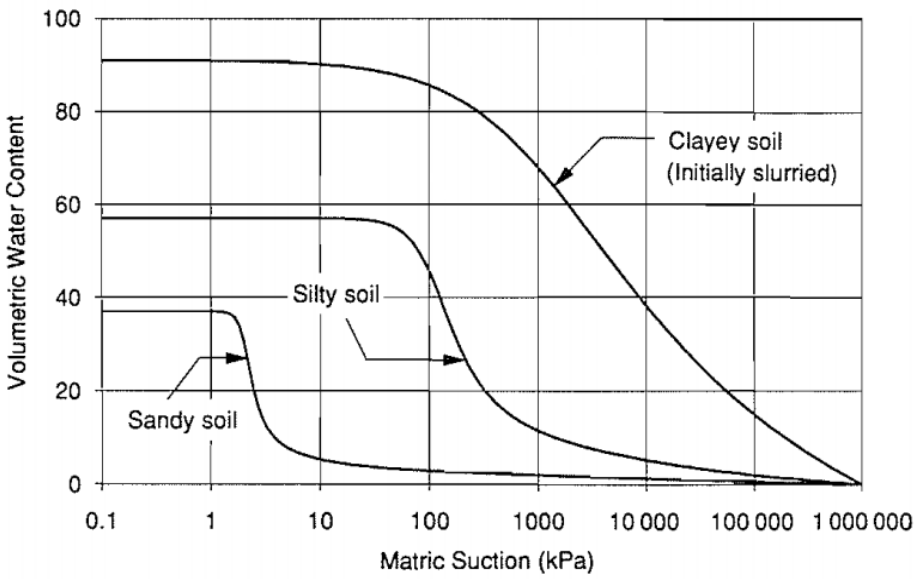

Figure 13: Typical SWRC for sandy soil, silty soil and clayey soil
(Fredlund & Xing, 1994)

SWRC is a function of soil suction (capillary pressure) and degree of saturation (water content). To measure the SWRC, it is necessary to measure these two parameters simultaneously.

2.2.1.1 Measuring the Soil Water Retention Curve

To measure the soil water retention curve, water content for corresponding soil suction should be known at different suction values. Generally, the test procedure involves a soil sample on top of a saturated membrane or a porous plate. Pairs of volumetric (or gravimetric) water content and suction values are obtained when the water in the sample is in equilibrium with the water the reservoir. SWRC can be obtained by plotting these values. The method that is used to measure these pair values can involve wetting or drying procedures. As it was mentioned earlier, the procedure to obtain SWRC is hysteretic (Maqsoud et al. 1975; Šimůnek et al. 1999). Because of that, the SWRC obtained for a given pressure head in the wetting process is normally less than the one that is obtained by drying process.

2.2.1.1.1 Axis Translation Technique

Cavitation is a phenomenon that can happen when the water pressure is relatively low. In soil science, cavitation is a problem that can happen when negative pore water pressure reaches zero. In measuring the soil water retention curve, the soil sample can be filled by air bubble when cavitation happens. Methods based on this technique, beside the hanging water column, are the common methods of studying hydraulic properties of unsaturated soils. Marinho et al. (2008) and Vanapalli et al. (2008) discussed the axis translation technique as a method to control suction in unsaturated soils. In this technique, the cavitation related to pressures greater than 100 *kPa* is eliminated by using a new procedure. The same amount of pressure is subjected to pore air and pore water pressures since the matric suction, $(u_a - u_w)$, will remain the same. The principle of the axis translation technique is shown in Figure 14 (Marinho et al., 2008). In this figure, matric suction is more than 100 *kPa*. This can cause metastable state in atmospheric pressure. To prevent this phenomenon, sample can be subjected to a large positive air pressure. In this condition, higher pore water pressures can be applied to the soil sample for the same matric suction value without being in metastable state (Marinho et al. 2008).

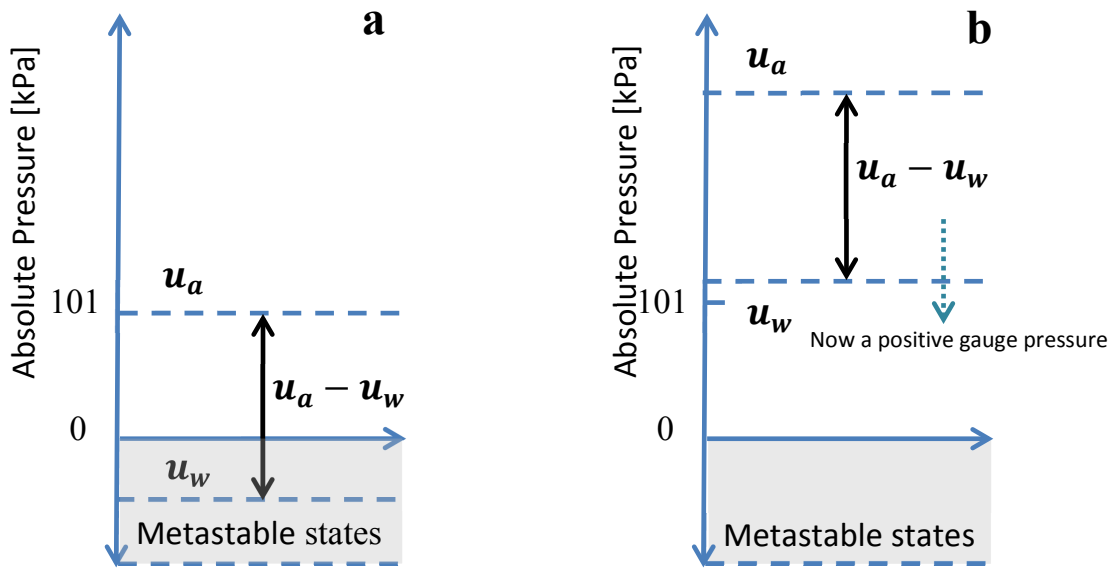

Figure 14: Use of the axis translation technique to avoid metastable states

(a) Atmospheric conditions (b) axis- translation (Marinho et al. 2008)

Axis translation technique can be used in a pressure plate apparatus or a Tempe Pressure Cell to measure soil water retention curve. Leong et al. (2004) and Wang and Benson (2004) described the design of pressure plate apparatus for measuring soil water retention curve. Wildenschild et al. (1997), Fujimaki & Inoue (2004) and Eching & Hopmans (1993) are some of the researchers who used axis translation technique to measure soil water retention curve.

2.2.1.1.2 Hanging (Negative) Water Column

Hanging column water that was originally proposed by Haines (1927, 1930) is proper for suctions between 0-80 *kPa.* This test is generally performed in a Buchner funnel. In Figure 15 (ASTM-D6836–02, 2012), a funnel is shown. Specimen chamber, an outflow measurement tube and a suction supply are three main parts of a hanging water apparatus. A schematic view of hanging water column apparatus is given in Figure 16 (ASTM-D6836–02, 2012). To perform the test, a manometer is used to measure the amount of applied suction. A capillary tube which is connected to the outlet of the funnel is used to measure the amount of the extracted water from the specimen while the test is running

(ASTM-D6836–02, 2012). The gas pressure that is applied to the sample is at atmospheric pressure (P_{atm}, P_a). Bulk water has sub-atmospheric pressure levels. This pressure can be provided by reducing the level of water in the reservoir or by decreasing the controlled gas pressure P_g. Gas can be dissolved from the bulk water, which can cause a problem in this test. Because of this fact, the suction apparatus has a minimum value which is -85 *kPa* at elevations near sea level (Dane & Topp, 2002).

In this test after reaching the desired matric suction, the final volumetric water content should be determined. To determine θ, the soil sample should be removed and after weighting should be place in an oven for about 48 hours at *105 °C,* so:

$$\theta = (M_1 - M_2)/\rho V \qquad \textit{Equation 12}$$

where θ is the volumetric water content. M_1 and M_2 are the soil mass before and after placing in the oven, respectively. ρ is the density of water and V is the volume of soil sample.

2.2.1.1.3 Pressure Plate Extractor

Hanging water column and pressure cell have an important limit that is related to their applicable minimum suction value that is equal to -8.5 m. Pressure plate extractor is a method that was developed for high suction values (Dane & Topp, 2002). To perform a test in high pressures with this method, a high air-entry porous ceramic plate is necessary. These ceramics are made of mixture of ball clays and are manufactured by a sintering process. During the test, these ceramics separate the air and the water phase (Leong et al. 2004).

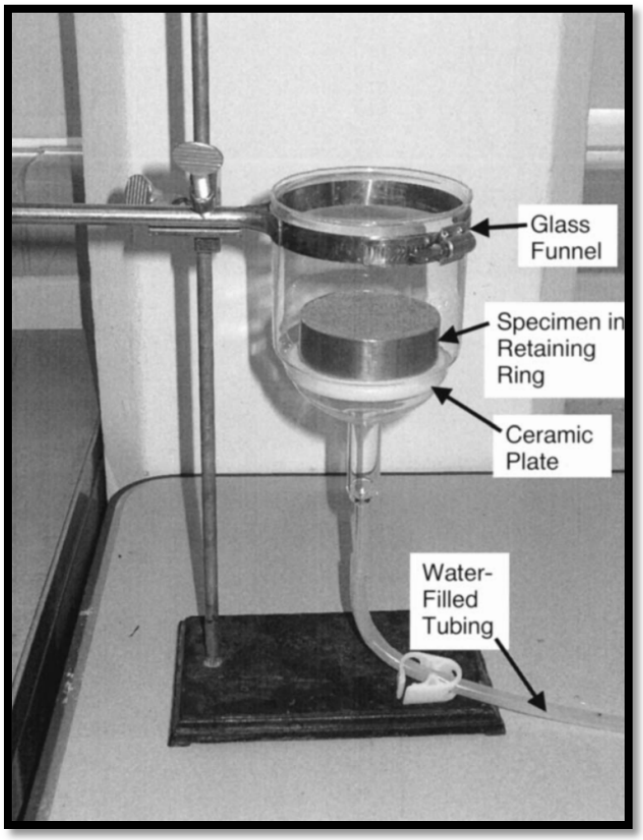

Figure 15: Photograph of a funnel used for hanging column apparatus (ASTM-D6836–02, 2012)

Pressure plate extractors are also called pressure plates. This apparatus can be used to determine soil water content in drying or wetting process. The procedure of this method can be found in "Methods of Soil Analysis" (Dane & Topp, 2002). Figure 17 (Soilmoisture Equipment Corp.) shows a 5-bar Pressure plate extractor. From 5 to 8 soil samples can be inserted on the ceramic plate in different models. This ceramic plate is normally supported by a pressure chamber that is equipped with some valves for air pressure inlet and an air release valve.

By using a pressure regulation system, air pressure can be applied to the system and water can flow out of the pressure chamber. When there is no more flow for a given pressure, the final water content of each sample can be determined weighing the sample. This is repeated for different pressure values to have pairs of suction and water content.

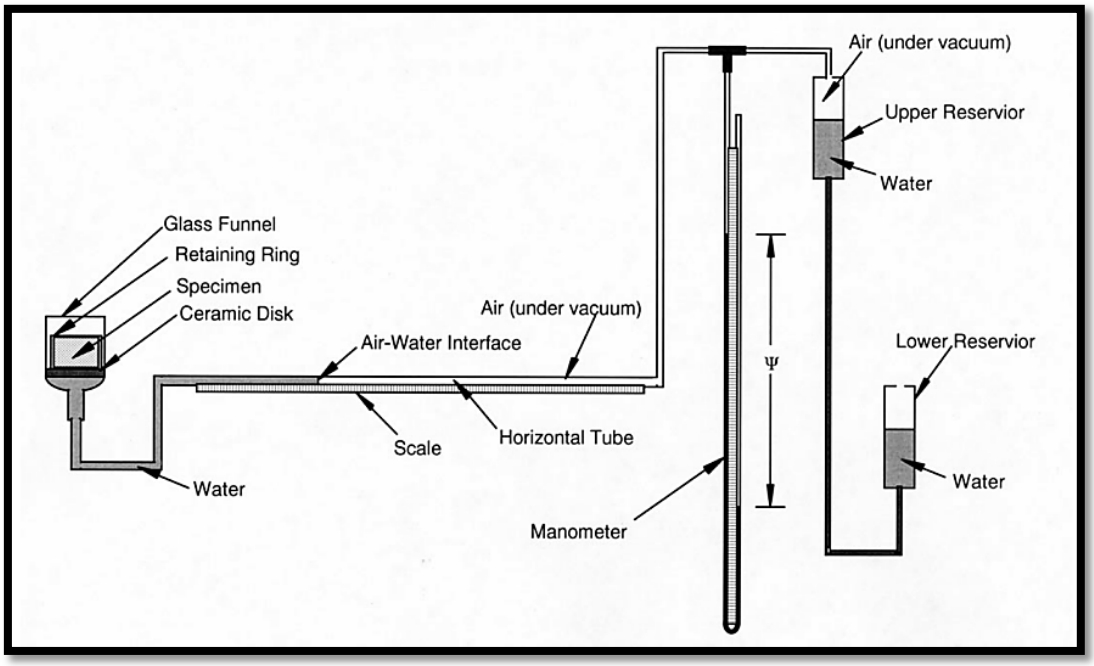

Figure 16 : Schematic view of a hanging column apparatus (ASTM-D6836–02, 2012)

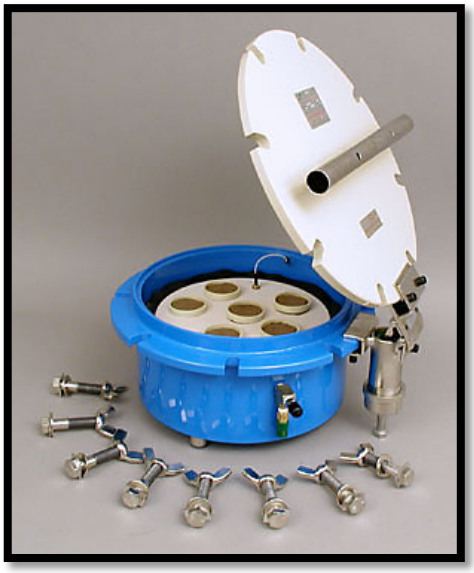

Figure 17 : 5 Bar Pressure Plate Extractor, picture from Soilmoisture Equipment Corp. (soilmoisture.com)

2.2.1.1.4 Tempe Pressure Cell

Tempe pressure cell is an apparatus that can be used to measure the soil water characteristic curve. This apparatus can be used for coarse and fine-grained soils. In this method an individual core of the soil sample is inserted on top of a porous ceramic plate. An air pressure inlet on top of the cell is used to apply pressure to the soil sample. This apparatus can be used for pressures between 0 to -100 kpa to prevent depressurization phenomena. Figure 18 (Soilmoisture Equipment Corp. 1995) shows a cross sectional view of the sketch of a Tempe Cell. The water outlet at the bottom of the cell allows the extracted water to flow towards the reservoir. A regulated gas pressure source is required to apply high pressures to the soil sample. Due to the pressure inside the soil sample, water will be extracted. Extracted water for each pressure value can be recorded and used to determine soil water retention curve with this method. This test can be performed in one-step or in multiple pressure steps. By performing this test in multiple steps, applied pressure increases in multiple steps and the extracted water value is measured for each pressure value.

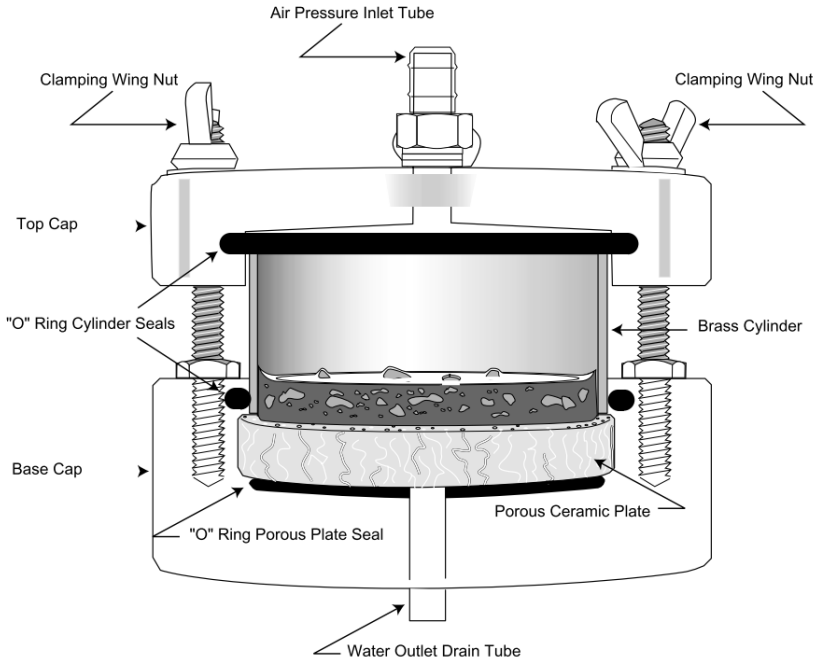

Figure 18: Cross sectional view of the sketch of a Tempe Cell
(Soilmoisture Equipment Corp. 1995)

In Figure 19 some methods of measuring SWRC and their corresponding matric suctions are given. Each method is suitable for a certain range of matric suction; for example, the psychrometer is better for higher matric suction values and the Tempe Cell is suitable for lower matric suctions.

2.2.1.2 Modelling Soil Water Retention Curve

It is time consuming and difficult to measure SWRC in laboratory. Different mathematical models were introduced by different peoples to represent SWRC based on their other properties. Some of these models are explained later in this chapter. Some of these models use soil's grain size distribution to estimate soil water retention curve.

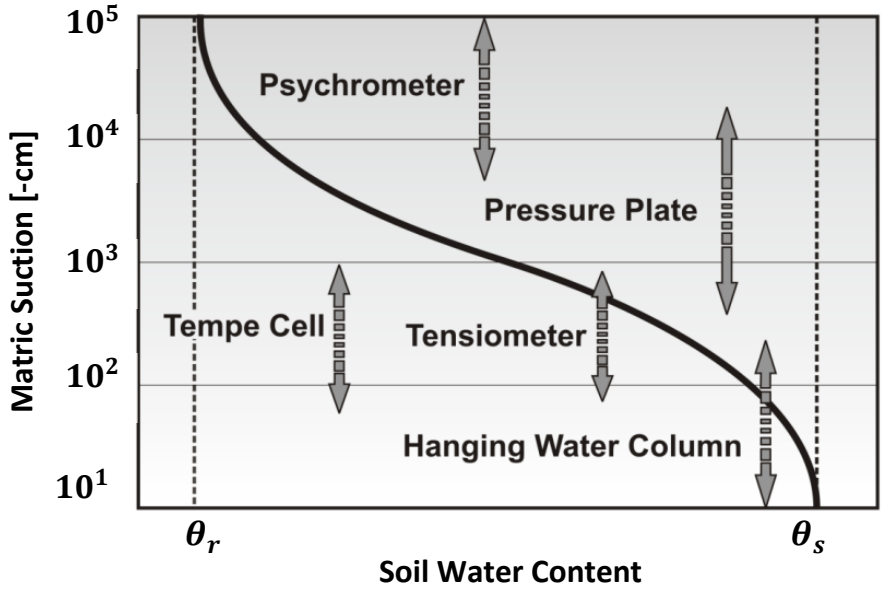

Figure 19: Some common soil water content measurement methods and their corresponding matric suction ranges (Tuller & Or, 2003)

2.2.1.2.1 Brooks and Corey

Brooks and Corey (1964) introduced a semi-empirical method to find unsaturated soils hydraulic properties. Brooks and Corey (BC) method gives better results for soils with coarse grain structure. As is it seen in Equation 13, for matric suctions (ψ) smaller than air-entry value (AEV), the effective degree of saturation (S_e) is equal to 1. If the matric suction

is greater than the *AEV*, S_e is found by using a correlation that is a function of matric suction and a dimensionless parameter (λ). λ is a constant that characterize pore size distribution and is called pore size distribution index.

$$S_e = 1 \qquad when \quad \psi < \psi_{AEV}$$

$$S_e = (\frac{\psi_{AEV}}{\psi})^{\lambda} \qquad when \quad \psi \geq \psi_{AEV} \qquad \textit{Equation 13}$$

and

$$S_e = \frac{\theta - \theta_r}{\theta_s - \theta_r} \qquad \textit{Equation 14}$$

where θ the volumetric water is content, θ_r is the residual water content and θ_s is the water content at saturation. Equation 13 can be re-written as:

$$\theta = \theta_s \quad when \quad \psi < \psi_{AEV} \qquad \textit{Equation 15}$$

$$\theta = \theta_r + (\theta_s - \theta_r)(\frac{\psi_{AEV}}{\psi})^{\lambda} \qquad when \quad \psi \geq \psi_{AEV} \qquad \textit{Equation 16}$$

where λ is the pore size distribution index. Figure 20 shows a comparison of SWRC results between Brooks and Corey (BC) model and experimental data for Pachappa loam (Assouline & Tartakovsky, 2001). As is shown in Figure 20, BC curve is formed of a straight line representing saturated part and a slope representing unsaturated part.

2.2.1.2.2 Arya and Paris

Arya and Paris (1981) proposed the first physico-empirical model to predict the SWRC by using particle size distribution and bulk density data. This model was developed for nonswelling soils with low degree of aggregation. They divided soil size distribution to several fractions and assumed that the bulk density of each fraction is equal to the bulk density of natural-structure soil. Based on this assumption they could find pore volume

related to each soil segment by using Equation 17. They approximated the solid volume to the volume of uniform size spheres, which is equal to mean particle radius for the segment and its pore volume is equal to uniform size cylindrical tube with diameter of the mean particle radius for that segment. By these assumptions, they could use Equation 23 to compute the pore radii. They translated particle size distribution into pore size distribution and used capillarity equations to find soil water pressure regarding to each pore radius (Arya & Paris, 1981). In this method pore volume (V_{vi}) is equal to:

$$V_{vi} = \left(\frac{W_i}{\rho_p}\right) * e \qquad \textit{Equation 17}$$

where W_i is the solid mass per unit sample mass in the *i*-th particle size range, ρ_p is the particle density and e is the void ratio and is equal to:

$$e = \frac{(\rho_s - \rho_b)}{\rho_b} \qquad \textit{Equation 18}$$

where ρ_s and ρ_b are particle and bulk densities, respectively.

Average volumetric water content of the midpoint of the *i*-th particle size range can be obtained as follows:

$$\theta_{vi} = \sum_{j=1}^{j=i} \frac{V_{vj}}{V_b}; \quad i = 1,2,\dots,n \qquad \textit{Equation 19}$$

$$V_b = \sum_{i=1}^{i=n} \frac{W_i}{\rho_b} = \frac{1}{\rho_b}; \quad i = 1,2,\dots,n \qquad \textit{Equation 20}$$

$$\theta_{vi}^* = (\theta_{vi} + \theta_{v\,i+1})/2 \qquad \textit{Equation 21}$$

where θ_{vi}^* is the average volumetric water content of the midpoint of a given (*i*-th) particle size range.

By using capillary correlation, suction related to each radius can be determined. The soil water pressure head ψ_i can be found with Equation 22.

$$\psi_i = 2T_s \cos\alpha / \rho_w g r_i \qquad \textit{Equation 22}$$

where T_s is the surface tension of water, α is the contact angle, ρ_w is the density of water, g is the gravity and r_i is the pore radius and r_i is equal to:

$$r_i = R_i\left[4en_i^{(1-\beta)}/6\right]^{1/2} \qquad \textit{Equation 23}$$

where r_i is the mean pore radius, R_i is the mean particle radius, n_i is the number of particles, and β is an empirical constant.

Arya and Paris set θ to 0 for $t=25^o\ C$, but if the contact angle can be used to adjust the results, if it is defined. To predict SWRC of aggregates, it was suggested to use aggregate size distribution in addition to particle size distribution. Results of Arya and Paris model shows a good agreement with measured data for several soils, but there is a considerable disagreement between measured and model values for some other soils (Arya & Paris, 1981). Figure 21 shows a comparison between Aria and Paris (1981) model measured data SWRC values for two Jersey soils. As is seen, there is a good agreement between predicted and measured data for these soils (Arya & Paris, 1981).

2.2.1.2.3 Fredlund and Xing (1994)

Fredlund and Xing (1994) proposed a new model for SWRC. They assumed that at suction equal to 1000 000 *kPa*, soil will be completely dry and the water content is *0*. This equation was based on the assumption that the shape of the SWRC is dependent on the pore size distribution.

$$\theta = \theta_s\, C(\psi)\left[\frac{1}{ln[e + (\psi/a)^n]}\right]^m \qquad \textit{Equation 24}$$

where a, n and m are fitting soil parameters, e is the Napier's constant, ψ is the soil suction and $C(\psi)$ is a correction factor which is equal to:

$$C(\psi) = \left[1 - \frac{ln(1 + \psi/\psi_r)}{ln(1 + 1000000/\psi_r)}\right] \qquad \textit{Equation 25}$$

where ψ_r is the residual soil suction.

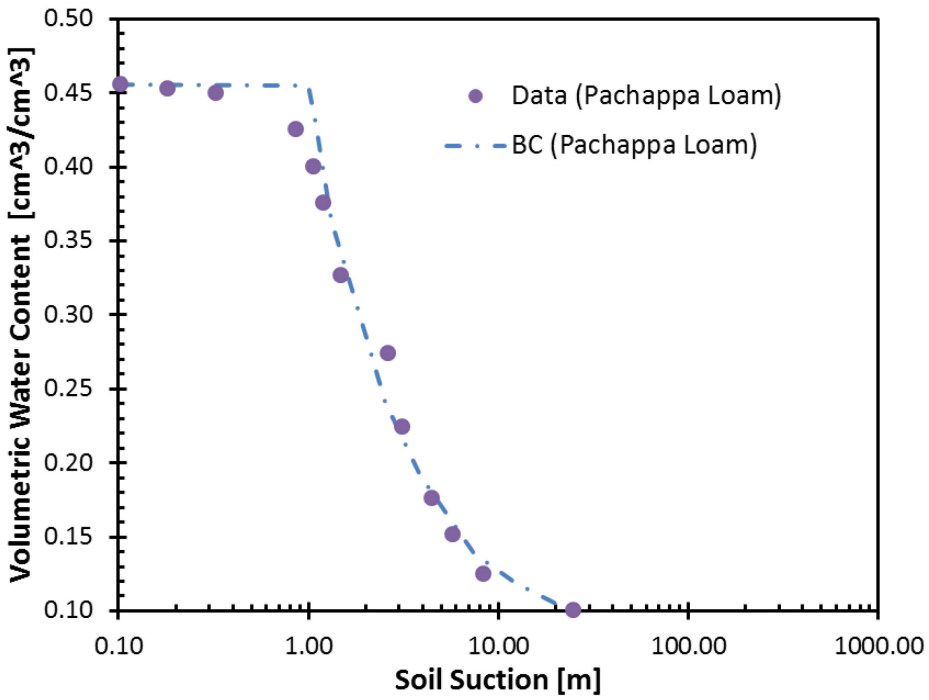

Figure 20 : Comparison of SWRC results between Brooks and Corey and data for Pachappa loam (Assouline & Tartakovsky, 2001)

In Figure 22 an example of applying Fredlund and Xing (1994) model to obtained experimental data is shown. As it is seen, the fitted curves are in a close agreement with the experimental data over the entire suction range.

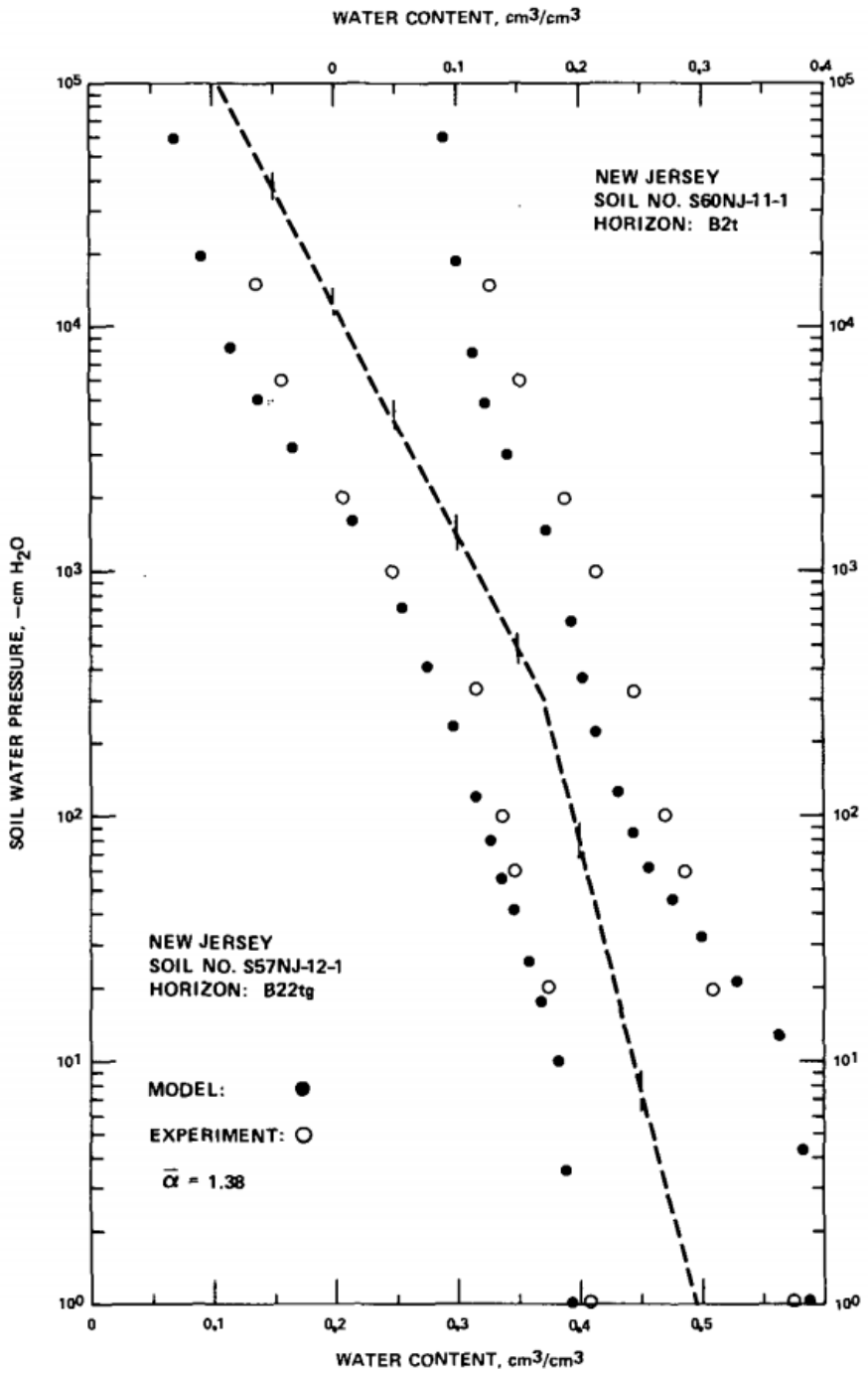

Figure 21 : Comparison between measured data and Aria and Paris (1981) model predicted values of SWRC for two Jersey soils (Arya & Paris, 1981)

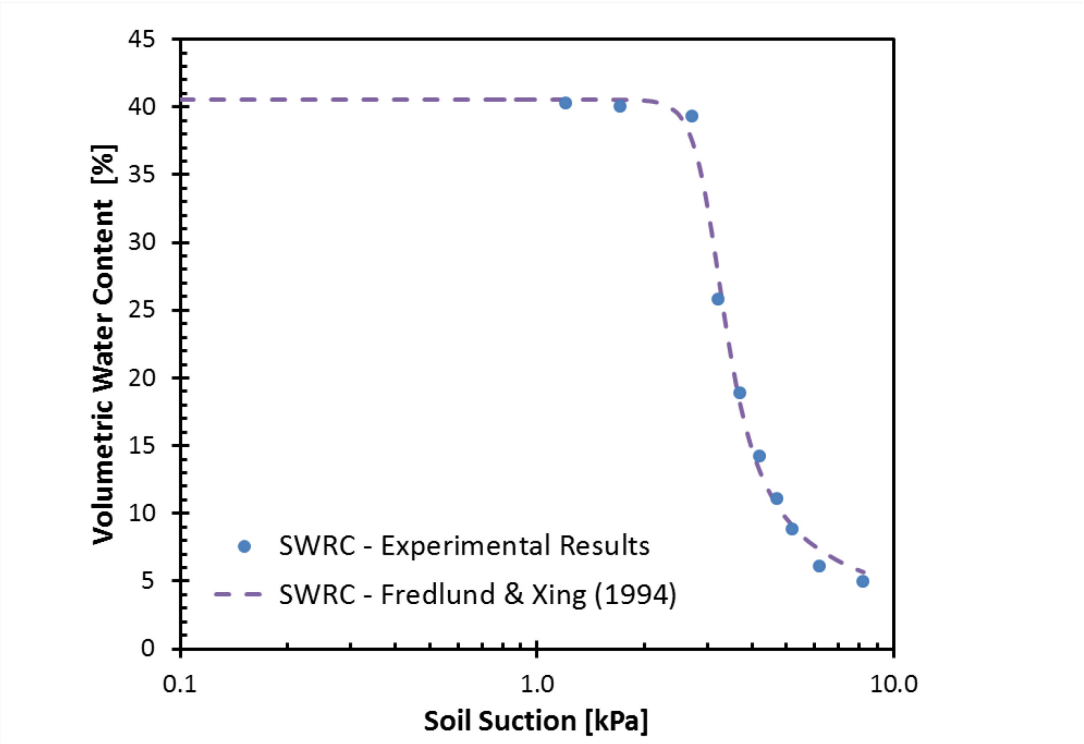

Figure 22 : A Fredlund & Xing (1994) model best-fit curve to the experimental data of a sandy material

2.2.1.2.4 van Genuchten (1980)

van Genuchten (1980) proposed new equations for SWRC. This model is applicable to different types of soils. By fitting van Genuchten (1980) model (VG) to the experimental data, three independent fitting parameters are obtained.

$$S_e = [1 + |\alpha\psi|^n]^{-m} \qquad \textit{Equation 26}$$

$$S_e = \frac{\theta - \theta_r}{\theta_s - \theta_r} \qquad \textit{Equation 27}$$

where S_e is the effective saturation, α (> 0) is a function of the inverse of the air-entry pressure, n (>1) is a function of pore size distribution and $m = 1 - 1/n$. ψ is the soil suction and θ is the volumetric water content and θ_r and θ_s are the residual and saturated

water contents, respectively. By combining Equation 26 and Equation 27, volumetric water content can be found as:

$$\theta = \theta_r + (\theta_s - \theta_r)\left[\frac{1}{1+(\alpha\psi)^n}\right]^m \qquad \textit{Equation 28}$$

To measure the suction by having the water content values, Equation 28 can be re-arranged as below:

$$\psi = \frac{1}{\alpha}\left[\left(\frac{\theta-\theta_r}{\theta_s-\theta_r}\right)^{-1/m} - 1\right]^{1/n} \qquad \textit{Equation 29}$$

By replacing m with $1 - 1/n$ as was suggested by Mualem (1976) fitting parameters will drop to two and the new equation will be re-written as below"

$$\theta = \theta_r + (\theta_s - \theta_r)\left[\frac{1}{1+(\alpha\psi)^n}\right]^{\left(1-\frac{1}{n}\right)} \qquad \textit{Equation 30}$$

In Figure 26-a, an example of applying van Genuchten model to Hygiene Sandstone experimental data (data from: Brooks & Corey, 1964) is shown. As it is seen, this model has a very good agreement with experimental data.

2.2.2 Hydraulic Conductivity of Unsaturated Soils

Hydraulic conductivity describes the capacity of the soil to transmit water. According to the Kozeny-Carman equation (Equation 31) hydraulic conductivity of saturated materials is affected by different parameters. This equation can be described as below (Carrier, 2003):

$$K = \frac{1}{CS_0^2}\frac{\gamma}{\mu}\frac{e^3}{(1+e)} \qquad \textit{Equation 31}$$

where K is the saturated hydraulic conductivity, γ is the unit of weight of permeant, μ is the viscosity of the permeant, e is the void ratio, C is the Kozeny-Carman empirical coefficient and S_0 is specific surface area per unit volume of particles $\left[\frac{1}{cm}\right]$.

Hydraulic conductivity decreases by decreasing soil unit weight. Soil temperature is another parameter that affects hydraulic conductivity of saturated materials. Void ratio, particle size, composition, fabric structure and degree of saturation also have influence on hydraulic conductivity of saturated materials. Soils with higher void ratio have higher hydraulic conductivity. D_{10} is inversely proportional to S_0. From Equation 31 it is evident that S_0 is inversely proportional to K, which implies D_{10} and K are directly proportional. Soils with bigger particles have higher permeability.

One of the properties of the soils that has a great influence on hydraulic conductivity of coarse-grained soils is the percentage of fine particles (Passing from No. 200 sieve). Existence of chemicals in fluids can also have some influences on hydraulic conductivity (Sharma & Lewis, 1994).

Darcy's law (Equation 10) defines hydraulic conductivity for saturated materials. Richards proposed an equation by applying Darcy's law for unsaturated soils. Hydraulic conductivity in unsaturated zone can be expressed in a relation with soil suction (ψ) or soil water content (θ). By increasing soil suction, hydraulic conductivity in soil decreases. Hydraulic conductivity of soils in unsaturated zone can be measured or estimated by different direct and indirect methods. To select the proper method for finding hydraulic conductivity, different parameters have to be considered. Time, cost, existence of equipment, skill of the staff who perform the test and type of the soil are some of these parameters. Different laboratory and field techniques were developed to measure hydraulic conductivity of unsaturated soils. Measuring methods are usually expensive and time consuming. Due to these problems, different attempts were done to find hydraulic conductivity by using indirect methods that are usually cheaper and faster than direct methods. Some methods of determining hydraulic conductivity of unsaturated soils are explained later in this chapter.

2.2.2.1 Direct Methods

Various direct methods were proposed by different researchers to measure hydraulic conductivity of unsaturated soils in field and laboratory. Steady state methods and unsteady

state methods are two major groups of direct methods of measuring hydraulic conductivity of unsaturated soils.

In steady state methods of determining unsaturated hydraulic conductivity $K(\theta)$, volumetric flux density and the hydraulic gradient are measured at given water content. A series of steady state flows are established and water flux and hydraulic gradient are recorded for each given water content value. The corresponding hydraulic conductivity for each θ value will be found by flux and hydraulic gradient data and using Equation 10, which is a finite –difference form of Darcy's equation.

Corey (1957, Cited by Masrouri et al. 2008) proposed a steady state method to find hydraulic conductivity of soils as a function of water content. He used a long column with some tensiometers which were installed on its wall. In this method, to have the hydraulic conductivity as a function of water content, a procedure should be done to measure water content as a function of soil suction. In this method for each step water will be entered form the top of the column (if wetting process is chosen) at a small steady rate. This will be continued till a steady flow into the column is reached and water content in the cell is constant. Therefore, the conductivity corresponding to that specific water content will be the same as flow rate for that step.

The most important limitation of this method is its necessity for a long homogenous soil column; so this method cannot be used for disturbed soil samples (Hopmans et al. 2002).

Beside proposed steady state methods, some researchers proposed unsteady methods to measure hydraulic conductivity of unsaturated soils. Instantaneous profile method (IPM) and Inflow-Outflow method are some of unsteady state methods.

Rose et al. (1965) was the first who developed the IPM method. This method is based on measuring hydraulic conductivity of soils for several depths as a function of water content. This method was then used and developed by some researchers like Watson (1966) and Chiu and Shackelford (1998) for determining the hydraulic conductivity of unsaturated materials.

Gypsum crusts were used by Bouma and Denning (1972) to find unsaturated soils hydraulic conductivity in field. To measure hydraulic conductivity of the soil by this method, a cylinder is made on soil surface. A mixture of gypsum and coarse sand is prepared. This mixture will be poured over that cylinder's surface. A flux is applied over the gypsum to have a constant head. Water potential at the bottom of the gypsum crust is measured by tensiometers. By measuring this flux rate and the diameter of the cylinder, hydraulic conductivity can be determined (ASTM-Standard-D5126).

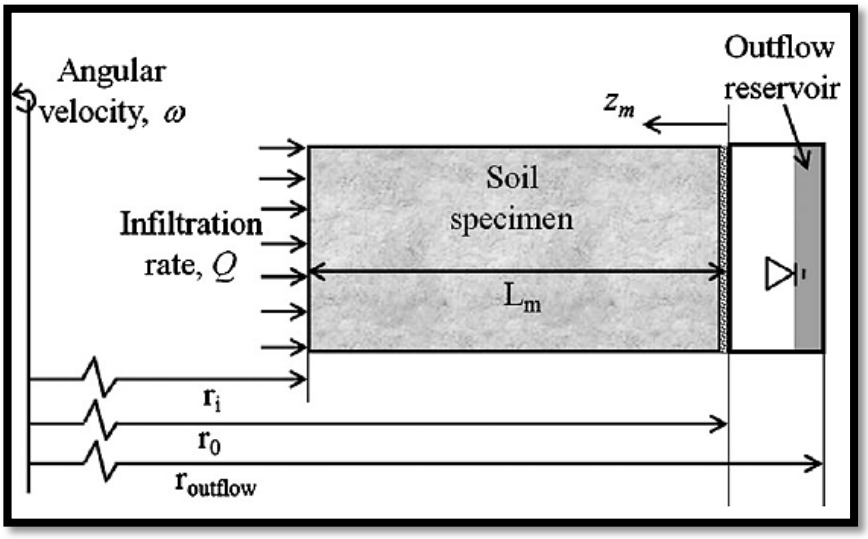

Figure 23 : Schematic view of a centrifuge permeameter with relevant variables (Reprinted from Zornberg & McCartney, 2010)

2.2.2.1.1 Evaporation

Evaporation method is one of the laboratory methods that can be used to determine SWRC and unsaturated hydraulic conductivity at the same time. This method was introduced by Gardner and Miklich (1962, Cited by Šimůnek et al. 1998). They imposed different evaporation rates to the sample. Each new rate was applied after equilibrium of the sample. The most popular procedure that is used to find hydraulic properties of the soils by evaporation method is a result of Wind (1966) efforts. He used a vertical cylinder filled with undisturbed soil material that was saturated with water. Sample was allowed to

evaporate only on its top. Wendroth et al. (1993) proposed an evaporation method to find soil hydraulic conductivity function and the water retention characteristic. They used a 6.0 *cm* high soil column and used two pressure tensiometers which were installed at 1.5 *cm* and 4.5 *cm* form the bottom of the cell. Top of the column was open, so the water could evaporate (Figure 24). They used numerical simulation to find hydraulic functions.

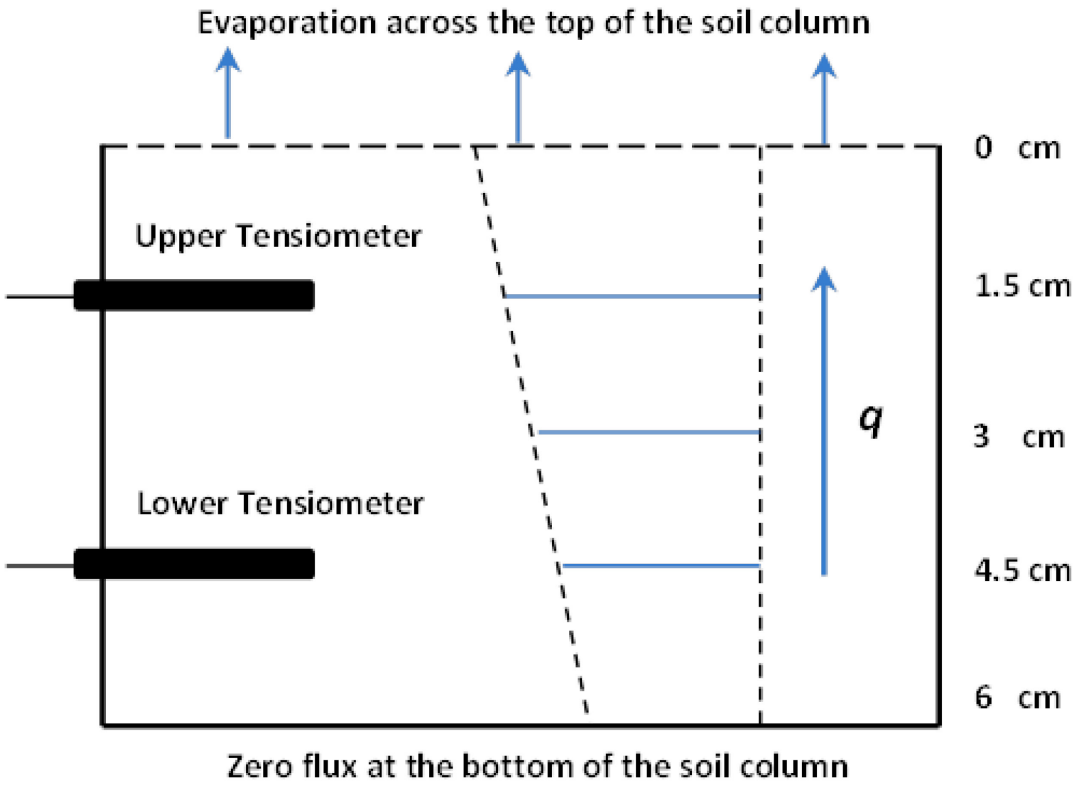

Figure 24 : Experimental setup for Wendroth et al. (1993)

2.2.2.2 Indirect Methods

Measuring unsaturated hydraulic conductivity by using direct methods is expensive and time consuming. Because of this problem, some indirect methods were developed to find hydraulic conductivity of unsaturated soils. Most of these methods use saturated hydraulic conductivity and SWRC to find hydraulic conductivity unsaturated soils.

2.2.2.2.1 Brooks and Corey (1964)

As it was described in 2.2.1.2.1, Brooks and Corey (1964) proposed some equations to relate soil's pore size distribution to its hydraulic properties. They proposed Equation 32 to estimate relative hydraulic conductivity, K_r, for given soil pressure:

$$K_r = 1 \qquad when \quad \psi < \psi_{AEV} \qquad \textit{Equation 32}$$

$$K_r = (\frac{\psi_{AEV}}{\psi})^{\eta} \qquad when \qquad \psi \geq \psi_{AEV}$$

where η is equal to $2 + 3\lambda$.

Relative hydraulic conductivity can be defined as the relationship between unsaturated hydraulic conductivity, K, and the saturated hydraulic conductivity, K_s.

$$K_r = \frac{K}{K_s} \qquad \textit{Equation 33}$$

However, this model gives better results for *J*-shaped retention data, and is not very good for *S*-shaped soils. Figure 25 shows a comparison of relative hydraulic conductivity, $K_{r,}$ results between BC model and experimental data for Pachappa loam (Assouline & Tartakovsky, 2001). There is a good agreement between BC model and experimental data.

2.2.2.2.2 van Genuchten (1980)

van Genuchten (1980) proposed a closed-form equation to predict hydraulic conductivity of unsaturated soils. van Genuchten (1980) method of predicting hydraulic conductivity is derived by applying this model's SWRC parameters to Mualem (1976). Unsaturated hydraulic conductivity can be described as:

$$K(\psi) = KS_e^l \left[1 - \left(1 - S_e^{1/m}\right)^m\right]^2 \qquad \textit{Equation 34}$$

where (ψ) is the unsaturated hydraulic conductivity, α, m are the curve fitting parameters. m is equal to $1 - (1/n)$, where n is also a van Genuchten equation curve fitting

parameter. l is an empirical pore connectivity parameter and can be fixed at 0.5 (Mualem, 1976).

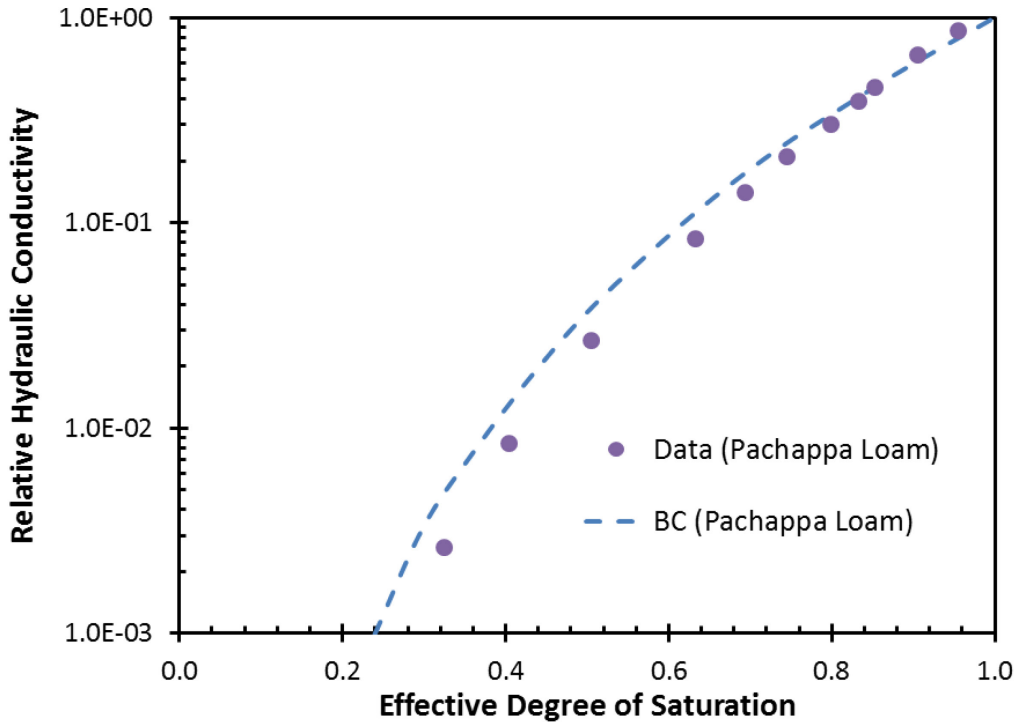

Figure 25: Comparison of relative hydraulic conductivity results between Brooks and Corey and experimental data for Pachappa loam (Assouline & Tartakovsky, 2001)

Soil water retention data obtained in laboratory can be used to find fitting parameters. By providing saturated hydraulic conductivity, (K), unsaturated hydraulic conductivity for the whole range of soil suction can be predicted. Figure 26 shows the SWRC data for a Hygiene Sandtone and its corresponding predicted unsaturated hydraulic conductivity. As it is seen, there is a good agreement between predicted unsaturated hydraulic conductivity results with the experimental data.

2.2.2.2.3 Fredlund et al. (1994)

Fredlund et al. (1994) proposed a model to determine hydraulic conductivity of unsaturated soils. Based on their relationship, relative hydraulic conductivity $K_r(\psi)$ can be found by using Equation 35. This model has a considerable deviation in high suction range.

$$k_r(\psi) = \frac{\int_{ln(\psi)}^{b} \frac{\theta(e^y)-\theta(\psi)}{e^y}\theta'(e^y)dy}{\int_{ln(\psi_{AEV})}^{b} \frac{\theta(e^y)-\theta_s}{e^y}\theta'(e^y)dy} \qquad \textit{Equation 35}$$

where ψ is the soil suction, y is a dummy variable, e is the Napier's constant, b is ln(1000000), ψ_{AEV} is the air-entry value of the soil under consideration, θ is the water content, θ_s is the saturated water content and θ' is the derivative of following equation:

$$\theta = \theta_s\, C(\psi)\left[\frac{1}{ln[e + (\psi/a)^n]}\right]^m \qquad \textit{Equation 36}$$

where a, n and m are fitting soil parameters, e is the Napier's constant, ψ is the soil suction and $C(\psi)$ is a correction factor which is equal to:

$$C(\psi) = \left[1 - \frac{ln(1 + \psi/\psi_r)}{ln(1 + 1000000/\psi_r)}\right]^m \qquad \textit{Equation 37}$$

ψ_r is the matric suction at the residual water content (θ_r).

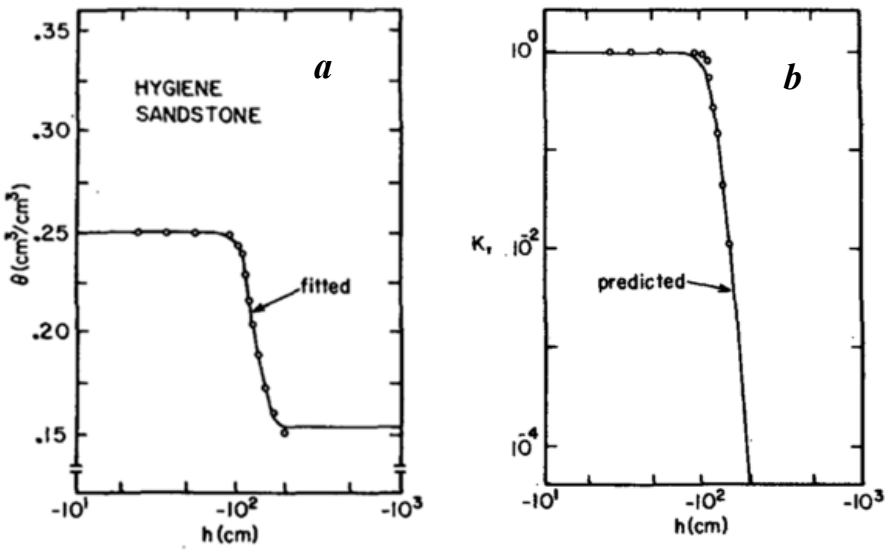

Figure 26 : A best-fit curve of van Genuchten Model to the experimental data of Hygiene Sandstone – (van Genuchten, 1980)

a) Soil water retention curve b) Unsaturated hydraulic conductivity

3 Inverse methods

3.1 Introduction

Inverse method is used to determine soil's retention and conductivity parameters simultaneously, and is widely used for ground water modelling. In this method, soil hydraulic parameters can be estimated by inverse modelling of transient inflow/outflow experiment. Inverse method can be defined as a mathematical approach to find unknown parameters based on their effects on specific observations (Hopmans et al. 2002). In soils, it can be described as an approach of finding soil hydraulic parameters based on soil suction and outflow/inflow measurements. Using inverse methods avoids many limitations of classic measurement methods, and allows finding both conductivity and retention curve parameters by a single experiment. This can decrease time and expense of measuring those parameters compare to direct methods (Durner et al. 1999).

Gardner (1956) applied inverse modelling method to Pressure Plate outflow experiment. He calculated the diffusivity of different suction intervals by measuring outflow of the sample as a function of time. Doering (1965, Cited by Hopmans et al. 2002) proposed a simplified method by applying Gardner's approach to one-step outflow experiment. This method was used and improved by several researchers like Kool et al. (1985), Kool et al. (1987), Parker et al. (1985), Hopmans et al. (2002) and Russo (1988). However, in one-step experiment outflow is highly sensitive to soil's condition. Due to the high water flux in this method, it has low applicability to the field conditions (van Dam et al. 1990). Toorman et al. (1992) have shown that one-step outflow method may not yield to a unique inverse solution. A multi-step outflow method was proposed by van Dam et al. (1994) to improve inverse modelling obtained results. Eching and Hopmans (1993) showed that by measuring soil pressure data and cumulative transient outflow data simultaneously, inverse modelling results will improve considerably. This pair of data is used to define the objective function to estimate soil hydraulic parameters.

3.2 Flow Theory and Optimization

As seen in Figure 27 (Hopmans et al. 2002), estimating soil hydraulic parameters using inverse modelling includes three different steps namely:

a) Controlled transient outflow experiment

b) Numerical solution; and

c) Nonlinear optimization

In transient outflow experiment, soil suction and cumulative outflow are measured simultaneously. A numerical flow model, that is based on Richards' equation (Equation 11) could be used to simulate transient flow regime. The final step includes an optimization algorithm that is used to estimate unknown parameters by minimizing the differences between the experimental and inverse modelling results. The multi-step outflow test is described in section 4.2.1. The flow simulation is then described in following section.

3.3 Water flow modelling

Richards' equation is the fundamental equation that can be used to describe flow in unsaturated materials. This equation can be written in three different forms. Equation 38 shows Richards' equation as θ-based form, where Equation 39 and Equation 40 show this equation as h-based form and mixed form, respectively (Celia et al. 1990):

$$\partial\theta/\partial t = \nabla.D(\theta)\nabla\theta + \partial K/\partial z \qquad \textit{Equation 38}$$

$$C(h)\,\partial h/\partial t = \nabla.K(h)\nabla h + \partial K/\partial z \qquad \textit{Equation 39}$$

$$\partial\theta/\partial t = \nabla.K(h)\nabla h + \partial K/\partial z \qquad \textit{Equation 40}$$

In these equations $D(\theta)$ is called unsaturated diffusivity and is equal to $[K(\theta) / C(\theta)]$, where $C(\theta)$ is called specific moisture content and is equal to $[d\theta / dh]$ and $K(h)$ is the unsaturated hydraulic conductivity. In these equations, z denotes the vertical dimension.

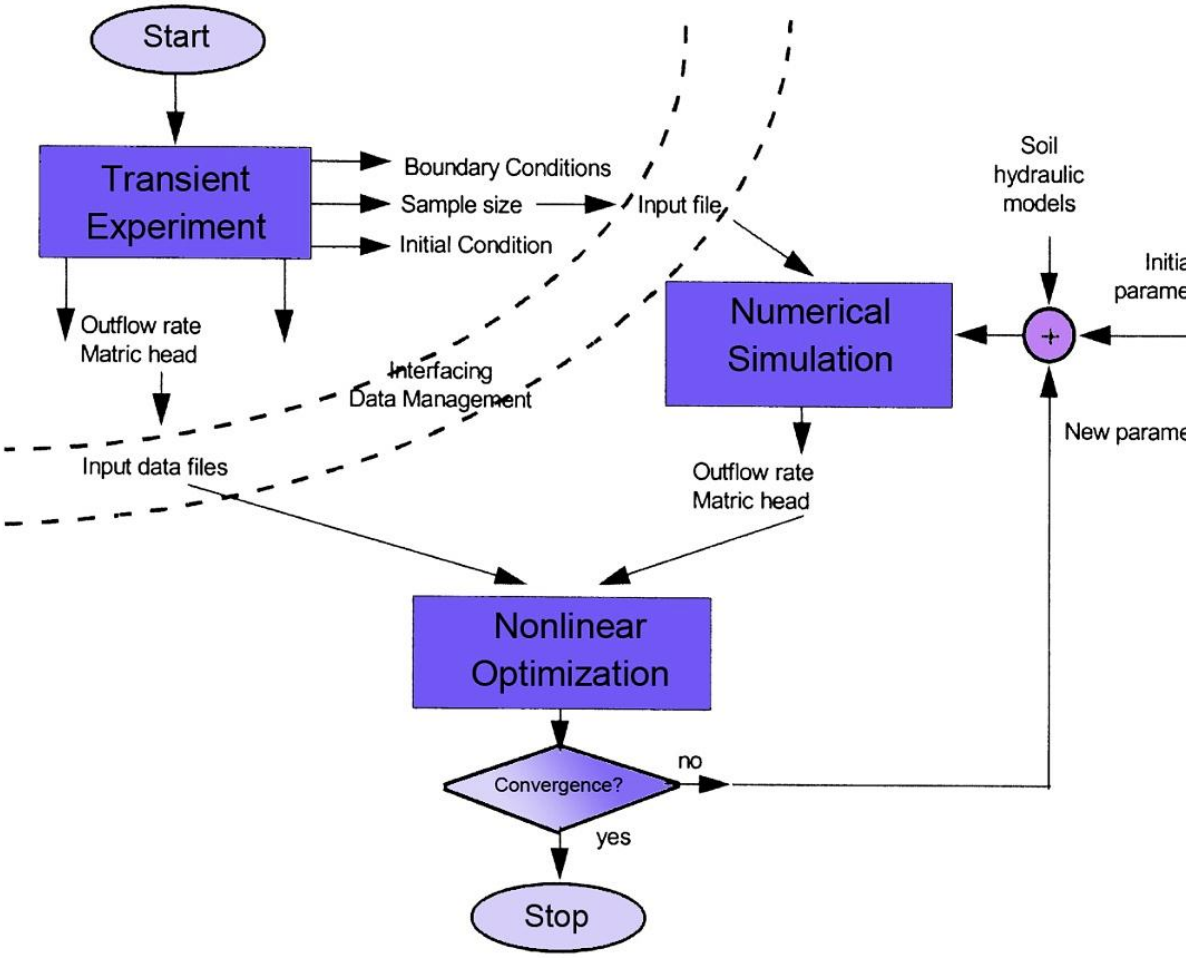

Figure 27: Flow chart of the inverse method illustrating the steps of inverse modelling (Reprinted from Hopmans et al. 2002)

To solve the Richards' equation numerically, generally the h-based form of Richards' equations is used. This form is normally written as:

$$\partial\theta/\partial t = \partial/\partial z\left[K(h)\left(\partial h/\partial z\right) + K(h)\right] \qquad \textit{Equation 41}$$

where θ is the volumetric water content, h is the soil water matric suction, $K(h)$ is the unsaturated hydraulic conductivity, z is a vertical coordinate and t is the time.

To solve this equation, it is necessary to solve the mass balance equation. Celia et al. (1990) proposed a simple mass conserving approximation to solve Richards' equation. They substituted $[C(h) * (\partial h \,/\, \partial t)]$ by $[\partial\theta \,/\, \partial t]$. This was a simple approximation based on the mixed form of Richards' equation . The new h-based form of Richard's equation will turn to Equation 42. This equation can be solved by easier procedures, where $C(h)$ denotes the moisture capacity function and is equal to $[d\theta \,/\, dh\,]$.

$$C(h)\,{}^{\partial h}/_{\partial t} = {}^{\partial}/_{\partial z}\left[K(h)\left(1 + \left({}^{\partial h}/_{\partial z}\right)\right)\right] \qquad \textit{Equation 42}$$

As it was discussed earlier, different expressions can be used to describe unsaturated hydraulic conductivity function or water retention. van Genuchten (1980) is one the expressions that can be used for this purpose:

$$S_e = [1 + |\alpha\psi|^n]^{-m} \qquad \textit{Equation 43}$$

$$S_e = \frac{\theta - \theta_r}{\theta_s - \theta_r}$$

where S_e is the effective saturation, α, n are fitting parameters and $m = 1 - 1/n$. ψ is the soil suction. θ_r and θ_s are the residual and saturated water contents, respectively. By applying van Genuchten (1980) SWRC parameters in Mualem (1976) hydraulic conductivity correlation, the unsaturated hydraulic conductivity will be:

$$K(\psi) = KS_e^l\left[1 - \left(1 - S_e^{\frac{1}{m}}\right)^m\right]^2 \qquad \textit{Equation 44}$$

where $K(\psi)$ is hydraulic conductivity for corresponding matric suction, and K is the soil saturated hydraulic conductivity, and l is the pore size interaction term.

3.4 Parameter optimization

An objective function *(Φ)* can be used to express the difference between experimental and modelling results. This function has to be minimized in order to determine the hydraulic parameters of the soils by using inverse modelling. Φ can be defined as (Hopmans et al. 2002):

$$\Phi(\beta, y) = \sum_{j=1}^{j=m_y} v_j \sum_{i=1}^{i=n_j} w_{i,j}\left[y_j^*(z,t_i) - y_j(z,t_i,\beta)\right]^2 \qquad \textit{Equation 45}$$

The right side of this equation represents the variation between measured and predicted space/time variables using the soil hydraulic parameters of the optimized parameter vector, β. These variables may include matric suction, and outflow values. y_j^* and y_j are measured and predicted variables, respectively. v_j and $w_{i,j}$ are weighting factors where *j* denotes the certain type of measurement. m_y is the number of different sets of measurements and n_j is the number of measurments in a particular sets of measurements. These measurements are at time, t_i, and at the specific location, z.

As it will be discussed later in section 6.1.2, during the inverse modelling, van Genuchten (1980) fitting parameters will be obtained by minimizing this objective function.

4 Materials and Experimental Procedure

4.1 Material

4.1.1 Origin and Characteristics of the Soil

The soil used in this study was granitic sand that was collected from Bédard quarry in Valcartier (Quebec). Multiple packs of this soil were dried, sieved and washed after it was collected. Energy Dispersive Spectroscopy (EDS) was used to microanalysis the soil sample. Figure 28 shows the EDS results of three particles of the tested soil. Results demonstrated that in the tested soil Silica is the main component. Presence of *Si, Al, Ca, Na, O* and *K* indicated that this soil might have different types of Feldspar.

This soil had a wide range of particle sizes. It was sieved and retained particles on each sieve was stored separately. Three samples with different particle size distribution were tested. The grain size distributions of these three samples are illustrated in Figure 29. Fillion (2008) measured the saturated hydraulic conductivities of these materials. Table 1 summarizes each sample's grain size characterization and Fillion (2008) measured *K* values.

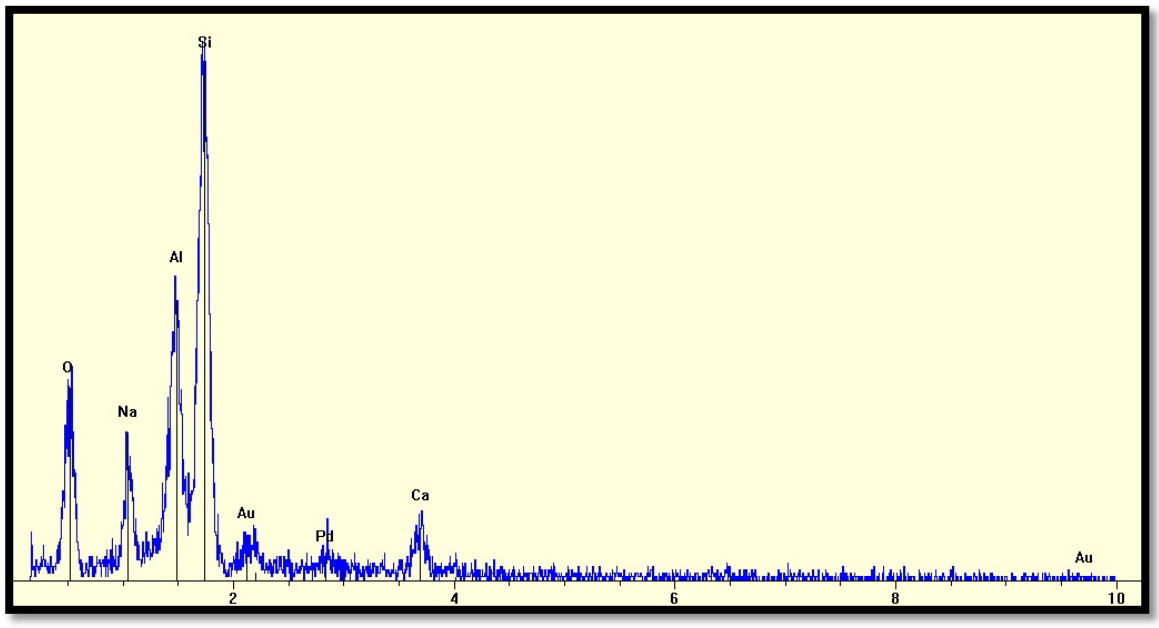

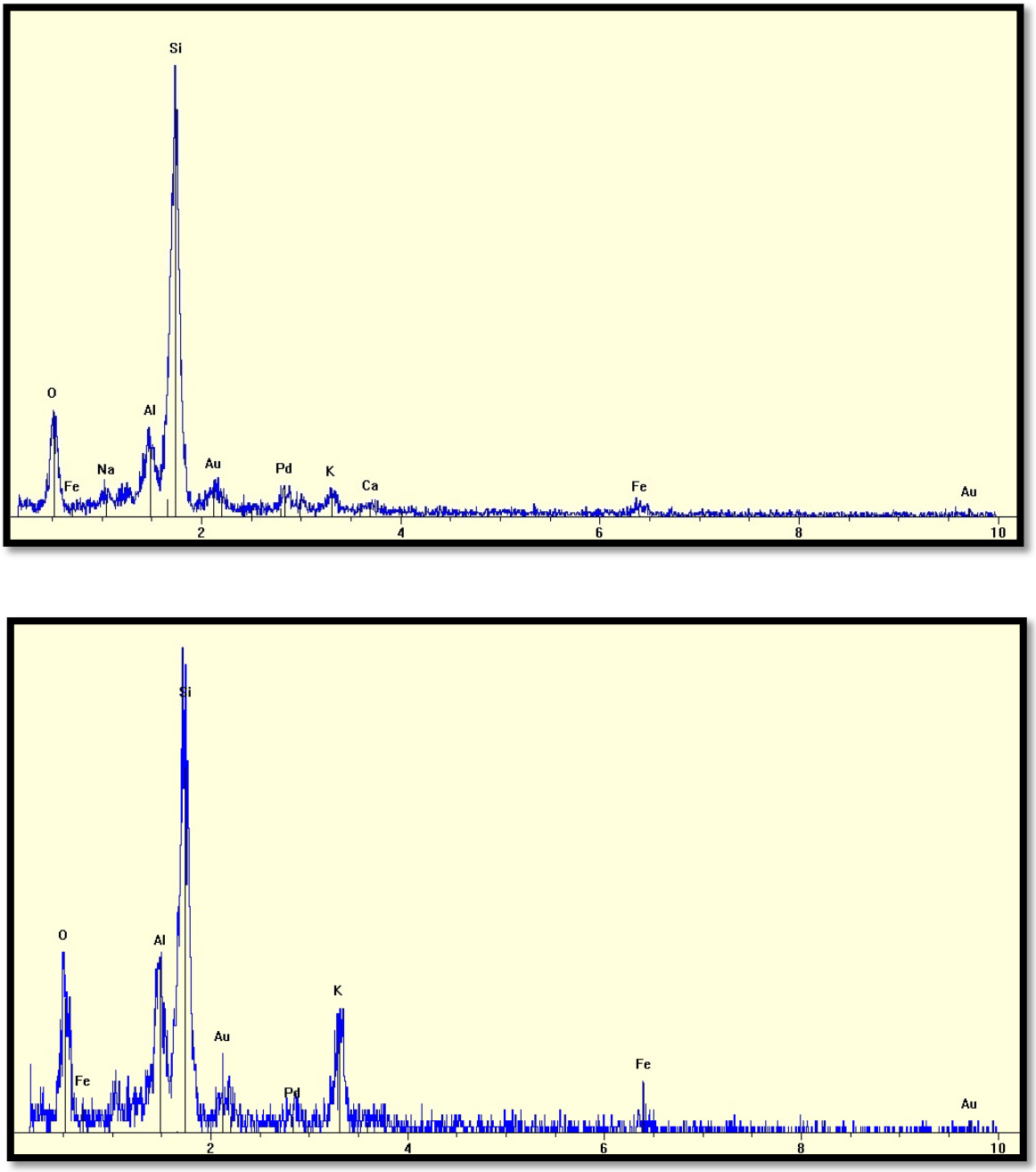

Figure 28: EDS results for three particles of the tested soil

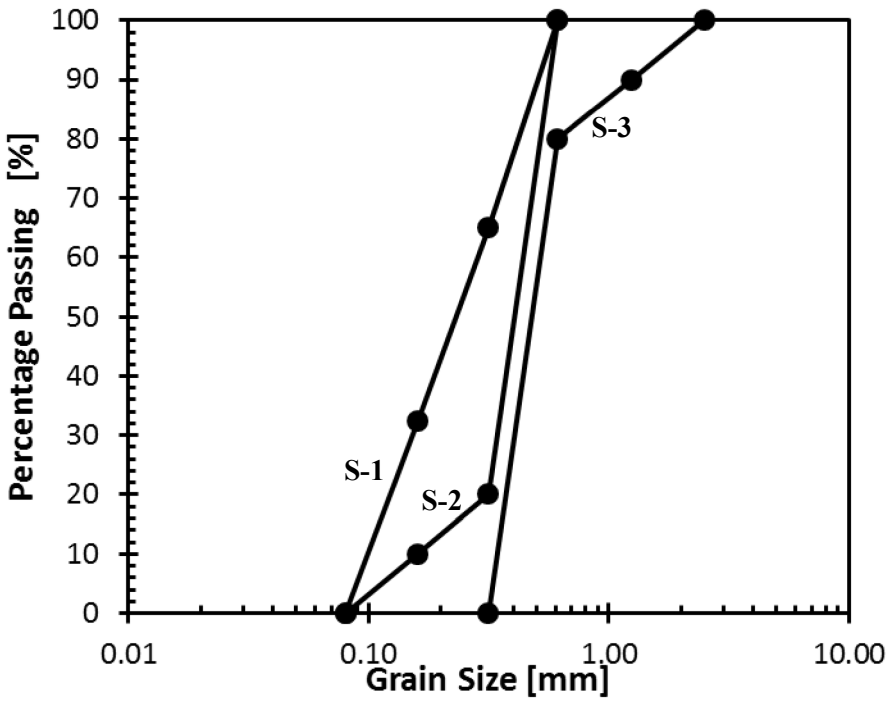

Figure 29: Soil samples grain size distribution

Table 1: Samples' grain size characteristics

Material	d_{10} *(mm)*	d_{30} *(mm)*	d_{60} *(mm)*	d_{50} *(mm)*	C_u	C_c	*K (cm/hr)* †
S-1	0.1	0.16	0.3	0.24	3	0.85	18
S-2	0.17	0.35	0.43	0.4	2.53	1.68	75.6
S-3	0.35	0.4	0.5	0.47	1.43	0.91	385.2

† Measured values from Fillion (2008)

Since soil is composed of different particles with different shapes and in different sizes, voids between these particles have irregular shapes. This irregularity plays an important role in water movement within soil material. A high-resolution camera was used to take detailed pictures of each soil specimen to analyse its particles macroscopic angularity and its surface shape. As is seen in Figure 30, particles are of different shapes and sizes.

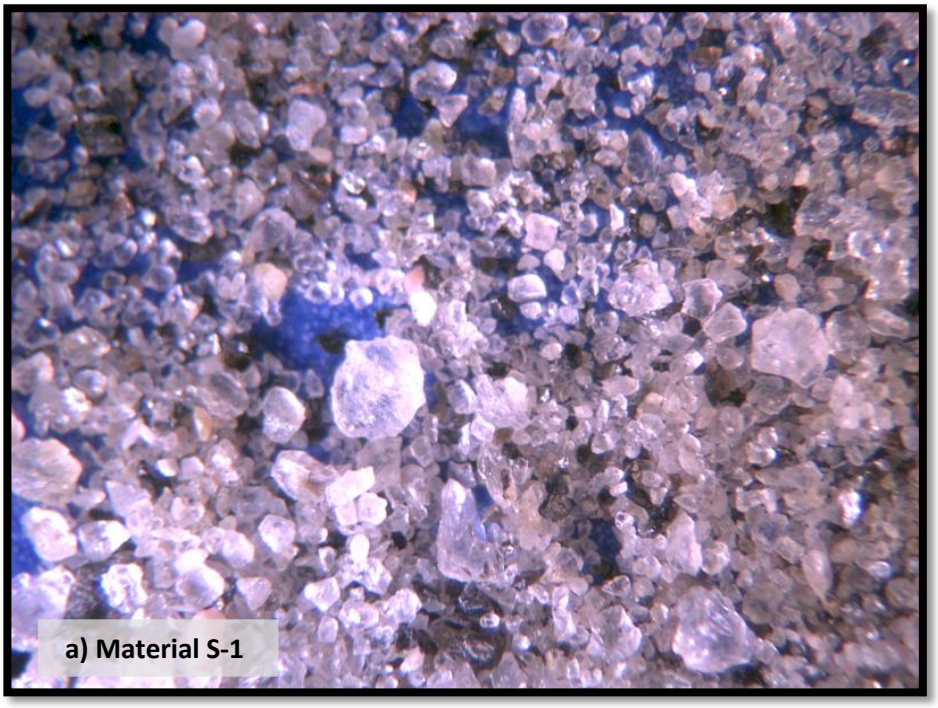

a) Material S-1

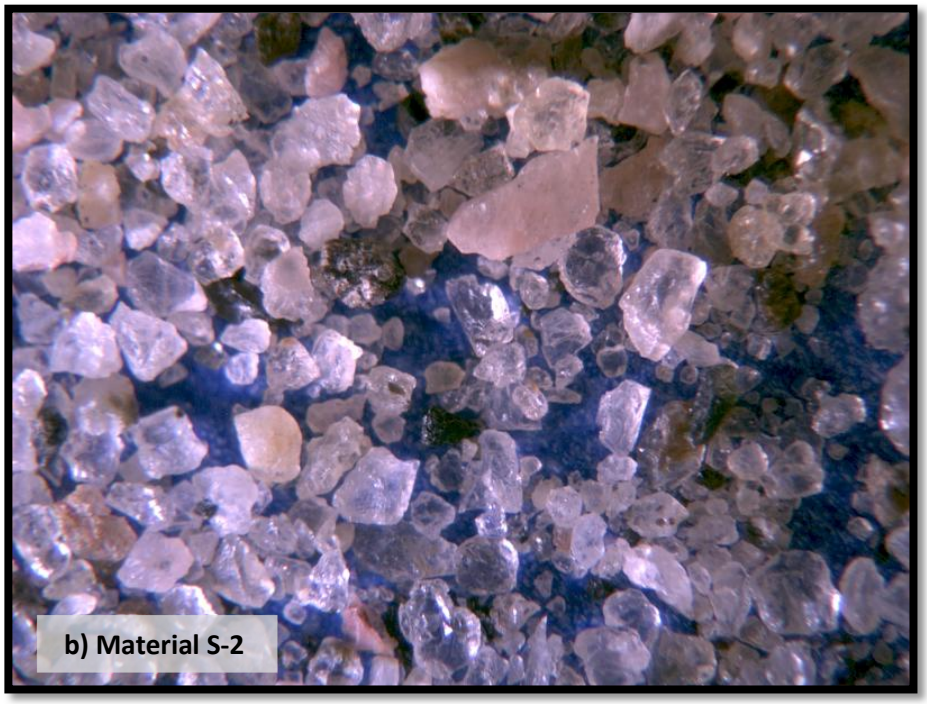

b) Material S-2

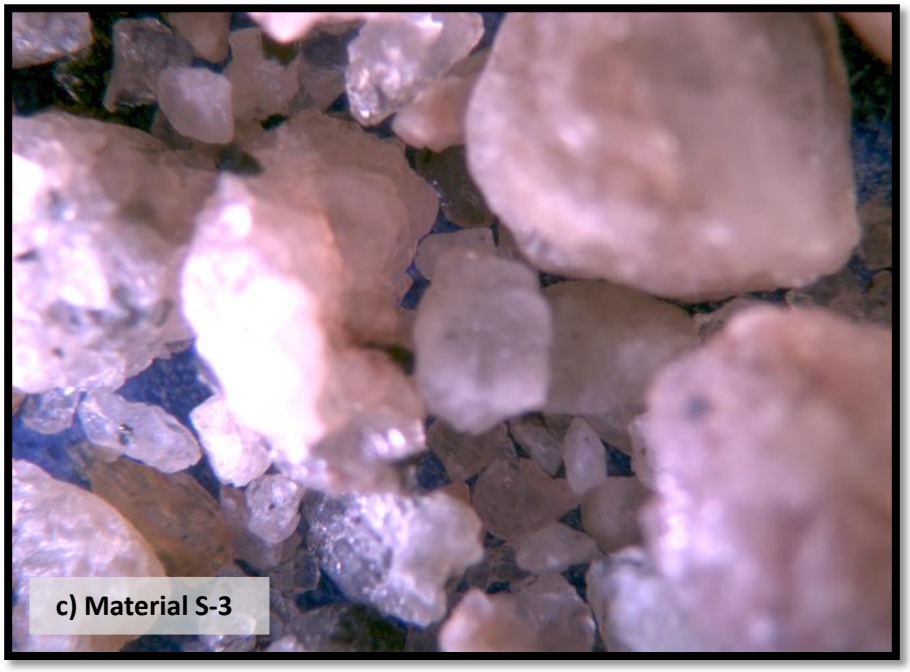

Figure 30: High-resolution pictures of tested soil samples

a) Material S-1 b) Material S-2 c) Material S-3

When soil suction reaches to its air-entry value, soil starts to desaturate. At certain suction, cavitation occurs is soil and liquid bridges forms between soil particles. At higher suctions, absorbed films of water will develop on soil particles. At high suction values, shape of the particles' surface will play a more important role in water movement. An electronic microscope was used to take microscopic photos of soil particles to better understand the reduction procedure in water flow (hydraulic conductivity) because of its particles' surface and shape. These photos are shown in Figure 31.

To perform each test for Valcartier Soil, different soil specimens were prepared with different soil particle distribution as is shown in Figure 29. Each sample was sieved after it was kept in an oven for 24 hours. Sieved soil was washed and dried again. Each specimen was prepared by mixing a specific amount of each particle size.

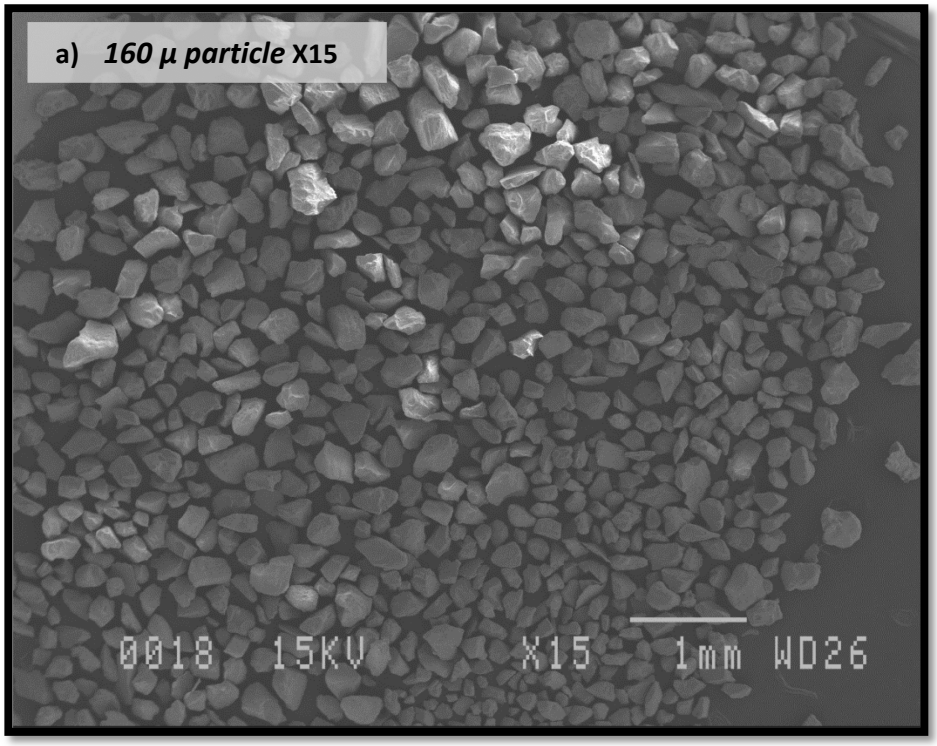
a) 160 µ particle X15
0018 15KV X15 1mm WD26

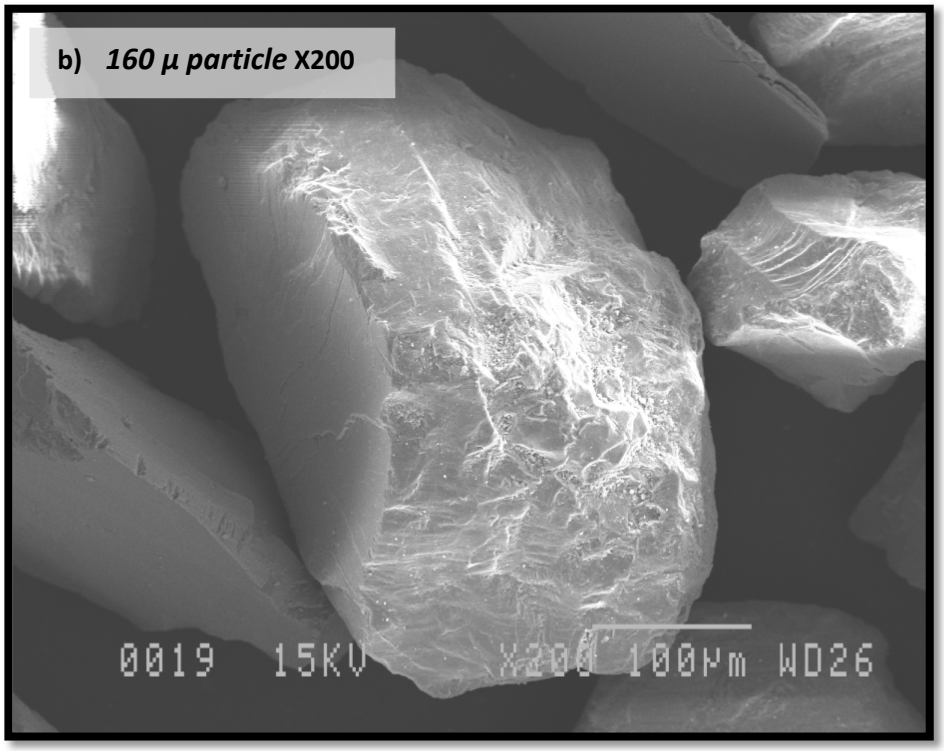
b) 160 µ particle X200
0019 15KV X200 100µm WD26

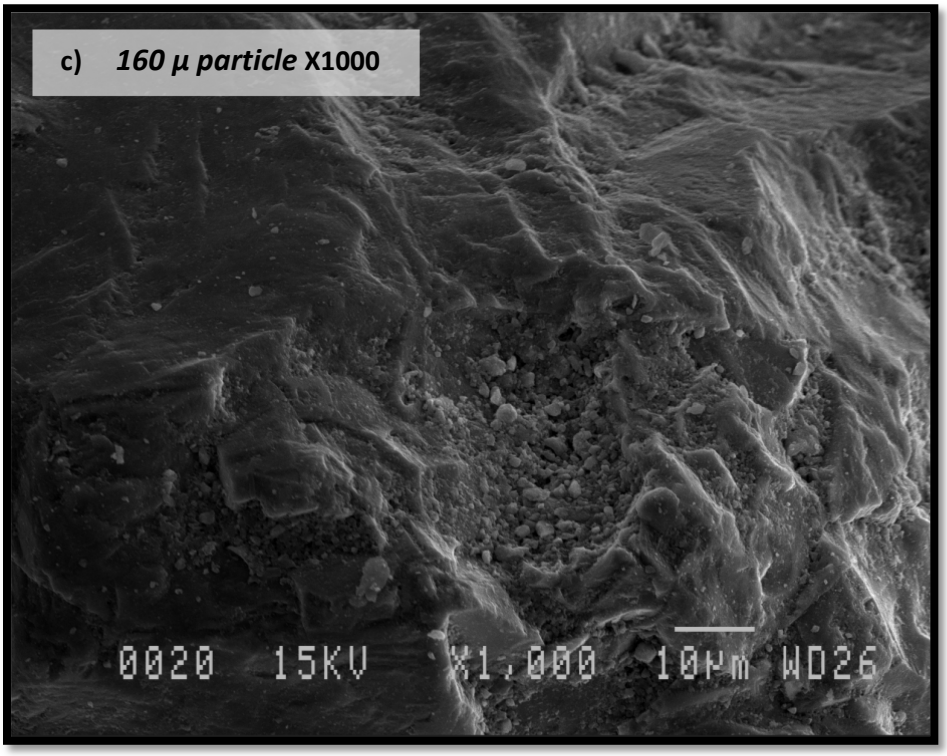

Figure 31: Electronic photo of a 160 µ particle

a) x15 b) x200 c) x1000

4.2 Experiment

4.2.1 Multi-step Outflow Experiment

Different types of outflow methods can be used to measure or estimate hydraulic properties of unsaturated soils. These methods in combination with numerical solutions can be used to estimate $K(h)$ and $\theta(h)$ simultaneously. These methods are generally flexible to boundary conditions (van Dam et al., 1990) and are cheaper compare to some other techniques of measuring or estimating hydraulic properties of unsaturated soils. Multi-step Outflow method (MSO) is one of the methods of determining soil water retention curve. Before using MSO, One-step Outflow method (OSO) was developed to study one-dimensional transient flow of water in porous media. Results of this test can be used to estimate SWRC and unsaturated hydraulic conductivity. Kool et al. (1985) were one of the first researchers who tried to used OSO method to determine hydraulic properties of unsaturated soils,

$K(h)$ and $\theta(h)$. They solved Richards' equation and optimized parameters of van Genuchten equation (Equation 26). They performed some tests on sandy loam and clay loam, and their results indicated that even for large pressure increments, the outflow data does not provide sufficient information to determine unique values for unknown van Genuchten parameters by using inverse modelling. By their studies about this method's sensitivity to errors, they showed that the measuring errors can cause considerable errors in the final results. van Dam et al. (1990) extended an error analysis on results of the OSO method compare to other methods. They showed that between θ_s and θ_r, only one of them can be estimated by the outflow experiment. They also analysed the effect of α, n, K_s and l. Their results showed that these parameters have their biggest influence when the experiment time is less than *4* hours. Due to their results, sensitivity has the lowest relativity to the K_s and l. Kool et al. (1985) used their results to find van Genuchten (1980) equation parameters. Performing OSO test is not representative for field condition. Testing soils in the one-step outflow method does not give a good sample of what really happen in field. By applying a high pressure in one step, a sudden flow of water can happen in soil which is not realistic.

van Dam et al. (1990) showed that simultaneous estimation of $\theta(h)$ and $K(h)$ based on results from outflow test after one pressure increase cannot be reliable due to inadequate information obtained from this test method. In OSO, a high flux is seen at the beginning of the test which is not realistic compare to the field situation. Pressure in soil sample is well distributed and pressure values near the bottom of the cell increases sharply.

To overcome these problems, a Multi-step outflow method (Eching & Hopmans 1993; van Dam et al. 1990) was developed. In this method, pressure is applied in multiple incremental steps and everything is measured in the same testing equipment.

The experimental process of the Multi-step outflow method (MSO) involves an almost saturated soil sample and a saturated porous plate. These materials are inserted in the experimental chamber. Cumulative outflow and soil water pressure head values are measured as a function of time. An instantaneous pneumatic pressure is applied to the top

of the sample (or suction at the bottom the porous plate). It is assumed that the flow in the soil sample follow Richards' equation for flow in one-dimensional porous media, (Equation 41). This testing method has a two-layer system. This includes the soil specimen and a porous plate.

4.2.2 Cell Design

To measure soil water content and soil suction in laboratory, an experimental cell was designed and manufactured in geotechnical laboratory of Laval University. The design of this cell was inspired from the Tempe Cell manufactured by Soilmoisture (Soilmoisture Equipment Corp.). This cell was made of Plexiglass. In order to measure soil suction within the soil specimen, two holes were made at *H2*=(H/4) and *H4*=(3H/4) where H is the height of the chamber (Figure 32). Two tensiometers (Figure 34) were installed in these holes to measure soil suction at *H2* and *H4*. Figure 33 shows different parts of the experimental cell. The internal diameter of the chamber was 8.5 *cm* and the height of the chamber was 6 *cm*.

A porous ceramic plate was used to create a barrier against the movement of the air at the bottom of the cell while allowing water to flow out of the sample. This plate was manufactured by "ROBU® Glasfilter-Geräte GmbH", and its specifications are summarized in Table 2.

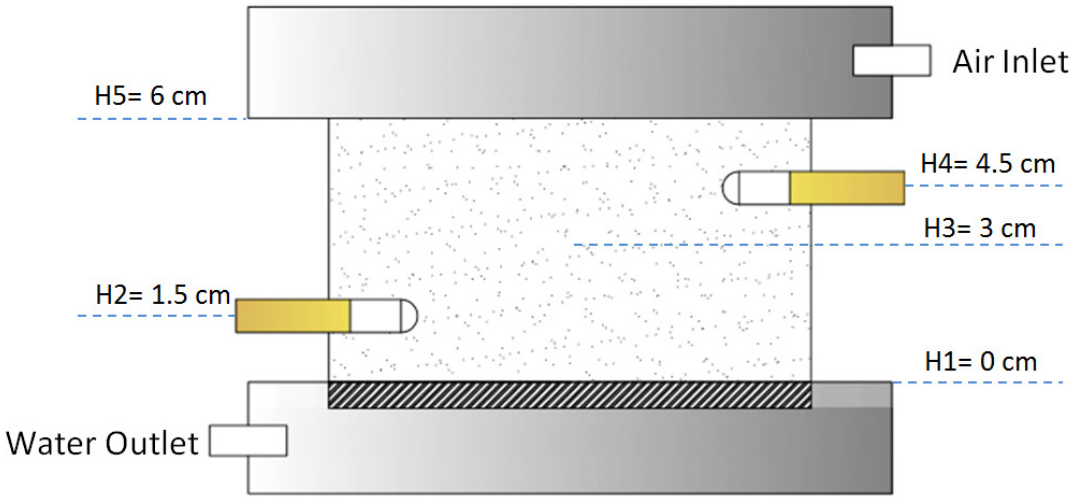

Figure 32: Sketch of the cell used in the scope of this study

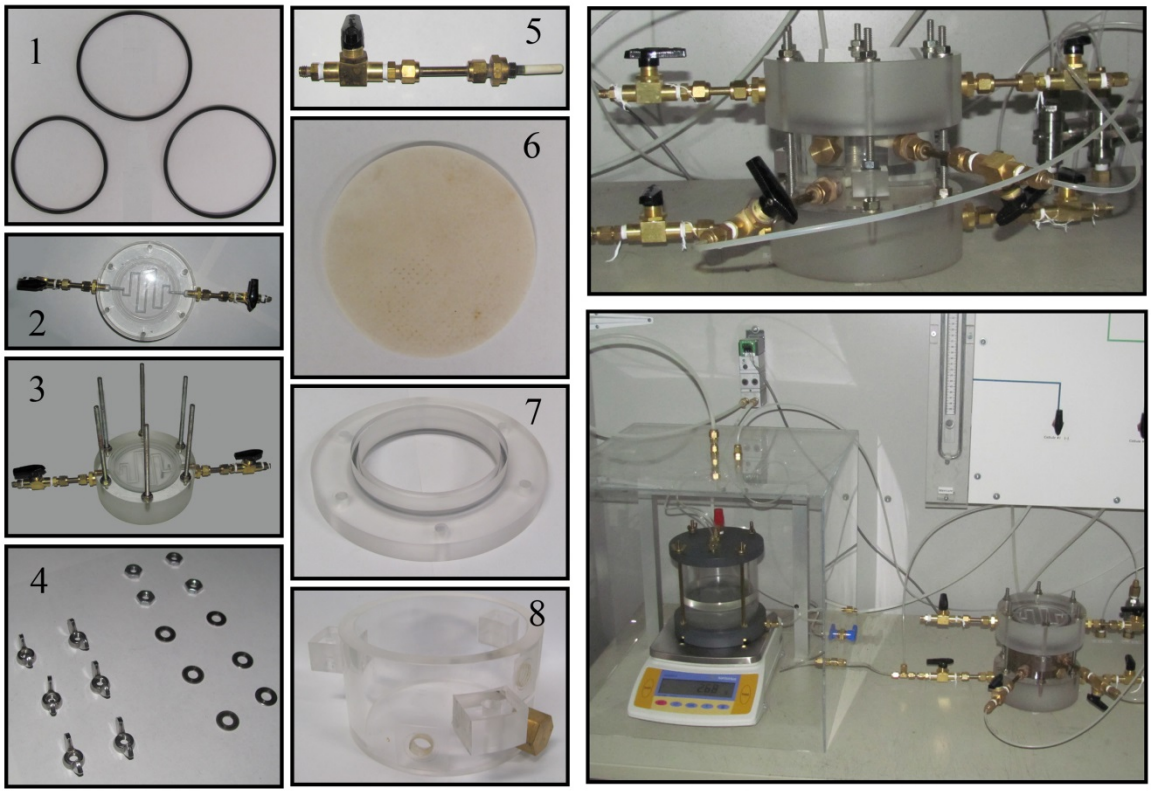

1. *Round Cross 'O' Ring*
2. *Top Plexiglass Cap*
3. *Bottom Plexiglass Cap*
4. *Wing nuts and Washers*
5. *Tensiometer*
6. *Porous Ceramic Plate*
7. *Extension (For Cylinder)*
8. *Plexiglass Cylinder*

Figure 33: Different parts of the developed cell in the scope of this study

Table 2: Hydraulic properties of the porous plate

	d [cm]	*K (cm/hr)*	*AEV [kPa]* †
Porous Plate	0.5	*2.8*	18

† Air-Entry Value

4.2.3 Tensiometers and Transducers

Tensiometers can be used to measure the soil suction. Different types of tensiometers were designed and used by different researchers. Two micro-tensiometers were used to measure the soil suction within the soil specimen. As it is illustrated in Figure 34, this type of tensiometers included a brass pipe with porous cup installed at its head. A valve was installed at the other side of the tensiometer. This valve was used to cut the connection of the tensiometer from the transducer. Transducers are instruments that can convert one form of energy to another. Transducers that were used in laboratory were pressure transducers (also called pressure sensors), and could convert pressure changes to electrical signal changes.

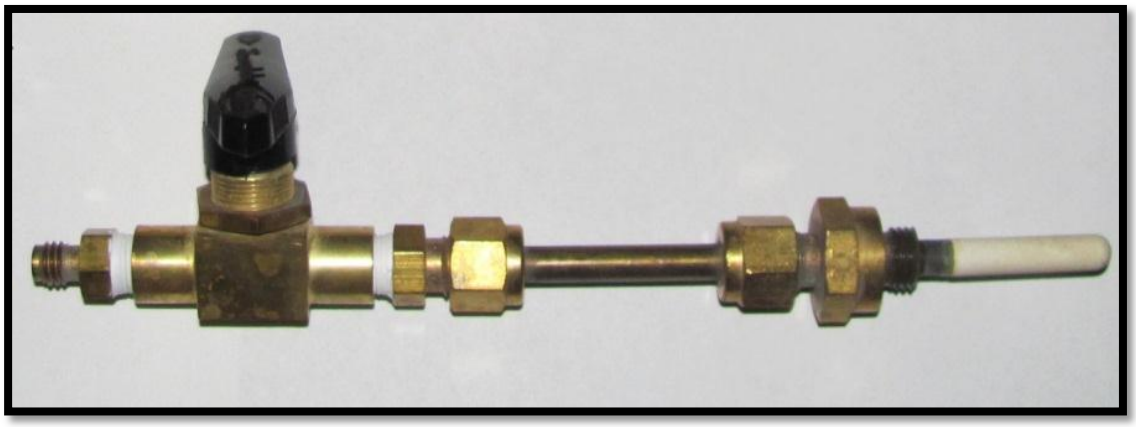

Figure 34: Tensiometer used in the scope of this research

4.2.4 Test Procedure

The design of the test setup to measure soil water retention data in laboratory was inspired from (ASTM-D6836-02, 2012). This test included a cylindrical container and an equipment to apply air pressure to the sample. The test procedure was controlled by DASYLab software (*DASYLab, 2000*) that was installed on a Personal Computer. The test procedure included:

1. Saturating the porous plate by using demineralized and deaerated water (Figure 35)

2. Filling the lower cap with demineralized and deaerated water and inserting o-ring in the cap

3. Inserting the porous plate in lower cap and inserting the cell chamber

4. Installing the collar to increase the height of the cell

5. Filling the cell with water and installing tensiometers

6. Filling the cell with prepared (saturated) soil

7. Shaking the specimen by using a vibrator (8 minutes)

8. Removing extra soil remained on the top of the chamber that hold the specimen

9. Putting the upper cap (with its O-ring) and fixing it with proper screws

10. Installing cell in the test setup (all connections has to be saturated with water except the air inlet tube):

    a) Saturating all the tubes with deaerated water

    b) Installing air inlet tube on top of the cell (upper cap)

    c) Connecting the controller of pressure changes and volume changes to its differential pressure sensors

    d) Connecting pressure and volume change controller to the lower cap

    e) Set the balance on zero

11. Measuring air volume in the air/water interface of the pressure and volume change controller (Figure 36) by using experimental calibration:

    a) Applying pressure in different steps and measuring the mass

    b) Measuring air volume by using equation (Lebeau & Konrad, 2006)

$$V_a = \frac{(\Delta M_{interface} - \Delta M_{\Delta V}^{interface})/\Delta P}{\Delta\rho_a/_{\Delta P}} \qquad \textit{Equation 46}$$

$$= \frac{(\Delta M_{interface} - \Delta M_{\Delta V}^{interface})/\Delta P}{M_m/_{R * (273.15 + T)}}$$

where V_a is the initial air volume, $\Delta M_{interface}$ is the mass change of the air/water interface and $\Delta M_{\Delta V}^{interface}$ is the mass change due to volume variations of the interface, ΔP is the pressure change and $\Delta\rho_a$ is the volumetric mass change of the air and M_m is the molar mass components due to dry air, *R* is the ideal gas constant and *T* is the temperature.

12. Starting the test:

    a) Entering temperature in DasyLab

    b) Closing all the valves before starting the test

    c) Applying the 100 *kPa* translation pressure

    d) Applying the first pressure step and opening the valves

    e) Applying next pressure step (repetitive to the last step)

    f) Closing the valve and removing 100 *kPa* translation pressure

    g) Opening tubes

    h) Measuring final water content of the specimen by using ASTM-D2216-10 (1963)

In DasyLab pressure values at *H1, H2* and *H4* were measured. Outflow of the sample was also measured and recorded every ten minutes during the test.

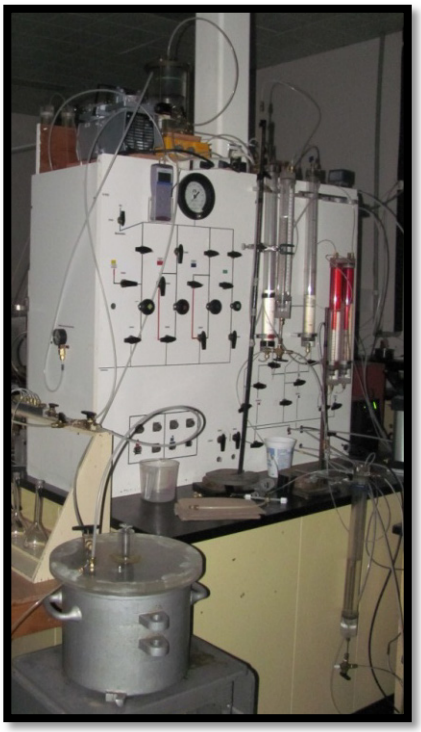

Figure 35: Apparatus that was used to saturate soil specimen and the porous plate

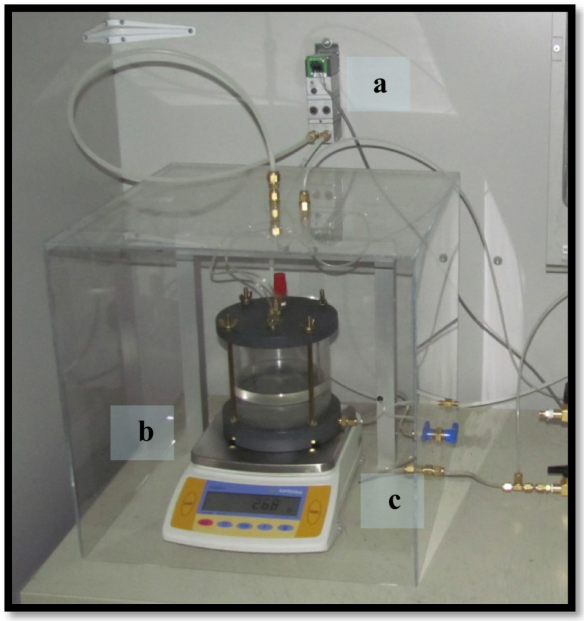

Figure 36: Pressure and volume change controller

a) Pressure transducer b) Air/water interface c) Balance

4.2.5 Setup and Specimen Preparation

Soil samples were prepared by combining different percentage of each particle size to achieve the proper particle size distribution.

Demineralized and deaerated water was used to saturate the soil specimen. A centrifugal suction machine was used to remove air bubbles from the demineralized water and make it deaerated. Soil was divided into six equal parts and was placed in six pycnometers. Deaerated water was added to the pycnometers to submerge the soil. Discussed apparatus is shown in Figure 37. All pycnometers were connected to the centrifugal suction instrument that could generate a negative pressure. Due to this suction, air bubbles tends to move out of the water in the soil. Based on the particle size distribution of each sample, it could take from *2* to *8* days to saturate the soil sample. Pycnometers were slightly shaken to ease the release of entrapped air bubbles presented between the soil particles. After saturating the soil sample, the pycnometers were fully filled with deaerated and demineralized water. To prevent entering air bubbles into the specimen during the transfer of the soil to the experimental cell, the opening of the pycnometer was put in the cell which was already full of deaerated water. By applying this method, soil particles in the pycnometer were replaced with water without entering any air bubbles. During the process, soil in the cell was mixed continually to have a homogenous mixture. Finally, the upper cap was placed and tightened by using six wing nuts.

5 Experimental Results and Discussion

5.1 Introduction

In order to characterize filter materials rock fill dams, several tests were done in laboratory in the scope of this study. Several soil samples and different methods were used to find the best procedure to obtain SWRC. Three different samples were tested during the experimental procedure. These samples were called *S-1*, *S-2* and *S-3* (Figure 29) with porosities of 0.34, 0.35 and 0.35, respectively. The following sections presents the experimental results.

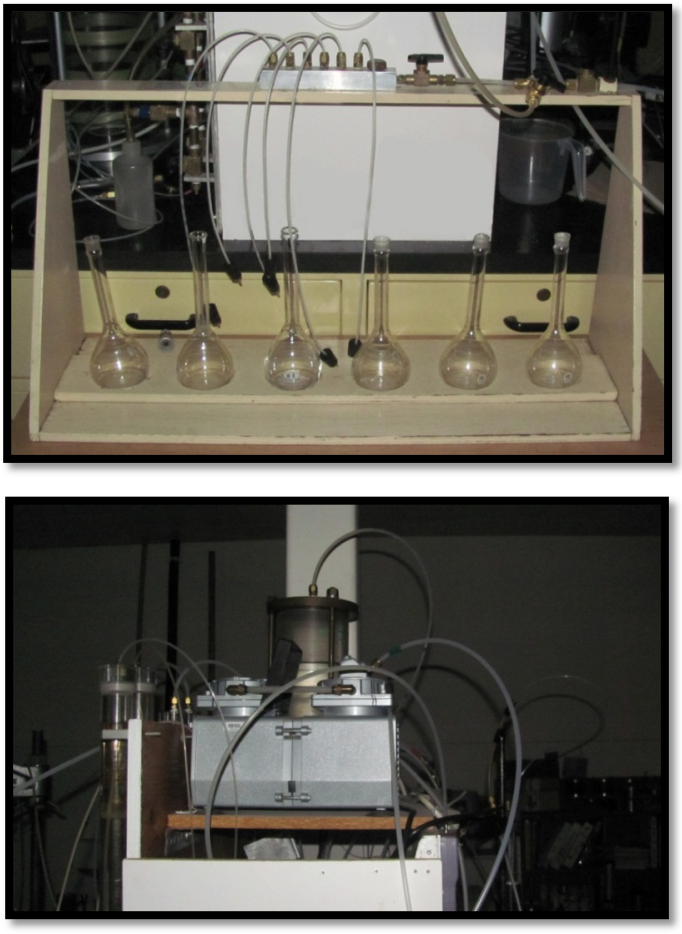

Figure 37: Apparatus that was used to saturate the soil specimens

5.2 Water Retention Curve

Laboratory tests were performed to determine water retention curve of all three samples. These tests were performed by using the cylindrical cell that was already described in the section 4.2.2. By using transient flow test, outflow rate and the suction at the bottom of the cell was measured and recorded. The final soil water content was also measured at the end of the test. These data were used to illustrate the soil water retention curve for each tested material. Soil volumetric water content for each step was calculated by using the measured outflow at the end of each pressure step and the final volumetric water content. These values represent the average water content for soil sample at each step. Measured suction at *H1* (Figure 38) represents the soil suction at the bottom of the cell. To relate the average water content to the average soil suction, soil suction at the middle of the cell was assumed as of Yang et al. (2004) and Lebeau and Konrad (2006). They assumed that the soil suction at each elevation of the soil profile above the bottom of the cell is the sum of the soil suction of the bottom of the cell hydrostatic pore-water pressure at that elevation. This assumption is based on negative pore-water pressure at elevations higher than the bottom of the cell. As it is seen in Figure 38 the soil suction in the middle of the cell is the sum of the soil suction of the bottom of the cell and the hydrostatic pore-water pressure at *H3*.

Figure 39, Figure 40 and Figure 41 show the cumulative outflow values and soil suctions of the middle of each soil sample profile versus time. The tests were started from an initially saturated soil state. Pressure was increased in several steps and as it is seen in these figures, by applying a new pressure step, outflow were monitored to reach steady state. In each step, the speed of the outflow is higher immediately after the new pressure is applied and it tails of slowly. In higher matric suctions, this process takes a longer time and the steady state is reached after a longer period. There are two markers on Figure 39. These markers are reflecting the marker point in Figure 45.

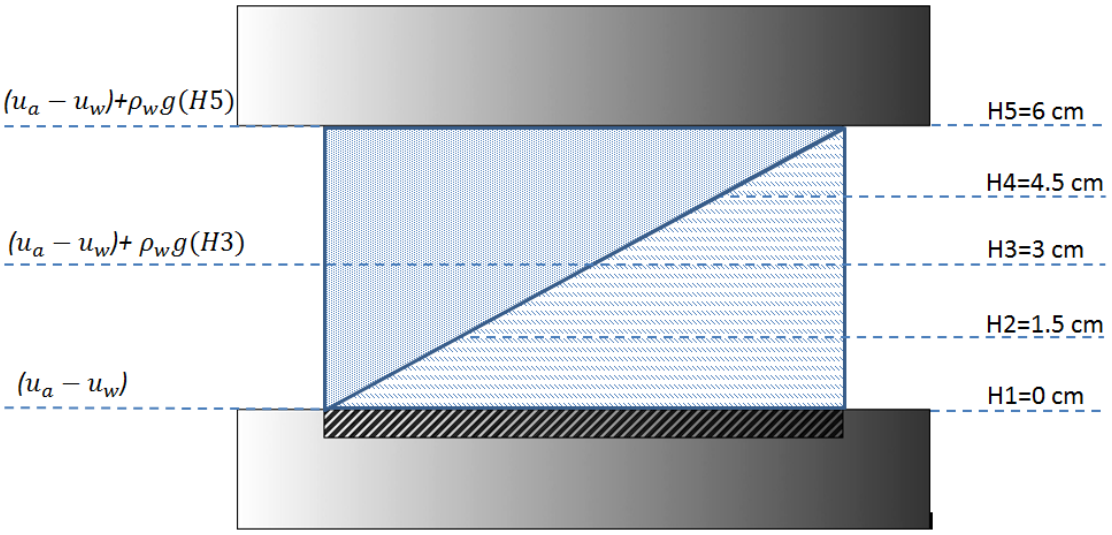

Figure 38: Schematic view of the soil suction in different elevations of the soil profile

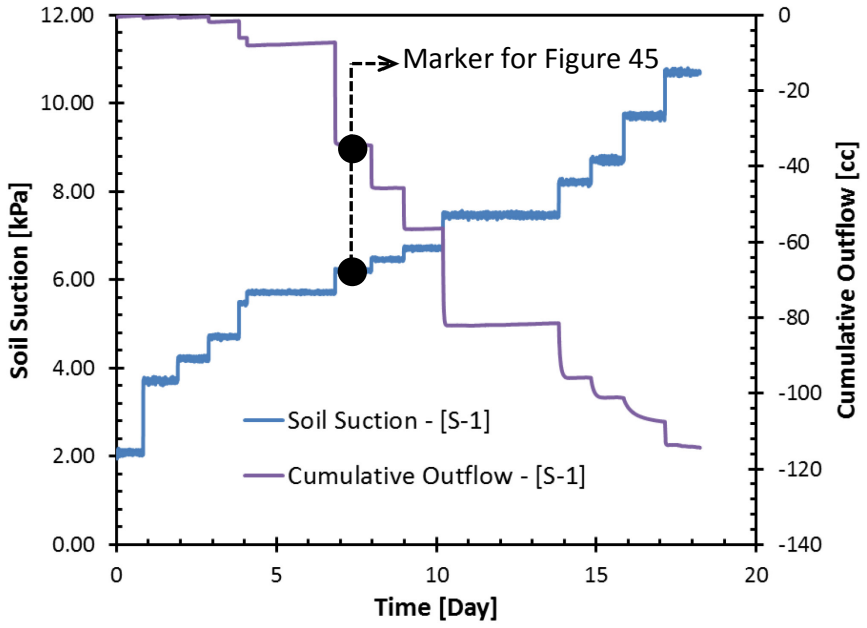

Figure 39: Cumulative outflow and soil suction curves obtained by laboratory results, [S-1]

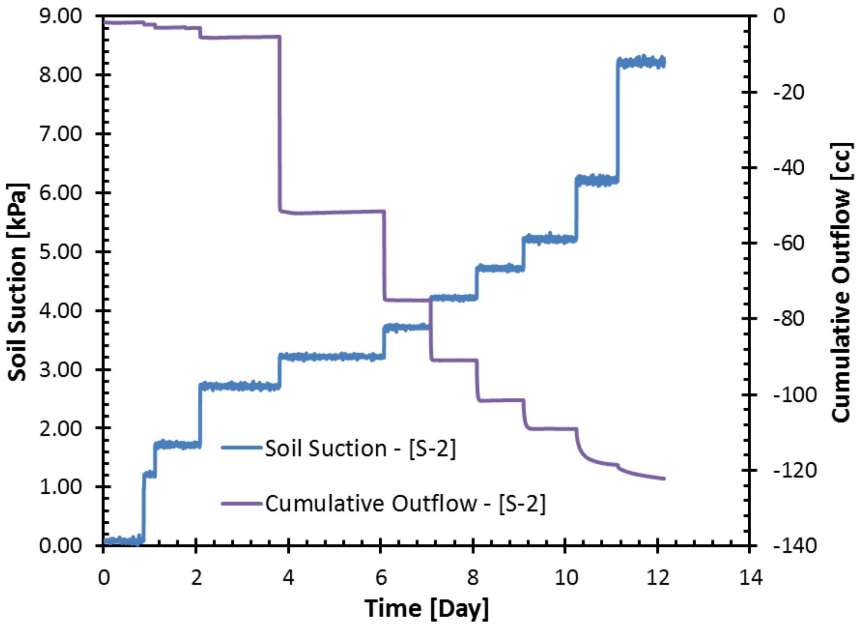

Figure 40: Cumulative outflow and soil suction curves obtained by laboratory results, [S-2]

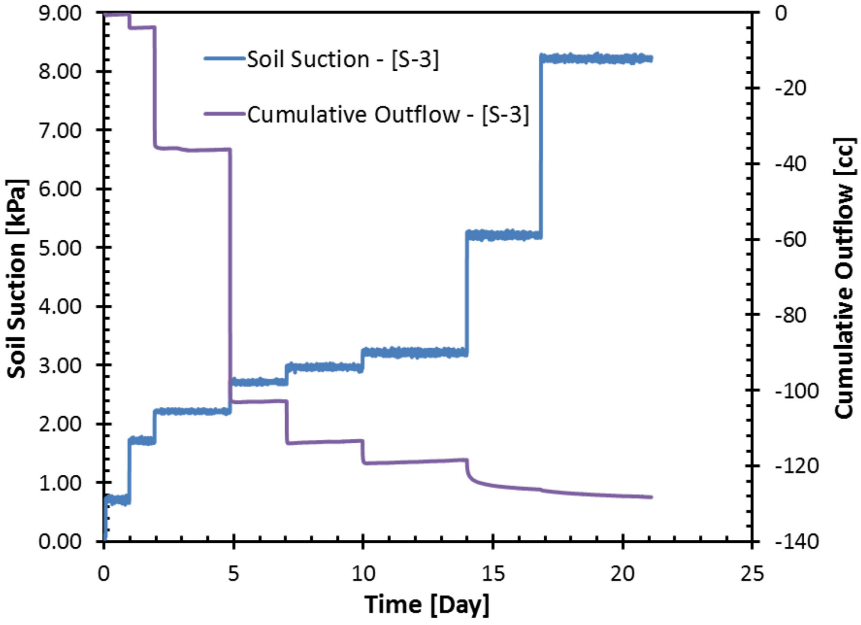

Figure 41: Cumulative outflow and soil suction curves obtained by laboratory results, [S-3]

Suction values were measured and recorded at three different depths during each test. Two tensiometers were installed at *H2* (*1.5 cm* above the bottom of the soil sample) and *H4* (*4.5 cm* above the bottom of the soil sample) on the cell chamber. The suction at the bottom of the cell were also recorded. Obtained values are plotted in Figure 42, Figure 43 and Figure 44. As it is seen, suction increases at higher elevations. Right figures are magnified portions of the left plots. Based on the recorded suctions and cumulative outflow and by using the final volumetric water content of each specimen, the water content curve were plotted for each sample.

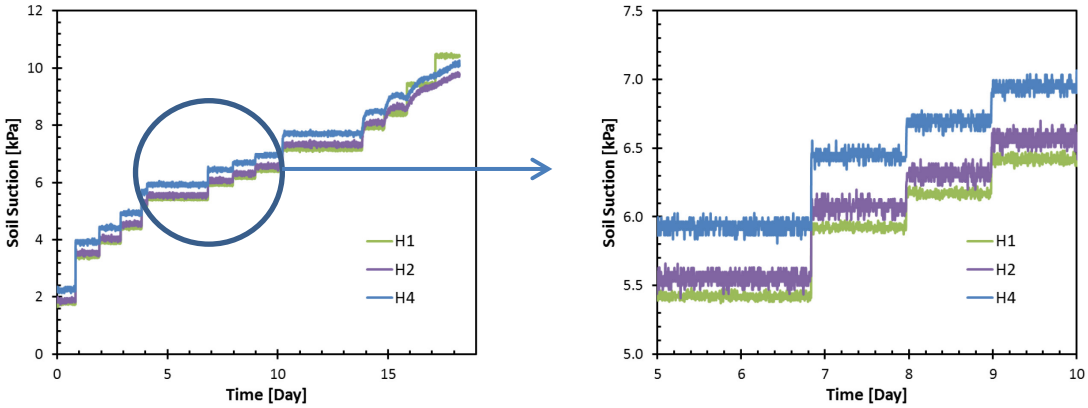

Figure 42: Measured suctions at three different levels in the soil profile, [S-1]

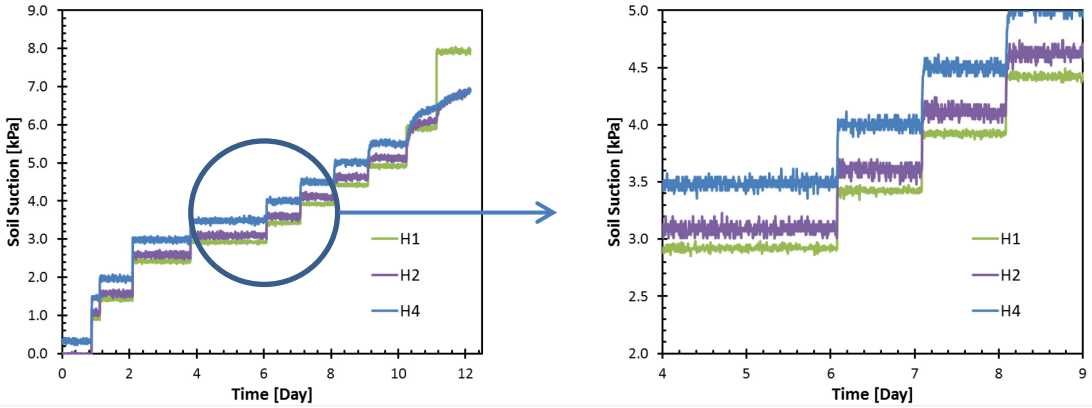

Figure 43: Measured suctions at three different levels in the soil profile, [S-2]

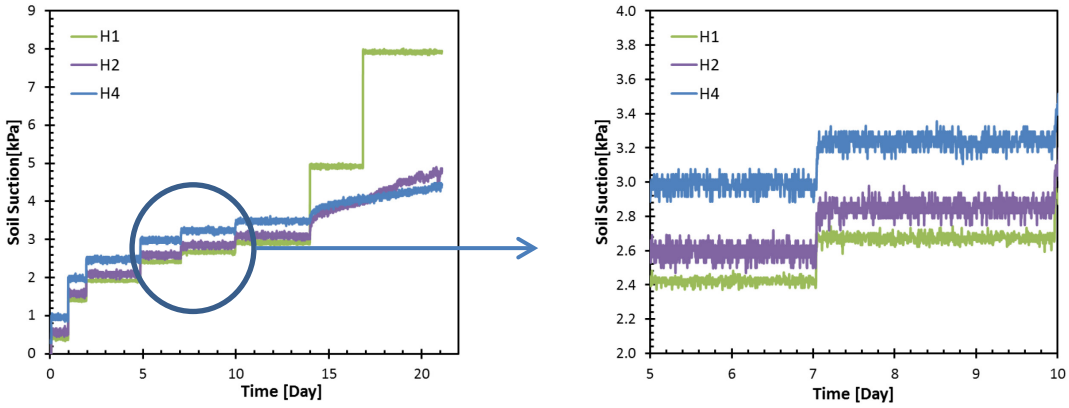

Figure 44: Measured suctions at three different levels in the soil profile, [S-3]

Recorded outflow and the suctions were used to determine SWRC. van Genuchten (1980) and Fredlund and Xing (1994) models were used to fit measured data. Evolutionary solving method in "*Microsoft Excel*" was used to fit the data. This method uses mechanisms that are based on biological evolution and are capable of finding a better solutions compare to local optimization. Table 3 and Table 4 summarize van Genuchten model and Fredlund & Xing model fitted parameters, respectively. These fitting parameters were used to illustrate the full curve for obtained laboratory results. These curves are shown in Figure 45, Figure 46 and Figure 47 for *S-1, S-2* and *S-3* materials, respectively. In these figures horizontal and vertical axis show the measured suction at the middle of the cell and the cell's average water content, respectively. Figure 45 illustrates the results of the *S-1* material. Laboratory results are shown with dots and are calculated by using measured soil suction and cumulative outflow in the transient Multi-step experiment. In this figure, the line shows the obtained curve using the van Genuchten model. After fitting laboratory results to this model, best fitting parameters were obtained and used to illustrate the full curve for the whole range of soil suction values. Dashed line shows the best fitting curve for Fredlund & Xing model. The procedure to obtain Fredlund & Xing model results was the same as van Genuchten model. As it is seen, each curve has two inflection points and is composed of three different parts. First part starts from saturated volumetric water content (θ_s), which is the water content of the sample when suction is equal to zero. This part represents the volumetric water content of the sample before it reaches to its first inflection point, which is

called air-entry value (*AEV*). After reaching *AEV*, the soil water retention curve has a sharp decrease in water content until its second inflection point that is called residual water content (θ_r). After this point water content has a gentle slope and tends to zero water content. As it was mentioned earlier in this chapter, the marker point in Figure 45 reflects the soil suction and cumulative outflow values that are marked in Figure 39.

Table 3: Inverse modelling initial and optimized values for van Genuchten model

	Fitted van Genuchten parameters		
	S-1	S-2	S-3
θ_s	0.387	0.405	0.397
θ_r	6.77E-02	6.43E-02	2.74E-02
α	1.48E-02	2.90E-02	4.10E-02
n	11.85	7.39	12.77
m †	0.92	0.86	0.92

† m=1-1/n

Table 4: Inverse modelling initial and optimized values for Fredlund & Xing model

	Fitted Fredlund & Xing parameters		
	S-1	S-2	S-3
θ_s	0.386	0.406	0.403
a	6.13	2.99	2.19
n	15.94	12.40	18.98
m	0.86	0.78	0.93

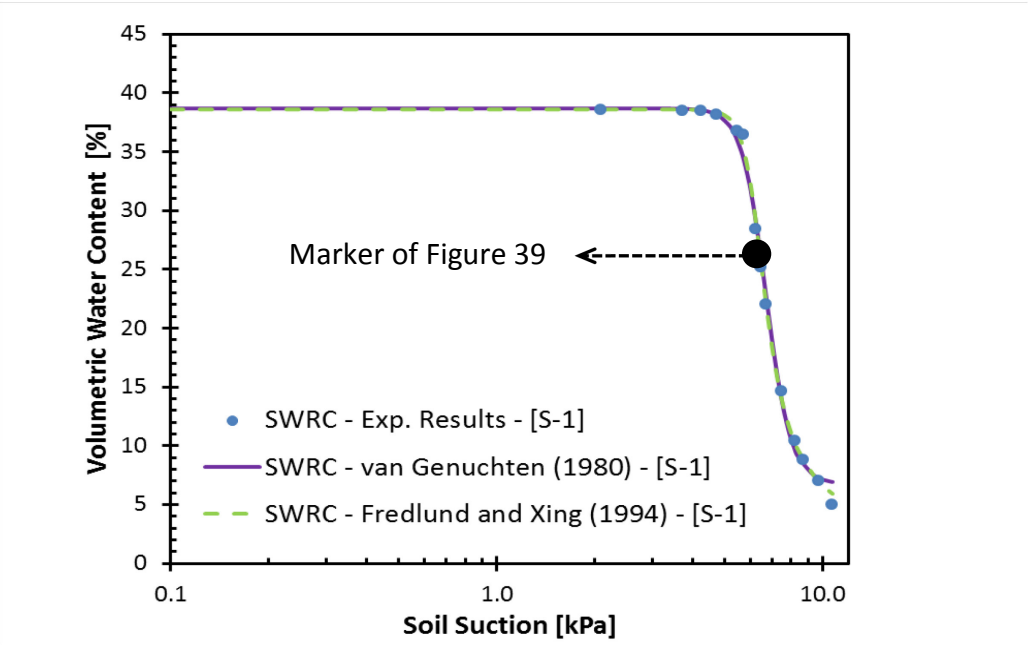

Figure 45: Soil water retention curve, experimental results, van Genuchten (1980) and Fredlund & Xing (1994) models fitted to measured data, [S-1]

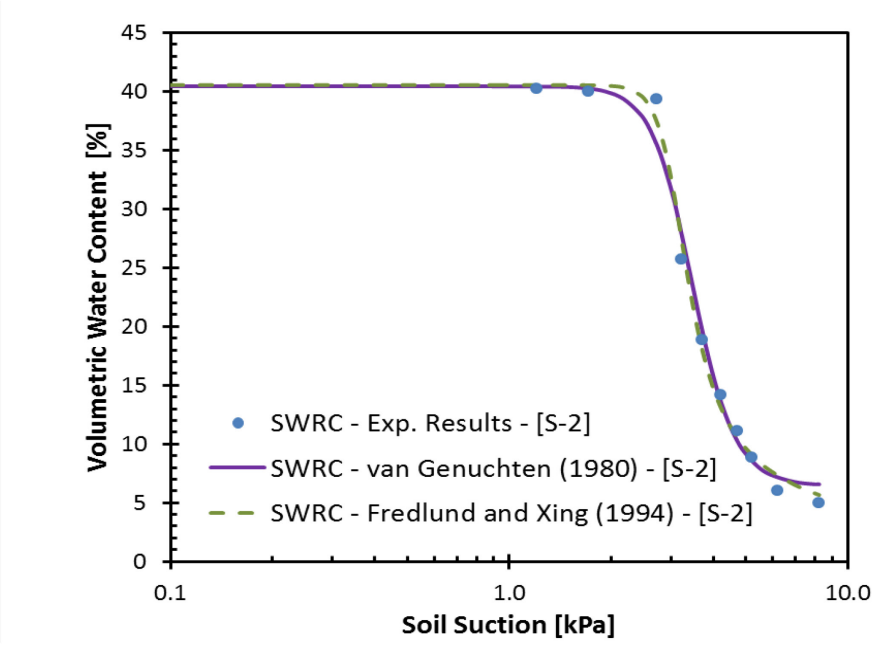

Figure 46: Soil water retention curve, experimental results, van Genuchten (1980) and Fredlund & Xing (1994) models fitted to measured data, [S-2]

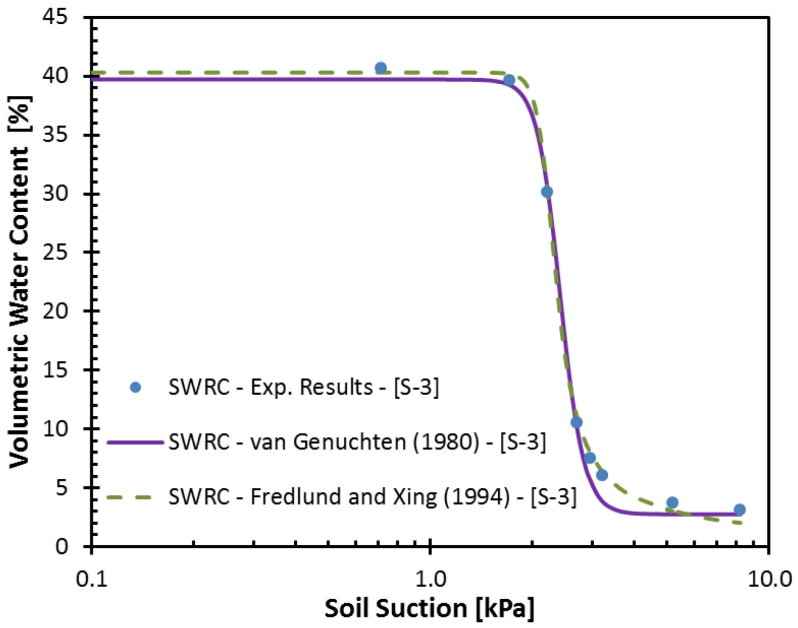

Figure 47: Soil water retention curve, experimental results, van Genuchten (1980) and Fredlund & Xing (1994) models fitted to measured data, [S-3]

To study the effect of d_{10} and coefficient of uniformity, *Cu,* on soil water retention behaviours, soil water retention curve of each material and their grain size distribution is plotted in Figure 48. Soil suction values for each soil, when volumetric water content is equal to 20 is marked on Figure 48-a. In Figure 48-b grain size distribution of each material is given with its coefficient of uniformity. It was seen that samples with lower d_{10} and higher *"Cu"* reach to the same volumetric water content at higher soil suctions.

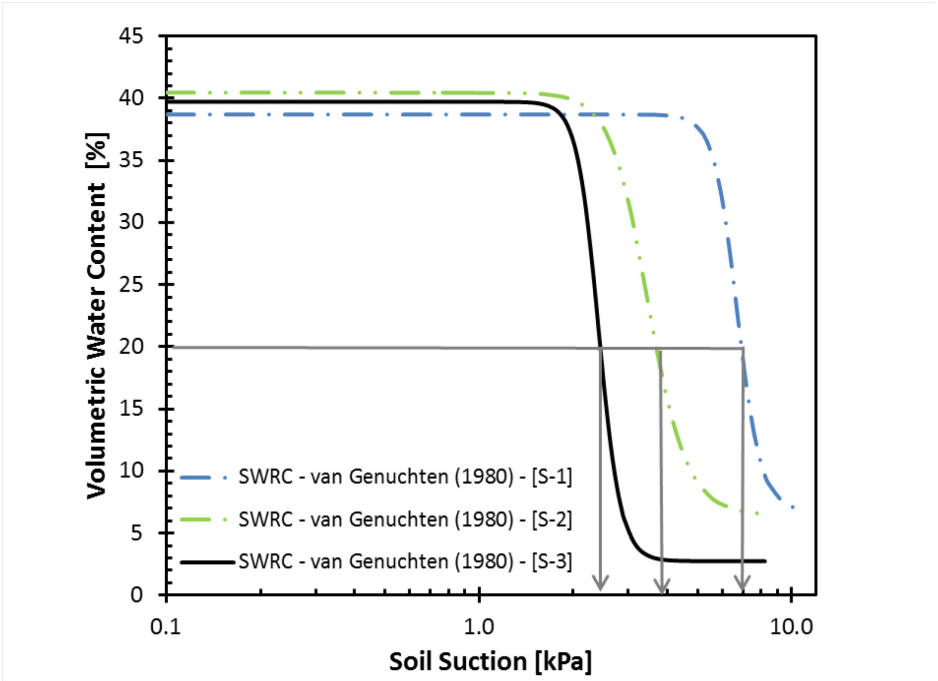

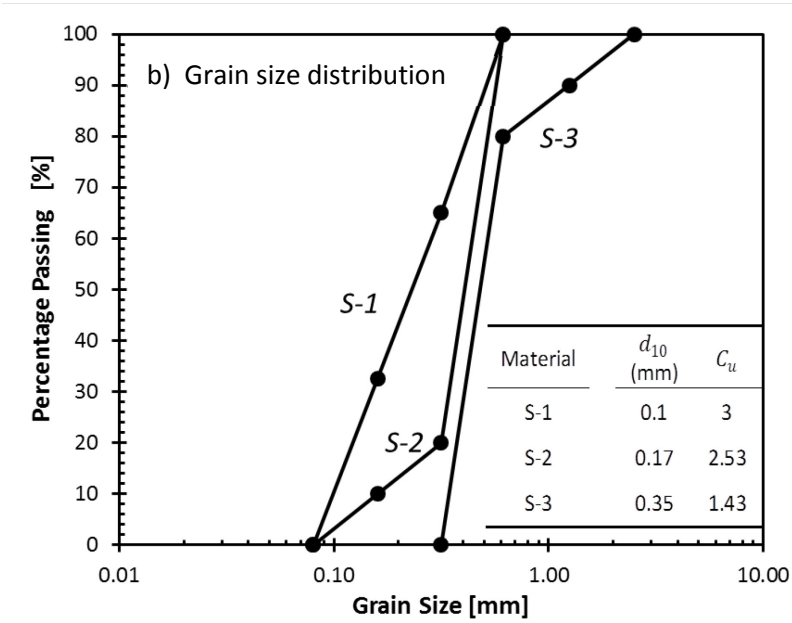

Figure 48: Effect of grain size distribution and coefficient of uniformity on soil water retention results of the soil samples

a) Fitted SWRC for S-1, S-2 and S-3 b) Grain size distribution for each sample

6 Hydraulic Conductivity of Unsaturated Sands and Discussion

Determining the unsaturated hydraulic conductivity is not an easy process. This can be done by laboratory tests or some numerical methods. Laboratory tests are not the best options to measure unsaturated hydraulic conductivity. They are difficult to perform, expensive and time consuming. Different methods have been developed to overcome these problems. As it was discussed earlier, some models have been introduced to determine unsaturated hydraulic conductivity. Numerical solutions can also be used for this purpose. Inverse modelling is a method that can be used to find unsaturated hydraulic conductivity by solving the flow equation and using some measured parameters. Measured soil water retention data (e.g. matric suction and outflow values) can be used to perform inverse modelling.

In this study, Fredlund et al. (1994) and van Genuchten (1980) methods were used to determine unsaturated hydraulic conductivity. SVFlux (*SVOffice 2009*), which is a seepage analysis program was used to find relative unsaturated hydraulic conductivity of each material based on its soil water content. Inverse modelling was another approach that was used to determine unsaturated hydraulic conductivity for tested soil samples. *HYDRUS-1D* is the software that was used to solve Richards' equation for each soil sample.

6.1.1 Estimated "*K*" Function using "van Genuchten (1980)" and "Fredlund et al. (1994)" Models

Relative unsaturated hydraulic conductivity was predicted by using van Genuchten (1980) and Fredlund et al. (1994) models which were already explained in sections 2.2.2.2.2 and 2.2.2.2.3. To use these models, SWRC data was provided by laboratory results. Obtained results are illustrated in Figure 49, Figure 50 and Figure 51 for *S-1*, *S-2* and *S-3* materials, respectively. In these figures horizontal and vertical axis represent soils suction and relative hydraulic conductivity, respectively. As it is seen in these figures, obtained results for van Genuchten (1980) model is lower than the obtained results for Fredlund et al. (1994) model. At higher suctions, where relative hydraulic conductivity tends to zero, this difference become smaller.

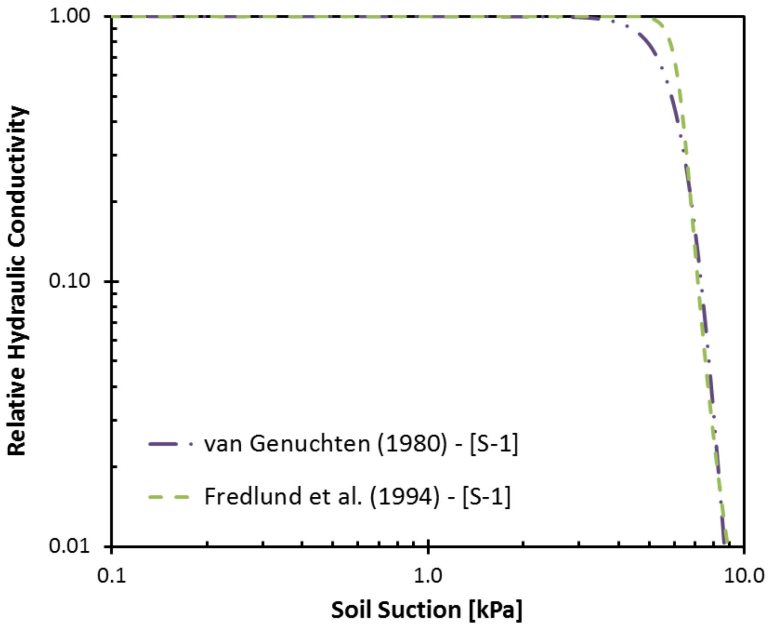

Figure 49: Comparison between predicted relative unsaturated hydraulic conductivities (Fredlund el al. and van Genuchten models), [S-1]

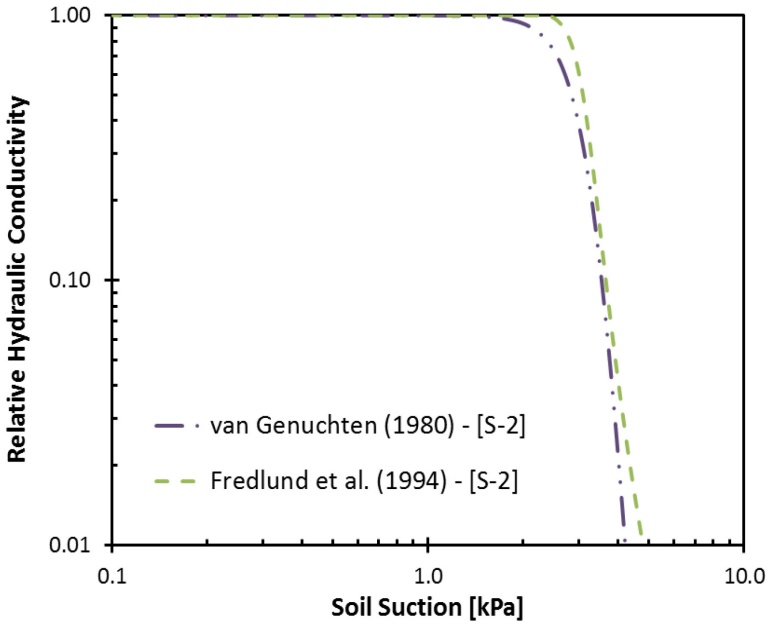

Figure 50: Comparison between predicted relative unsaturated hydraulic conductivities (Fredlund et al. and van Genuchten models), [S-2]

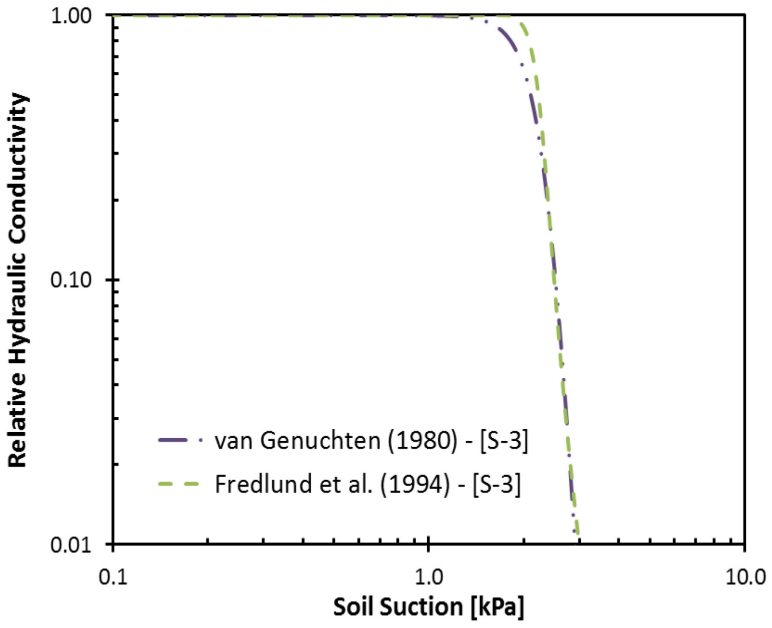

Figure 51: Comparison between predicted relative unsaturated hydraulic conductivities (Fredlund et al. and van Geunchten models), [S-3]

6.1.2 Inverse Modelling of Hydraulic Conductivity

6.1.2.1 HYDRUS- 1D

HYDRUS-1D code (Hopmans et al., 2002; Šimůnek et al. 2005; Šimůnek & van Genuchten, 1997) was used to perform the inverse modelling.

Richards' equation was solved numerically using standard Galerkin-type linear finite element schemes. It uses a Marquardt-Levenberg type parameter optimization algorithm for inverse estimation of soil hydraulic parameters. There are different parameters that are involved to find the solution. Time, geometry, initial conditions, boundary conditions, initial parameters and observed data have to be provided to use this method. These parameters have to be known in order to find the unsaturated hydraulic conductivity. Dimensions of the cell were already given in section 4.2.2. In *HYDRUS-1D,* the sample was modelled with 101 vertical nodes, which were discretized non-variably. Soil and Porous Plate were modelled as two different materials. Two observation points were inserted at *H2*

and *H4* (Figure 32). A set of data for each test were prepared. These data included steps of matric suctions at the bottom of the cell (top of the Porous Plate) versus time, measured matric suctions at *3H/4* and outflow values for the period of the test.

To solve Richards' equation (see chapter 2, Equation 11), van Genutchen-Mualem analytical model was used for hydraulic properties.

The initial and boundary conditions of the tests of this study are as Hopmans et al. (2002), which is:

$$h_m(z,t) = h_{m,i}(z) \qquad t = 0,\ 0 < z < L$$

$$q(z,t) = 0 \qquad t > 0,\ z = L$$

$$h_m(z,t) = h(z,t) - h_a \qquad t > 0,\ z = 0$$

where $h_{m,i}$ is the initial matric head, q is the flux density, *z=0* is the bottom of the porous plate, *z=L* is the top of the soil and $h(z,t)$ is the water pressure head at the bottom of the porous plate. h_a is the pneumatic gas pressure applied to the top of the soil *(z=L)* (or suction applied beneath the porous plate).

For this simulation:

$$h_{m,i}(z) = -2 - z \qquad t = 0\ , 0 < z < L$$

where *z=L=6.5 cm.*

6.1.2.2 Parameter Optimization

By using evolutionary solving method (solver in *Microsoft office Excel*), the best fit for van Genuchten SWRC parameters was obtained. Results are summarized in Table 3. Pairs of laboratory results of soil suction and volumetric water content values were prepared and used for inverse modelling. These data were used to solve Equation 45 by using *HYDRUS-1D* software.

A set of data was prepared as an input for *HYDRUS-1D*. This includes a set of pressure steps with time. In addition, a set of cumulative outflow values versus time and suction values at *H2* were prepared for inverse modelling. Saturated volumetric water content, θ_s, values were measured in laboratory and the same values were used for optimization. Pore connectivity coefficient, *l,* values were also fixed as 0.5 [(Mualem, 1976) and (Hopmans et al. 2002)]. Table 5 shows θ_s and *l* values used for each sample in the optimization process.

Table 5: Inverse modelling fixed values for van Genuchten model

	S-1	S-2	S-3
θ_s	0.387	0.405	0.397
l	0.5	0.5	0.5

6.1.2.3 Results and Discussion

HYDRUS-1D uses a local fitting algorithm, so different analysis had been done for each sample with different initial parameters. Several trials have been done to find the proper results for this method, and to reduce errors. Since the *HYDRUS-1D* uses local optimization method, it was important to provide proper first guess for parameters and a proper range for their allowable changes for optimization. Fillion (2008) results for saturated hydraulic conductivity (Table 1) were used as to find a proper range for initial saturated hydraulic conductivity. Experimental results were fitted to the van Genuchten (1980) equation by using evolutionary solving method (solver in *Microsoft Excel*). Obtained results were used as initial guesses for optimization. After several attempts, best results were obtained for each sample by using initial van Genuchten equation parameters that are summarized in Table 6.

The results with the highest r^2 between observed and simulated data was used. Figure 52, Figure 53 and Figure 54 show the comparison between laboratory observed and inverse modelling predicted values for *S-1, S-2* and *S-3,* respectively. Figure 52-a, Figure 53-a and Figure 54-a compare cumulative outflow versus time for each soil sample. In these figures,

soil suction at the point where lower tensiometer were installed (*H2*) were compared. The highest obtained r^2 values for each simulation were equal to 0.99616, 0.99658 and 0.99965 for *S-1, S-2* and *S-3*, respectively. There was a good agreement between observed and fitted values for all three samples. Gaps between values in these figures indicate changing of pressure step.

Table 6: Inverse modelling initial and optimized values for van Genuchten model

	Initial values			Optimized values		
	S-1	S-2	S-3	S-1	S-2	S-3
θ_r	6.77E-02	6.43E-02	2.74E-02	5.46E-03	5.28E-02	3.21E-02
K †	30	80	300	25.79	112.19	339.98
α	1.48E-02	2.90E-02	4.10E-02	1.54E-02	2.98E-02	4.10E-02
n	11.85	7.39	12.77	8.40	6.42	14.00

† cm/hr

Sensitivity of the experimental apparatuses such as pressure transducers, and existence of air bubbles in the experimental system can cause some minor errors in laboratory results. Besides, local optimization method, which is used by *HYDRUS-1D* has some limitations compare to global optimization method. Due to the errors of laboratory results and limitations of local optimization method some errors during the optimization was encountered.

Figure 55-a, Figure 55-b and Figure 55-c illustrate the soil water retention curves obtained by inverse modelling and compare these results with the experimental data for material *S-1*, *S-2* and *S-3,* respectively. In these figures, the line represents the inverse modelling results and dots represent the experimental results. As it is seen in these figures, experimental results are in a very good agreement with the *HYDRUS-1D* results. For *S-1* material, at lower soil suctions a better agreement was seen between these two approaches. At higher soil suctions, there is a slight difference between the obtained soil water retention curves. Limitations of *HYDRUS-1D'*s local optimization method can be a reason for the difference between the obtained results of the soil water retention curve *S-1* material.

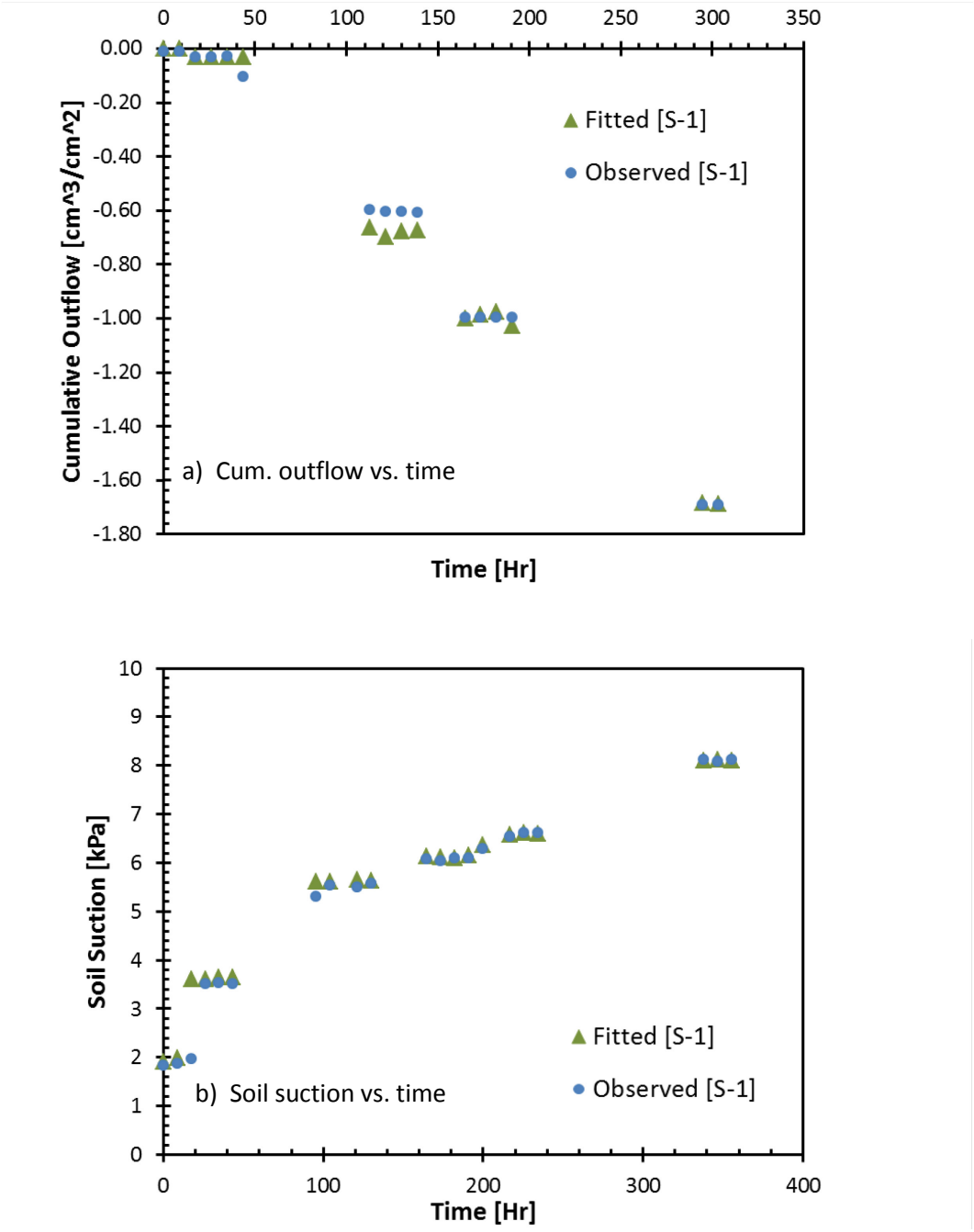

Figure 52: Comparison between observed and inverse modelling fitted values, [S-1]

a) Cumulative Outflow vs. time b) Soil suction vs. time (at H2)

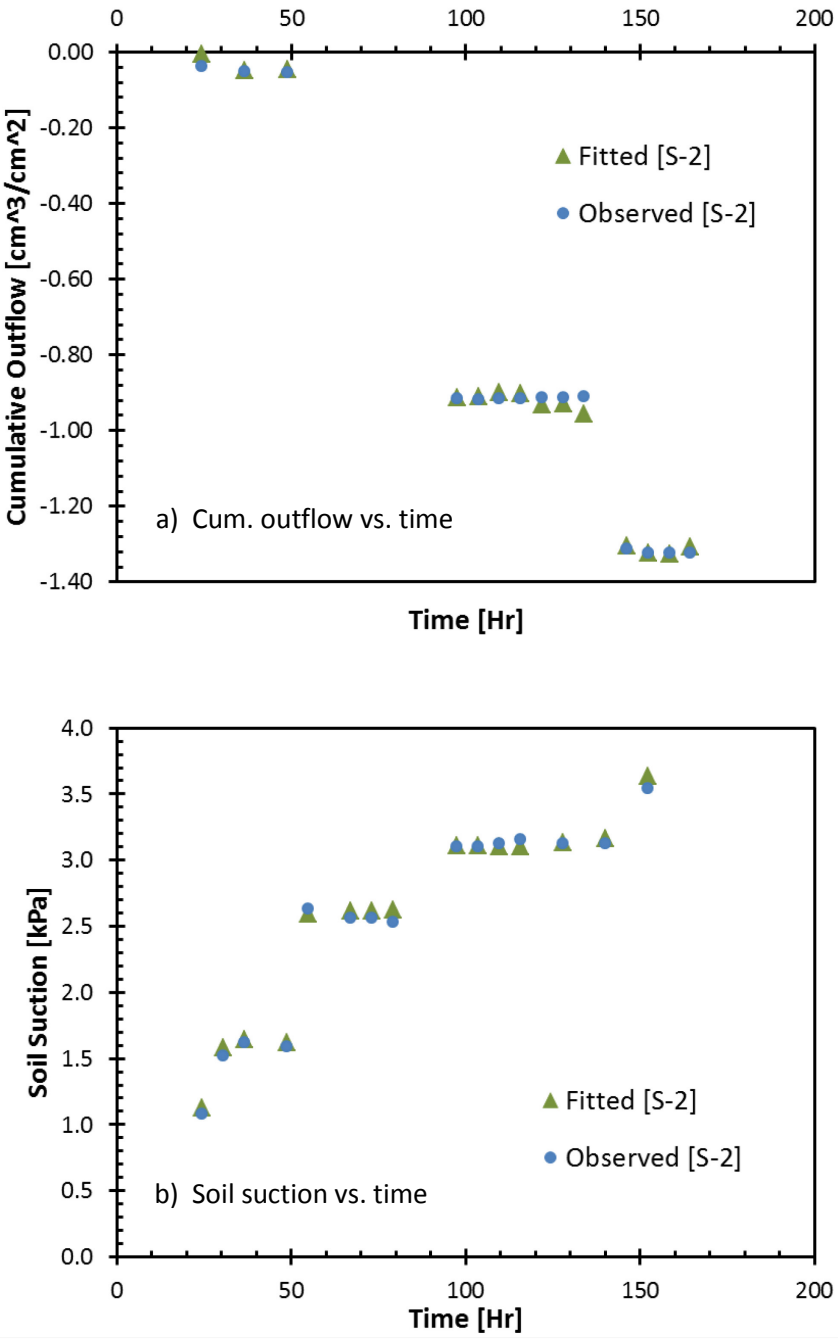

Figure 53: Comparison between observed and inverse modelling fitted values, [S-2]

a) Cumulative Outflow vs. time b) Soil suction vs. time (at H2)

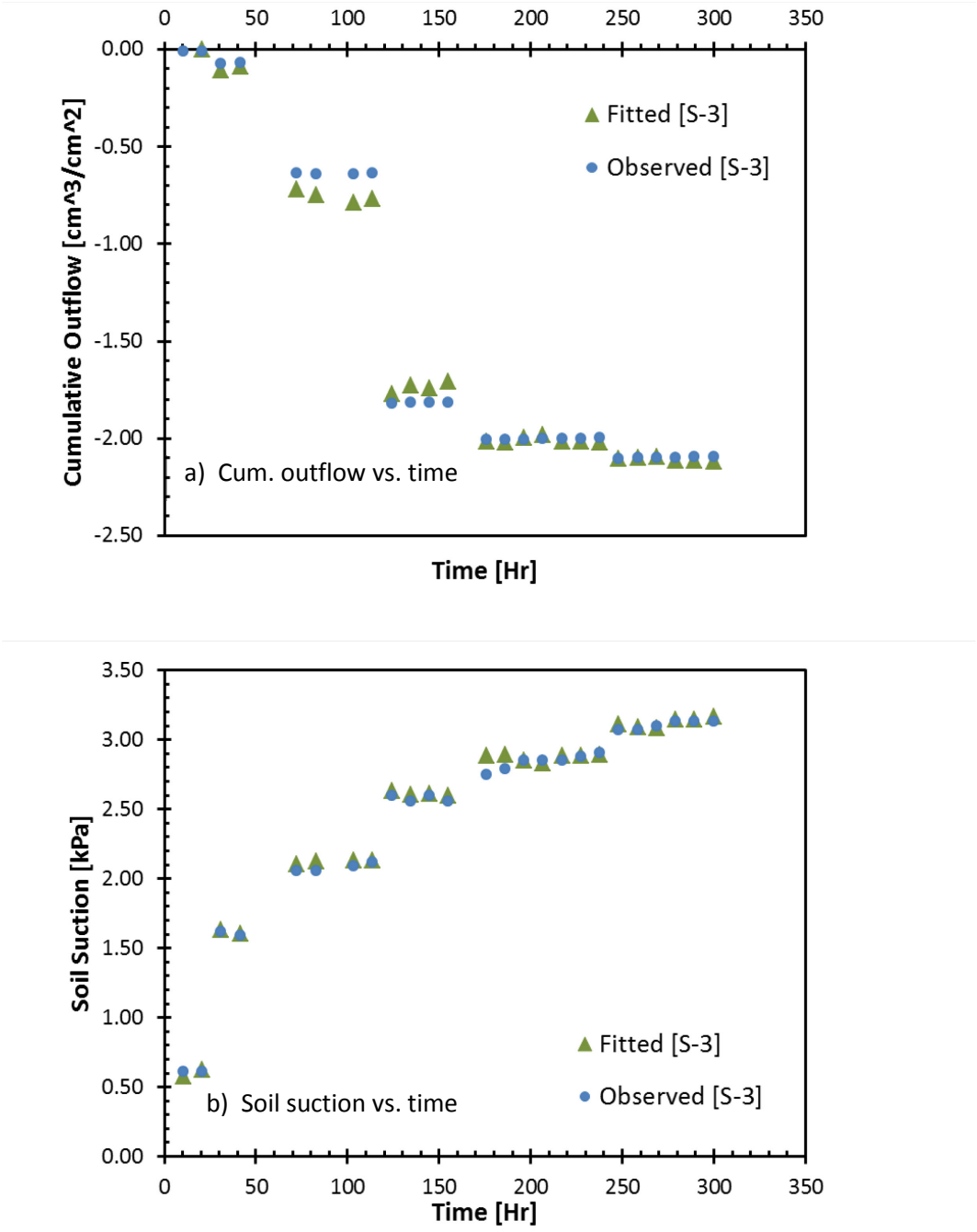

Figure 54: Comparison between observed and inverse modelling fitted values, [S-3]

a) Cumulative Outflow vs. time b) Soil suction vs. time (at H2)

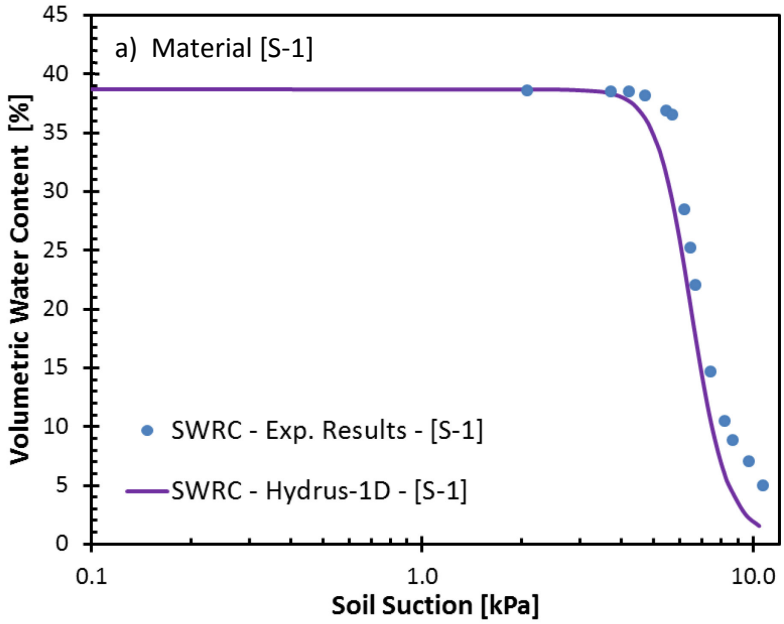
a) Material [S-1]
Volumetric Water Content [%]
45
40
35
30
25
20
15
10
5
0
0.1
1.0
10.0
Soil Suction [kPa]
SWRC - Exp. Results - [S-1]
SWRC - Hydrus-1D - [S-1]

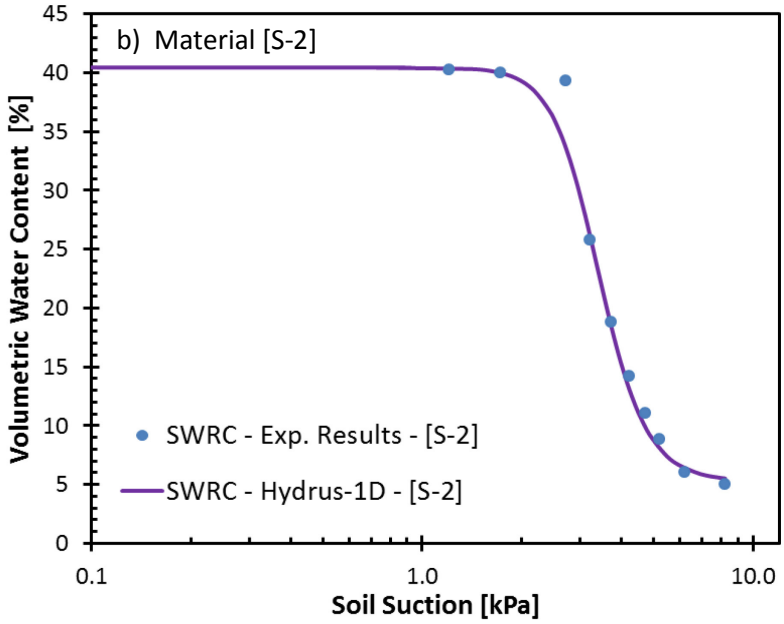
b) Material [S-2]
Volumetric Water Content [%]
45
40
35
30
25
20
15
10
5
0
0.1
1.0
10.0
Soil Suction [kPa]
SWRC - Exp. Results - [S-2]
SWRC - Hydrus-1D - [S-2]

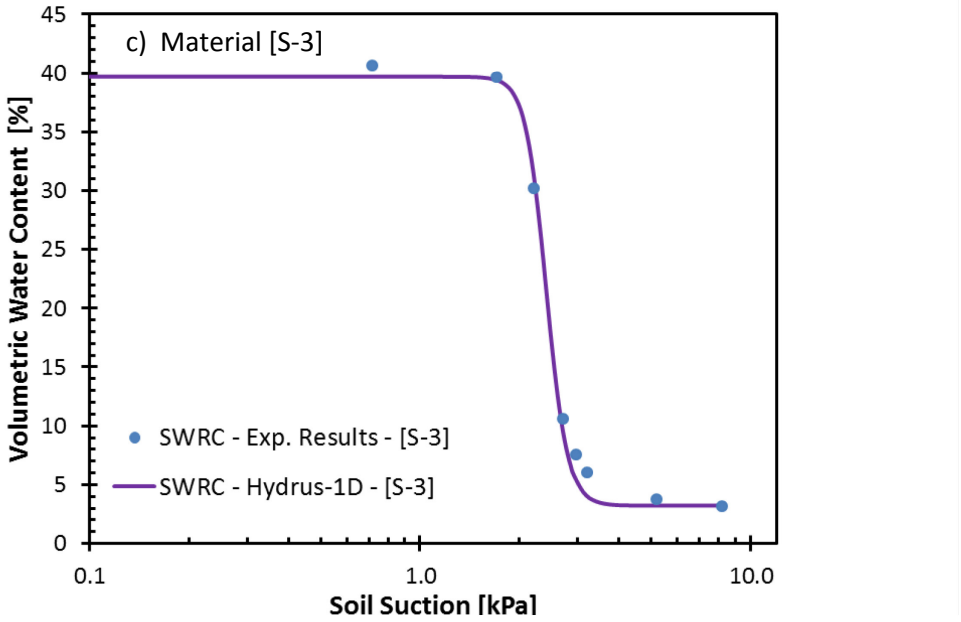

Figure 55: Comparison between laboratory and inverse modelling SWRC results

a) S-1 b) S-2 c) S-3

By using the inverse solution, the unsaturated hydraulic conductivity of each material was determined. As it is seen in Figure 56-a, Figure 57-a and Figure 58-a, the hydraulic conductivity decreases when the soil suction increases. Hydraulic conductivity has a sharp decrease when the soil suction reaches to the air entry value.

Figure 56-b, Figure 57-b and Figure 58-b show hydraulic conductivity of each material versus its water content. As it is seen in these figures, hydraulic conductivity and volumetric water content are directly proportional. At lower water contents, hydraulic conductivity has a gradual increase compare to the higher water contents.

In Figure 56-c, Figure 57-c and Figure 58-c, the unsaturated hydraulic conductivity for different elevations of the specimen at different time steps are illustrated for *S-1, S-2* and *S-3,* respectively. In these figures, depth equal to 0 shows the top of the cell and -6 *cm* is the bottom of the cell. As it is seen in these figures, hydraulic conductivity for Porous Plate (-6 *cm* to -6.5 *cm)* is constant during the test. In the saturated specimen, hydraulic conductivity at all elevations of soil profile is the same.

In the soil sample, the higher the elevation, the higher the soil suction is; because of that, for each time step, higher elevations have less hydraulic conductivities. In initial steps, when the specimen is saturated, hydraulic conductivity along the sample is constant and equal to the saturated hydraulic conductivity. By applying new steps, suction at higher elevations in the soil profile is higher than the suction at the bottom of the soil sample. Therefore, water content in soil profile will not be constant. The higher the elevation, the higher the suction and the lower the volumetric water content will be. As a result, Figure 56-c, Figure 57-c and Figure 58-c show that the hydraulic conductivity is decreasing when the elevation is increasing.

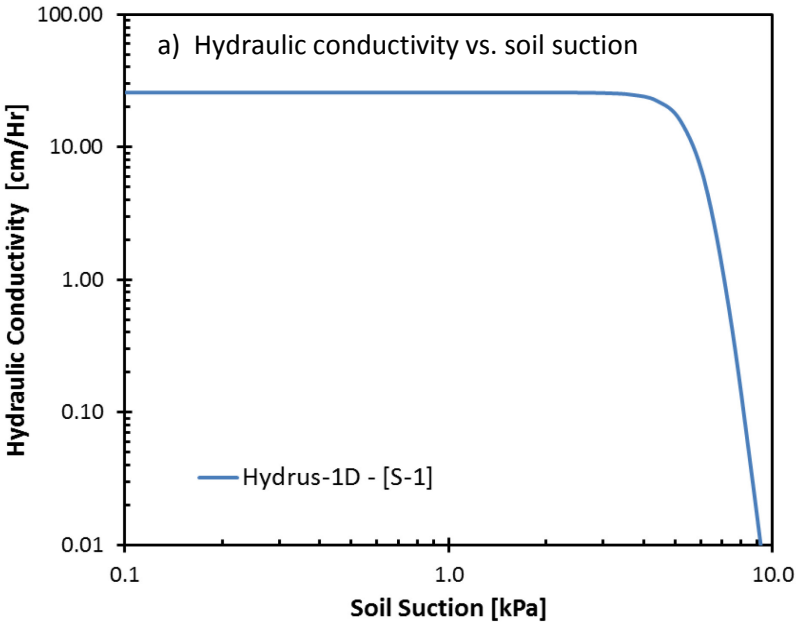

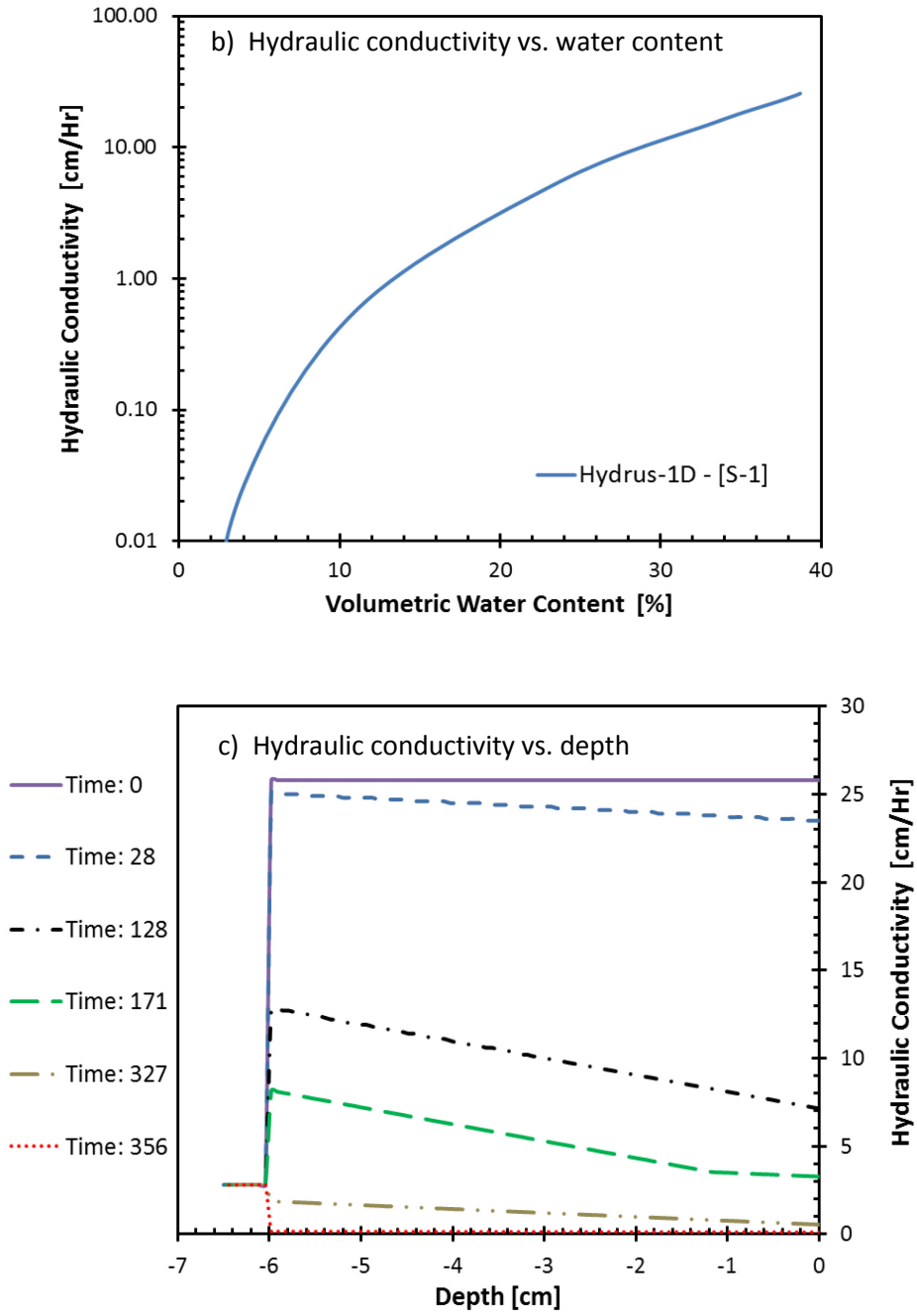

Figure 56: Unsaturated hydraulic conductivity obtained by inverse modelling, [S-1]

a) Hydraulic conductivity vs. soil suction b) Hydraulic conductivity vs. water content

c) Hydraulic conductivity vs. depth

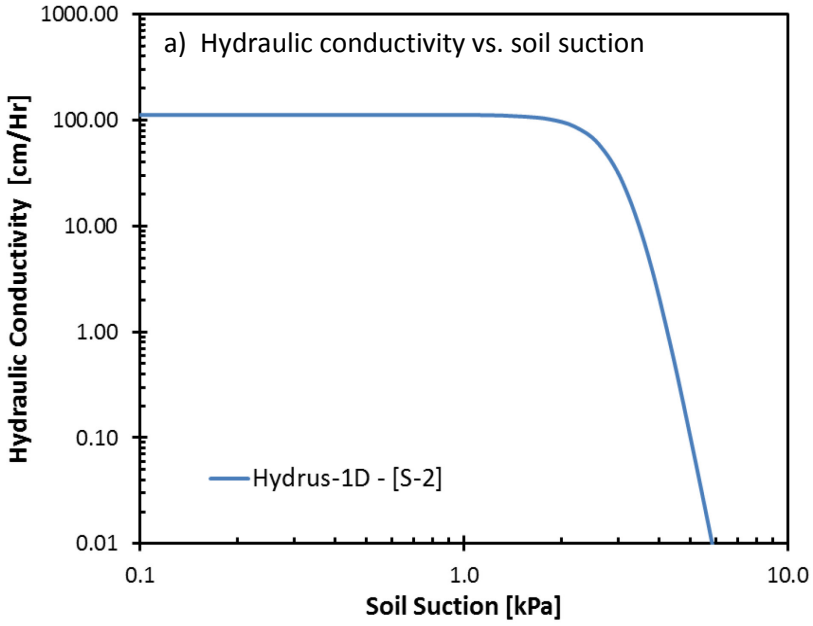
a) Hydraulic conductivity vs. soil suction
Hydraulic Conductivity [cm/Hr]
1000.00
100.00
10.00
1.00
0.10
0.01
0.1
1.0
10.0
Soil Suction [kPa]
Hydrus-1D - [S-2]

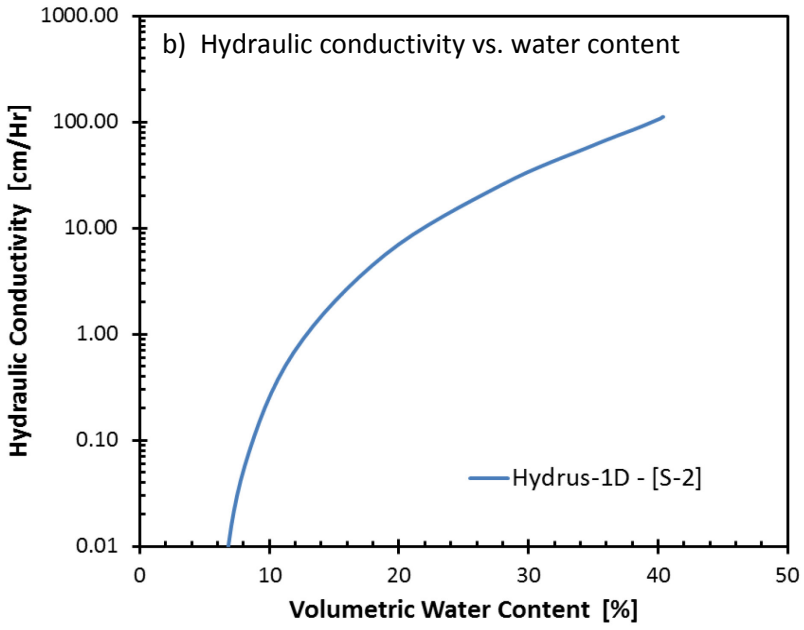
b) Hydraulic conductivity vs. water content
Hydraulic Conductivity [cm/Hr]
1000.00
100.00
10.00
1.00
0.10
0.01
0
10
20
30
40
50
Volumetric Water Content [%]
Hydrus-1D - [S-2]

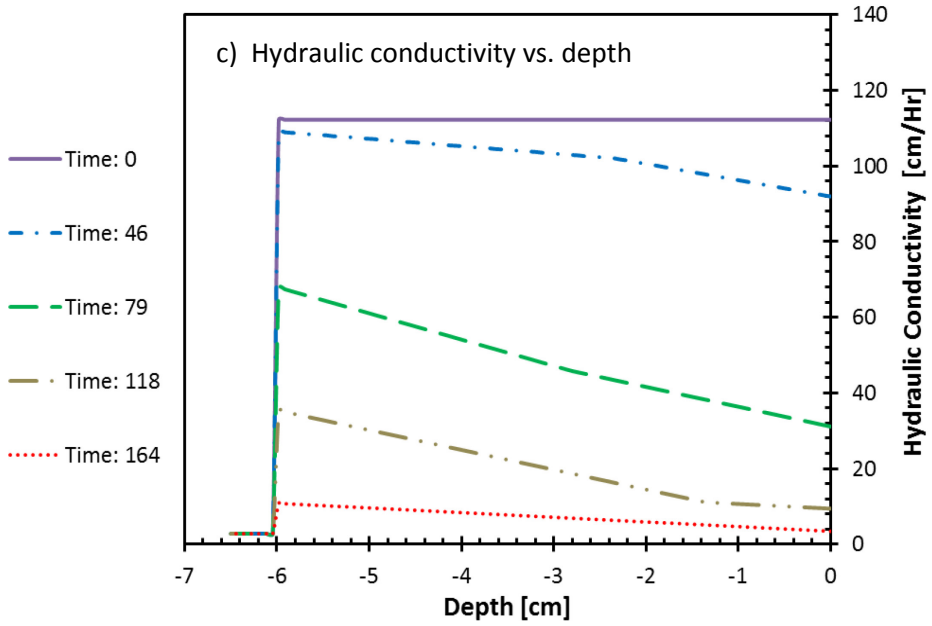

Figure 57: Unsaturated hydraulic conductivity obtained by inverse modelling, [S-2]

a) Hydraulic conductivity vs. soil suction b) Hydraulic conductivity vs. water content

c) Hydraulic conductivity vs. depth

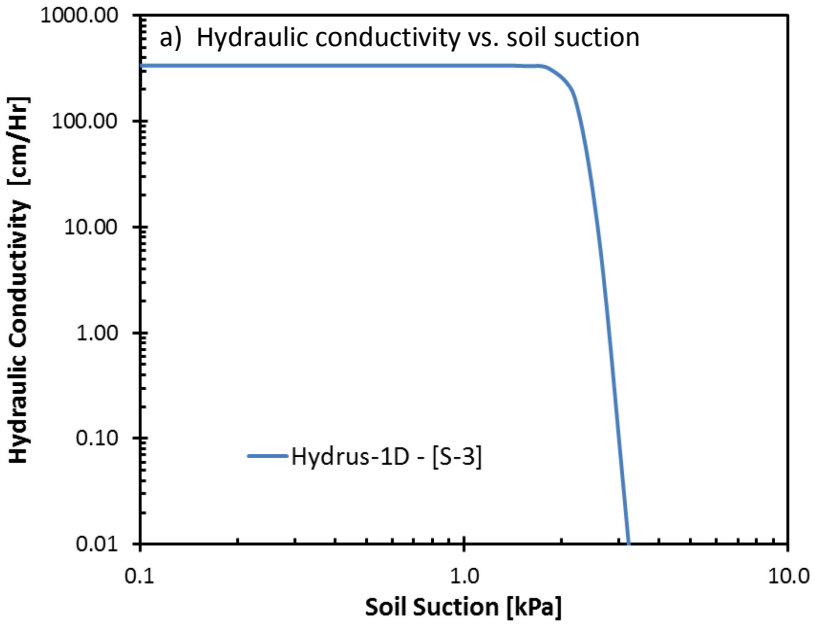

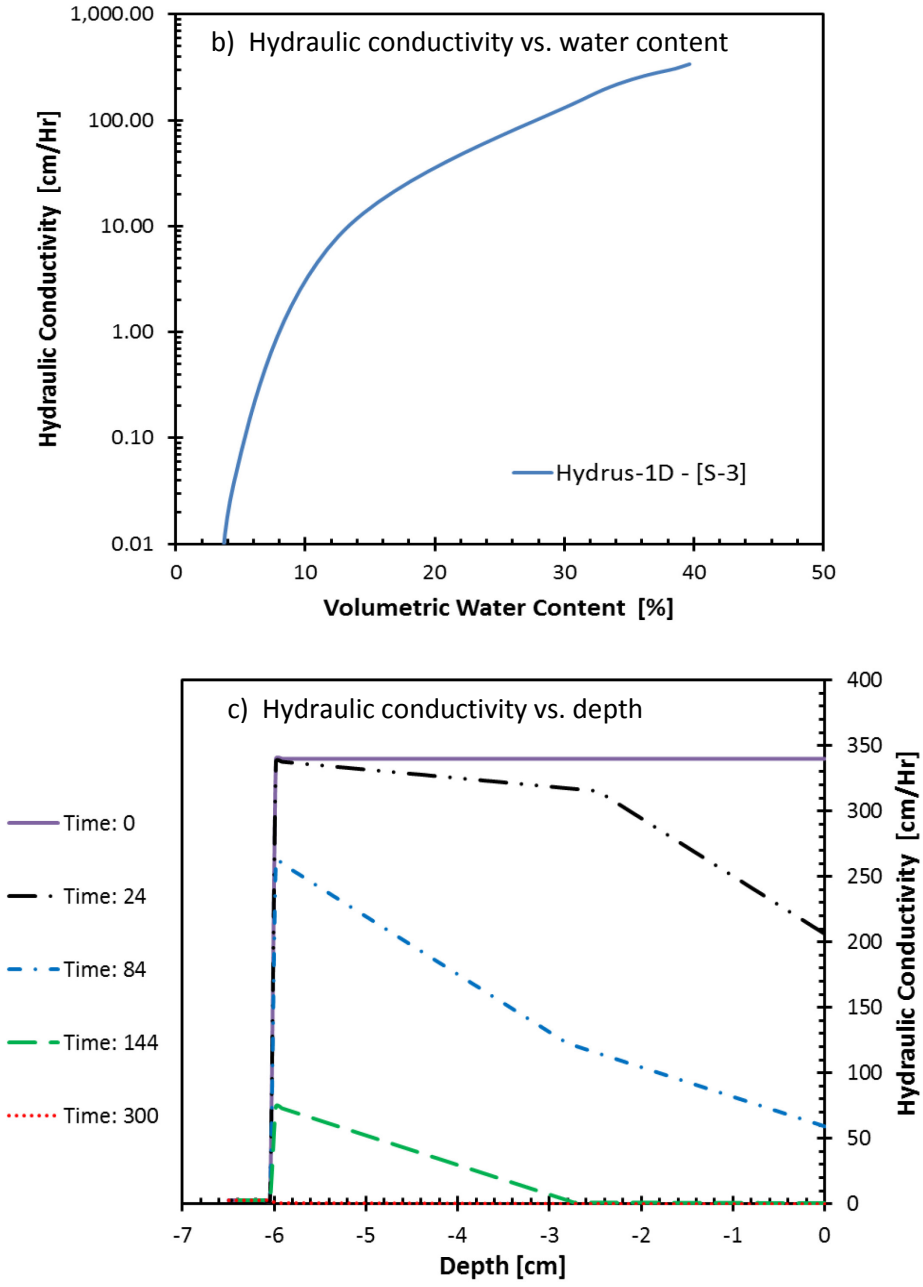

Figure 58: Unsaturated hydraulic conductivity obtained by inverse modelling, [S-3]

a) Hydraulic conductivity vs. soil suction b) Hydraulic conductivity vs. water content

c) Hydraulic conductivity vs. depth

In Table 7, the porosity and the fitted saturated hydraulic conductivity of each material are summarized. Fillion (2008) results for each sample are also presented in this table. Comparing the inverse modelling results and the Fillion (2008) measured saturated

hydraulic conductivities shows a good agreement between the two studies. As it is seen in Table 7 and Figure 59, for *S-1* and *S-2* materials with a higher porosity compare to Fillion (2008), fitted saturated hydraulic conductivity values are higher than the measured values from Fillion (2008) that is as expected. For *S-3* material, with higher porosity, fitted saturated hydraulic conductivity values is lower than the measured value from Fillion (2008). This can be explained by homogeneity of each specimen, and experimental errors. Limitations of *HYDRUS-1D* in optimizing parameters can be another reason for this difference.

Table 7: Comparison between porosity and saturated hydraulic conductivity of tested materials with Fillion (2008) values

Material	***Porosity (n)***	***K [cm/hr]***
S-1 [Hydrus-1D]	0.387	25.79
S-1 [Fillion, 2008]	0.353	18
S-2 [Hydrus-1D]	0.404	112.19
S-2 [Fillion, 2008]	0.373	75.6
S-3 [Hydrus-1D]	0.397	339.98
S-3 [Fillion, 2008]	0.396	385.2

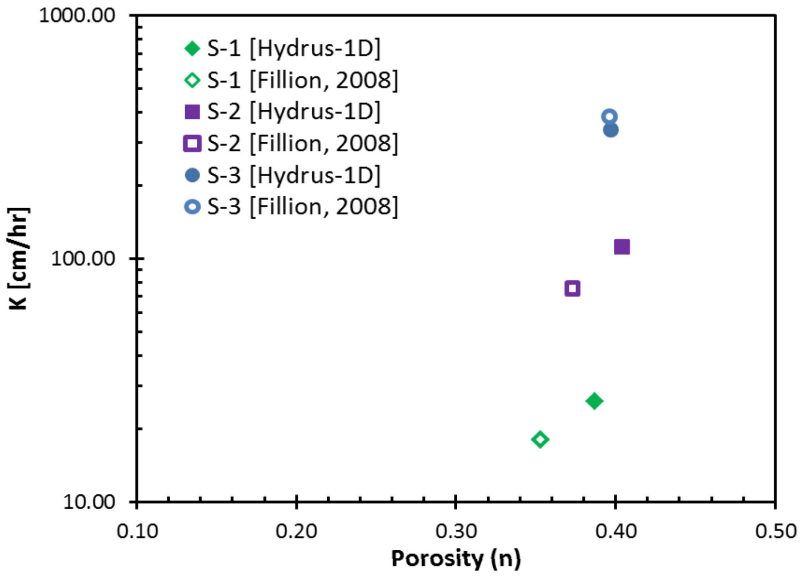

Figure 59: Comparison between porosity and saturated hydraulic conductivity of tested materials with Fillion (2008) obtained values

Comparing results of relative unsaturated hydraulic conductivity of the tested materials (Figure 60) demonstrated that samples with lower d_{10} and higher coefficient of uniformity, *Cu,* need higher suction to reach a same relative hydraulic conductivity. The hydraulic conductivity results have a sharp inclination. Uniform materials have a narrow grain size distribution, so a narrow pore size distribution. Since all pores have almost the same size, they all desaturate at the same suction.

One of the problems that can be encountered while using predictive models to find the unsaturated hydraulic conductivity is related to the saturated hydraulic conductivity. Inverse modelling can fit the saturated hydraulic conductivity based on laboratory results. This helps to obtain more precise values of unsaturated hydraulic conductivities compare to predictive models. Figure 61-a, Figure 61-b and Figure 61-c show the comparison between relative hydraulic conductivities obtained by inverse method, van Genuchten model and Fredlund et al. model for material *S-1*, *S-2* and *S-3,* respectively.

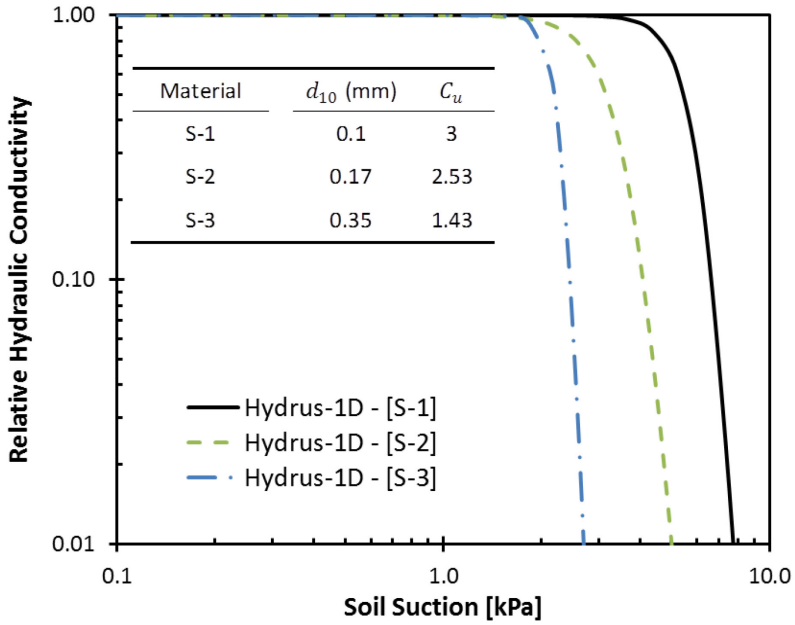

Figure 60: Comparison of relative hydraulic conductivities of tested samples

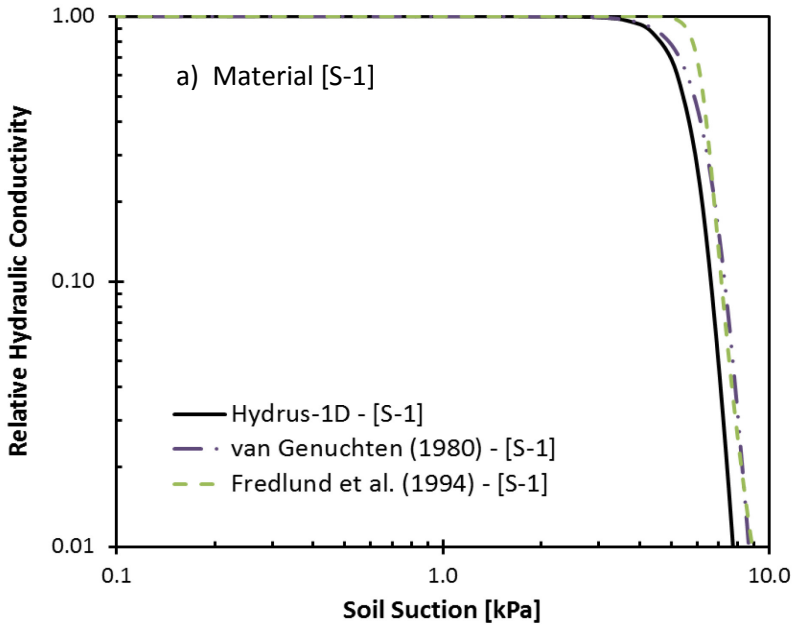
a) Material [S-1]
Relative Hydraulic Conductivity
1.00
0.10
0.01
0.1
1.0
10.0
Soil Suction [kPa]
Hydrus-1D - [S-1]
van Genuchten (1980) - [S-1]
Fredlund et al. (1994) - [S-1]

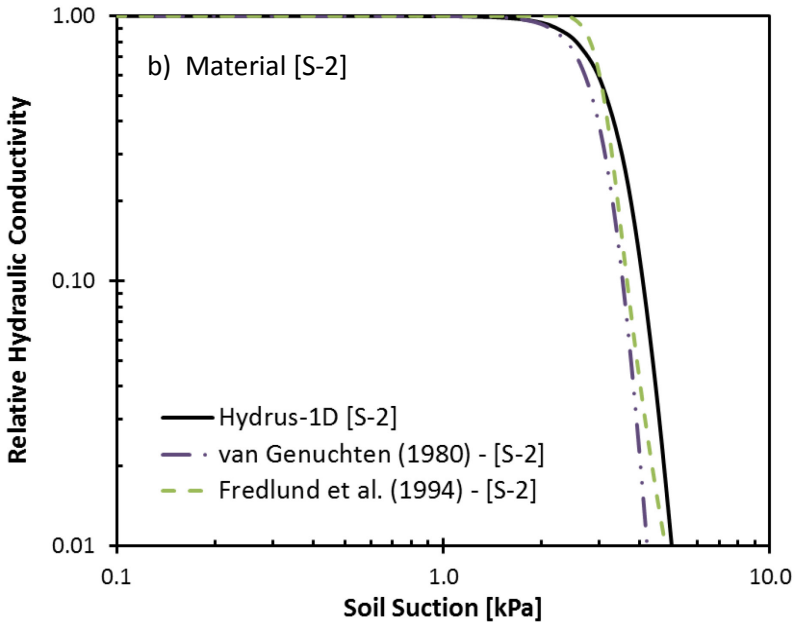
b) Material [S-2]
Relative Hydraulic Conductivity
1.00
0.10
0.01
0.1
1.0
10.0
Soil Suction [kPa]
Hydrus-1D [S-2]
van Genuchten (1980) - [S-2]
Fredlund et al. (1994) - [S-2]

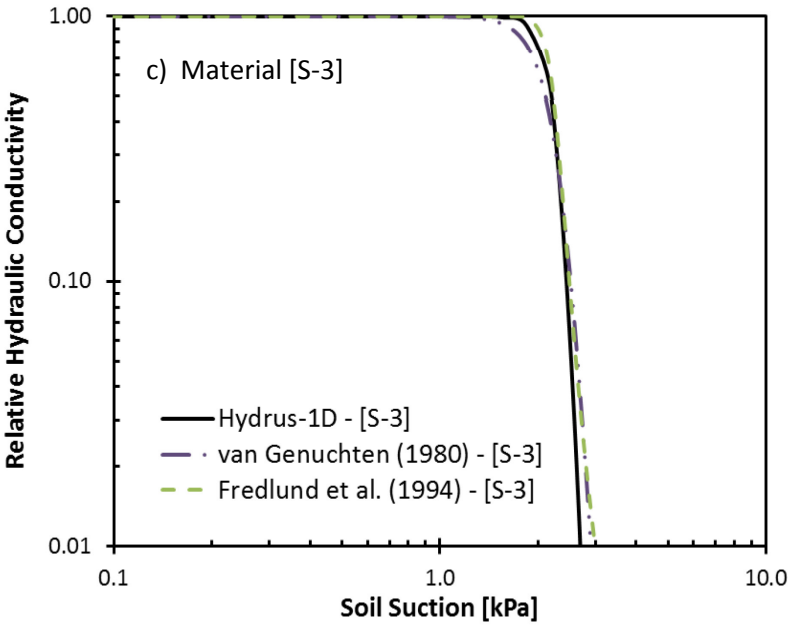

Figure 61: Comparison of relative unsaturated hydraulic conductivities obtained by inverse solution, Fredlund model and van Genuchten model

a) S-1 b) S-2 c) S-3

7 Conclusion

Multistep transient outflow test and inverse modelling method were used to determine the hydraulic properties of Bédard Valcartier (Québec) granite sand. A cell was designed and made by Plexiglass at the Department of Civil Engineering of the Laval University. In order to measure the soil suction within the soil sample during the multistep transient outflow test, two holes were made at two different elevations of the experimental cell Figure 32. Two tensiometers were installed in the manufactured holes and were connected to the pressure transducers to measure matric suction at *H2* and *H4* during the test. To perform the test, pressure was applied in multiple steps. Measured suctions and outflow were automatically recorded every ten minute. Moisture content of each sample was measured at the end of each transient outflow test. These data were used to illustrate the soil water retention curves of the tested materials. Laboratory results were fitted to van Genuchten (1980) and Fredlund and Xing (1994) models. The difference between these models' fitted soil water retention curves was not considerable. Obtained soil water retention curves for the three tested samples were compared by their coefficient of uniformity, C_u, and it was observed that samples with higher coefficient of uniformity need higher soil suctions for the same volumetric water content. Relative hydraulic conductivities of each sample was find by using van Genuchten (1980) and Fredlund et al. (1994) models and the experimental soil water retention results. It was observed that these models' obtained results in lower soil suctions have more difference compare to higher soil suctions.

HYDRUS-1D software was used to perform inverse modelling on laboratory results to find the unsaturated hydraulic conductivity of the tested samples. van Genuchten (1980) was solved by this software and this equation unknown parameters were determined. Since *HYDRUS-1D* uses local optimization method, some limitations have been encountered during the optimization process. The initial guess for van Genuchten (1980) equation unknown parameters needed to be close enough to the optimized values, so the software could find the fitted parameters with an accepted precision. Comparing the soil water retention curves of testes materials showed that in higher soil suctions, there is a difference between the experimental results and the *HYDRUS-1D* results. This difference can be

explained by limitations of the optimization method, which is used by *HYDRUS-1D* or the experimental limits to measure actual outflow values in higher soil suction when the water content is close to its residual amount.

Saturated and unsaturated hydraulic conductivity of the tested materials were obtained by using inverse modelling. Comparing the *HYDRUS-1D* obtained saturated hydraulic conductivity results with the Fillion (2008) measured values for the same soil samples, showed a very good for all samples.

The relative hydraulic conductivity that was obtained by using inverse modelling method, van Genuchten (1980) model and Fredlund et al. (1994) model were compared for each sample. It was seen that the relative hydraulic conductivity for the three methods are in close agreement over the entire soil suction.

References

Agus, S. S., & Schanz, T. (2005). Comparison of Four Methods for Measuring Total Suction. *Vadose Zone Journal*, *4*(4), 1087. doi:10.2136/vzj2004.0133

Alonso, E. E., Gens, A., & Josa, A. (1990). A constitutive model for partially saturated soils. *Géotechnique*, *40*(3), 405–430. doi:10.1680/geot.1990.40.3.405

Arya, L. M., & Paris, J. F. (1981). A Physicoempirical Model to Predict the Soil Moisture Characteristic from Particle-Size Distribution and Bulk Density Data. *Soil Science Society of America Journal*, *45*(6), 1023–1030. doi:10.2136/sssaj1981.03615995004500060004x

Assouline, S., & Tartakovsky, D. M. (2001). Unsaturated hydraulic conductivity function based on a soil fragmentation process. *Water Resources Research*, *37*(5), 1309–1312. doi:10.1029/2000WR900332

ASTM-5298-10. (2010). Standard Test Method for Measurement of Soil Potential (Suction) Using Filter Paper. *ASTM International*, 1–6. doi:10.1520/D5298-10.2

ASTM-D2216-10. (1963). Standard Test Method for Laboratory Determination of Water (Moisture) Content of Soil and Rock by Mass. *ASTM International, West Conshohocken, PA*, (Approved 2010), 1–7. doi:10.1520/D2216-10.N

ASTM-D5126. (1990). Standard Guide for Comparison of Field Methods for Determining Hydraulic Conductivity in the Vadose Zone. *ASTM International, West Conshohocken, PA*.

ASTM-D6836-02. (2012). Standard Test Methods for Determination of the Soil Water Characteristic Curve for Desorption Using Hanging Column, Pressure Extractor, Chilled Mirror Hygrometer, or Centrifuge. *ASTM International*, *02*. doi:10.1520/D6836-02R08E02.characteristic

ASTM-D6836–02. (2012). Standard Test Methods for Determination of the Soil Water Characteristic Curve for Desorption Using Hanging Column, Pressure Extractor, Chilled Mirror Hygrometer, or Centrifuge. *ASTM International, West Conshohocken, PA*, *02*(Reapproved 2008). doi:10.1520/D6836-02R08E02.characteristic

Bouma, J., & Denning, J. L. (1972). Field Measurement of Unsaturated Hydraulic Conductivity by Infiltration Through Gypsum Crusts 1. *Soil Science Society of America Journal*, *36*(5), 846–847. doi:10.2136/sssaj1972.03615995003600050042x

Brooks, R. H., & Corey, A. T. (1964). Hydraulic Properties of Porous Media. In *P.3 , Hydrology Papers, Colorado State University, Fort Collins* (Vol. 3).

Buckingham, E. (1907). Studies on the Movement of Soil Moisture. *U.S. Department of Agriculture, Burreau of Soils*, *38*, 61.

Bulut, R., Park, S. W., & Lytton, R. L. (2000). Comparison of total suction values from psychrometer and filter paper methods. In *Unsaturated soils for Asia. Proceedings of the Asian Conference on Unsaturated Soils, UNSAT-ASIA 2000, Singapore, 18-19 May, 2000 2000 pp. 269-273*. Rotterdam.

Cardoso, R., Romero, E., Lima, A., & Ferrari, A. (2007). A Comparative Study of Soil Suction Measurement Using Two Different High-Range Psychrometers. *Experimental Unsaturated Soil Mechanics*, *112*, 79–93.

Carrier, W. D. (2003). Goodbye, Hazen; Hello, Kozeny-Carman. *Journal of Geotechnical and Geoenvironmental Engineering*, *129*(11), 1054–1056. doi:10.1061/(ASCE)1090-0241(2003)129:11(1054)

Celia, M. A., Bouloutas, E. T., & Zarba, R. L. (1990). A General Mass-Conservative Numerical Solution for the Unsaturated Flow Equation. *Water Resources Research*, *26*(7), 1483. doi:10.1029/WR026i007p01483

Chiu, T.-F., & Shackelford, C. D. (1998). Unsaturated Hydraulic Conductivity of Compacted Sand-Kaolin Mixtures. *Journal of Geotechnical and Geoenvironmental Engineering*, *124*(2), 160–170. doi:10.1061/(ASCE)1090-0241(1998)124:2(160)

Cokca, E. (2000). Comparison of suction and oedometer methods for the measurement of swell pressure. *Quarterly Journal of Engineering Geology and Hydrogeology*, *33*(2), 141–147. doi:10.1144/qjegh.33.2.141

Corey, A. T. (1957). Measurement of Water and Air Permeability in Unsaturated Soil. *Soil Science Society of America Journal*.

Dane, J. H., & Topp, G. C. (Eds.). (2002). *Methods of Soil Analysis. Part 4. Physical Methods*. Madison, Wisconsin, USA: American Society of Agronomy, Soil Science Society of America.

Darcy, H. (1856). *Les Fontaines Publiques de la Ville de Dijon. VII-647 p. ; in-4*. Dalmont, Paris.

Doering, E. J. (1965). Soil-Water Diffusivity By the One-Step Method. *Soil Science*, *99*(5), 322–326.

Durner, W., Schultze, B., & Zurmühl, T. (1999). State-of-the-art in inverse modeling of inflow/outflow experiments. In *Workshop on Characterization and Measurement of the Hydraulic Properties of Unsaturated Porous Media* (pp. 661–681).

Eching, S. O., & Hopmans, J. W. (1993). Optimization of Hydraulic Functions from Transient Outflow and Soil Water Pressure Data. *Soil Science Society of America Journal*, *57*(5), 1167–1175.

Eching, S. O., Hopmans, J. W., & Wendroth, O. (1994). Unsaturated Hydraulic Conductivity from Transient Multistep Outflow and Soil Water Pressure Data. *Soil Science Society of America Journal*, *58*(3), 687–695. doi:10.2136/sssaj1994.03615995005800030008x

Eijkelkamp Agrisearch Equipment. (2014). Retrieved from http://en.eijkelkamp.com/

Enfield, C. G., & Hsieh, J. J. C. (1971). Application of Thermocouple Psychrometers to Soil Water Transport. *Water Resources Research*, *7*(5), 1349–1353.

Farouk, A., Lamboj, L., & Kos, J. (2004). A Numerical Model to Predict Matric Suction Inside Unsaturated Soils. *Acta Polytechnica*, *44*(4), 3–10.

Fillion, M.-H. (2008). *Mesure de la Conductivité Thermique et de la Perméabilité Intrinsèque d'Assemblage de Cailloux*. Université Laval.

Fredlund, D. G., & Rahardjo, H. (1993). *Soil mechanics for unsaturated soils*. *Civil Engineering*. Wiley-Interscience.

Fredlund, D. G., Sheng, D., & Zhao, J. (2011). Estimation of soil suction from the soil-water characteristic curve. *Canadian Geotechnical Journal*, *48*(2), 186–198. doi:10.1139/T10-060

Fredlund, D. G., & Wong, D. K. H. (1989). Calibration of Thermal Conductivity Sensors for Measuring Soil Suction. *Geotechnical Testing Journal*, 188–194.

Fredlund, D. G., Xing, A., & Huang, S. (1994). Predicting the permeability function for unsaturated soils using the soil-water characteristic curve. *Canadian Geotechnical Journal*, *31*(4), 533–546. doi:10.1139/t94-062

Fredlund, D., & Xing, A. (1994). Equations for the soil-water characteristic curve. *Canadian Geotechnical Journal*, *31*, 521–532.

Fredlund, M. D., Fredlund, D. G., & Wilson, G. W. (2000). Estimation of volume change functions for unsaturated soils. In *Unsaturated Soils for Asia,*.

Fujimaki, H., & Inoue, M. (2003). Reevaluation of the Multistep Outflow Method for Determining Unsaturated Hydraulic Conductivity. *Vadose Zone Journal*, *2*, 409–415. doi:10.2136/vzj2004.0317

Gardner, R. (1937). A Method of Measuring the Capillary Tension Of Soil Moisture Over a Wide Moisture Range. *Soil Science*, *43*(4), 277–284.

Gardner, W. R. (1956). Calculation of Capillary Conductivity from Pressure Plate Outflow Data 1. *Soil Science Society of America Journal*, *20*(3), 317–320. doi:10.2136/sssaj1956.03615995002000030006x

Gardner, W. R., & Miklich, F. J. (1962). Unsaturated Conductivity and Diffusivity Measurements By A Constant Flux Method. *Soil Science*, *93*(4), 271–274. doi:10.1097/00010694-196204000-00008

Haines, W. B. (1927). Studies in the physical properties of soils: IV. A further contribution to the theory of capillary phenomena in soil. *The Journal of Agricultural Science*, *17*(02), 264–290. doi:10.1017/S0021859600018499

Haines, W. B. (1930). Studies in the physical properties of soil. V. The hysteresis effect in capillary properties, and the modes of moisture distribution associated therewith. *The Journal of Agricultural Science*, *20*(01), 97–116. doi:10.1017/S002185960008864X

Hopmans, J. W., Šimůnek, J., Romano, N., & Wolfgang Durner. (2002). Methods of Soil Analysis. Part 4. Physical Methods. In *Methods of Soil Analysis , Part 1-Physical and Mineralogical Methods* (pp. 963–1004). Soil Science Society of America, Soil Science Society of America Book Series Number 5.

Karkare, M. V., & Fort, T. (1993). Water Movement in “Unsaturated” Porous Media Due to Pore Size and Surface Tension Induced Capillary Pressure Gradients. *Langmuir*, *9*(9), 2398–2403. doi:10.1021/la00033a023

Kay, B. D., & Low, P. F. (1970). Measurement of the Total Suction of Soils by a Thermistor Psychrometer 1. *Soil Science Society of America Journal*, *34*, 373–376.

Kool, J. B., Parker, J. C., & van Genuchten, M. T. (1985). Determining Soil Hydraulic Properties from One-step Outflow Experiments by Parameter Estimation: I. Theory and Numerical Studies 1. *Soil Science Society of America Journal*, *49*, 1348–1354. doi:10.2136/sssaj1985.03615995004900060004x

Kool, J. B., Parker, J. C., & van Genuchten, M. T. (1987). Parameter estimation for unsaturated flow and transport models — A review. *Journal of Hydrology*, *91*, 255–293. doi:10.1016/0022-1694(87)90207-1

Lebeau, M., & Konrad, J.-M. (2006). *Développement d'une méthodologie de sélection des matériaux de fondation routière* (pp. 1–410).

Leong, E. C., Tripathy, S., & Rahardjo, H. (2004). A Modified Pressure Plate Apparatus (Technical Note). *Geotechnical Testing Journal*, *27*(3), 322–331.

Leong, E. C., Zhang, X.-H., & Rahardjo, H. (2012). Calibration of a thermal conductivity sensor for field measurement of matric suction. *Geotechnique*, *62*, 81–85.

Leong, E.-C., Tripathy, S., & Rahardjo, H. (2003). Total suction measurement of unsaturated soils with a device using the chilled-mirror dew-point technique. *Géotechnique*, *53*(2), 173–182. doi:10.1680/geot.2003.53.2.173

Likos, W. J., & Lu, N. (1981). Filter Paper Technique for Measuring Total Soil Suction. *Transportation Research Record 1786, Paper No. 02-2140*, 120–128.

Maqsoud, A., Bussière, B., Mbonimpa, M., & Aubertin, M. (2004). Hysteresis Effects on the Water Retention Curve a Comparison between Laboratory and Predictive Models. In *57th Canadian Geotechnical Conference, Geo Quebec 2004* (pp. 8–15).

Marinho, F. A. M., & Oliveira, O. M. (2006). The Filter Paper Method Revisited. *Geotechnical Testing Journal*, *29*(3), 1–9.

Marinho, F. A. M., Take, W. A., & Tarantino, A. (2008). Measurement of Matric Suction Using Tensiometric and Axis Translation Techniques. *Geotechnical and Geological Engineering*, *26*, 615–631. doi:10.1007/s10706-008-9201-8

Masrouri, F., Bicalho, K. V., & Kawai, K. (2008). Laboratory Hydraulic Testing in Unsaturated Soils. *Geotechnical and Geological Engineering*, *26*, 691–704. doi:10.1007/s10706-008-9202-7

Mualem, Y. (1976). A New Model for Predicting the Hydraulic Conductivity of Unsaturated Porous Media. *Water Resources Research*, *12*(3), 513–522. doi:10.1029/WR012i003p00513

Parker, J. C., Kool, J. B., & van Genuchten, M. T. (1985). Determining Soil Hydraulic Properties from One-step Outflow Experiments by Parameter Estimation: II. Experimental Studies 1. *Soil Science Society of America Journal*, *49*, 1354–1359. doi:10.2136/sssaj1985.03615995004900060005x

Rawlins, S. L., & Dalton, F. N. (1967). Psychrometric Measurement of Soil Water Potential without Precise Temperature Control 1. *Soil Science Society of America Journal*, *31*, 297–301. doi:10.2136/sssaj1967.03615995003100030007x

Richards, L. A. (1931). Capillary Conduction of Liquids Through Porous Mediums. *Physics*, *1*, 318–333. doi:10.1063/1.1745010

Richards, L. A. (1941). Soil moisture tensiometer materials and construction. *U.S. Department of Agriculture*, 241–248.

Richards, L. A., & Gardner, W. (1936). Tensiometers for Measuring the Capillary Tension of Soil Water 1. *Journal of the American Society of Agronomy*, *28*(5), 352 – 358.

Richardson, S. J., Knuteson, R. O., & Tobin, D. C. (1999). A Chilled Mirror Dew Point Hygrometer for Field Use. In *Ninth ARM Science Team Meeting Proceedings* (pp. 1–5). San Antonio, Texas.

Rose, C. W., Stern, W. R., & Drummond, J. E. (1965). Determination of hydraulic conductivity as a function of depth and water content for soil in situ. *Australian Journal of Soil Research*, *3*, 1–9. doi:10.1071/SR9650001

Russo, D. (1988). Determining Soil Hydraulic Properties by Parameter Estimation: On the Selection of a Model for the Hydraulic Properties. *Water Resources Research*, *24*(3), 453–459. doi:10.1029/WR024i003p00453

Sattler, P., & Fredlund, D. G. (1989). Use of thermal conductivity sensors to measure matric suction in the laboratory. *Canadian Geotechnical Journal*, *26*, 491–498. doi:10.1139/t89-063

Sharma, H. D., & Lewis, S. P. (1994). Low-Permeability Liner and Drainage Materials. In *Waste Containment Systems, Waste Stabilization, and Landfills: Design and Evaluation*. John Wiley & Sons.

Shaw, B., & Baver, L. D. (1939). Heat Conductivity as an Index of Soil Moisture 1. *Journal of the American Society of Agronomy*, 886–891.

Šimůnek, J., Genuchten, M. T. van, & Šejna, M. (2005). The HYDRUS-1D Software Package for Simulating the One-Dimensional Movement of Water, Heat, and Multiple Solutes in Variably-Saturated Media. *HYDRUS Software Series 1, Department of Environmental Sciences, University of California Riverside, Riverside, California, USA,*, *Version 3*.

Šimůnek, J., Kodesova, R., Gribb, M. M., & van Genuchten, M. T. (1999). Estimating hysteresis in the soil water retention function from cone permeameter experiments. *Water Resources Research*, *35*(5), 1329–1345. doi:10.1029/1998WR900110

Šimůnek, J., & van Genuchten, M. T. (1999). Using the HYDRUS-1D and HYDRUS-2D Codes for Estimating Unsaturated Soil Hydraulic and Solute Transport Parameters. In *p.1523–1536. In M.Th. van Genuchten et al. (ed.) Proc. of the Int. Workshop on*

Characterization and Measurement of the Hydraulic Properties of Unsaturated Porous Media. 22–24 Oct. 1997. Univ. of California, Riverside, CA. (pp. 1523–1536).

Šimůnek, J., van Genuchten, M. T., & Wendroth, O. (1998). Parameter Estimation Analysis of the Evaporation Method for Determining Soil Hydraulic Properties. *Soil Science Society of America Journal*, *62*(4), 894. doi:10.2136/sssaj1998.03615995006200040007x

Smajstrla, A. G., & Harrison, D. S. (1998). Tensiometers for Soil Moisture Measurement and Irrigation Scheduling. *CIR487, Agricultural and Biological Engineering Department, Florida Cooperative Extension Service, Institute of Food and Agricultural Sciences, University of Florida*, 1–8.

Soilmoisture Equipment Corp. Operating Instructions: 1400/1405 Tempe Pressure Cell (1995).

Soilmoisture Equipment Corp. (2014). Retrieved from http://www.soilmoisture.com/

Spanner, D. C. (1951). The Peltier Effect and its Use in the Measurement of Suction Pressure. *Journal of Experimental Botany*, *2*(5), 145–168. doi:10.1093/jxb/2.2.145

Sun, D. A., Matsuoka, H., Cui, H. B., & Xu, Y. F. (2003). Three-dimensional elasto-plastic model for unsaturated compacted soils with different initial densities. *International Journal for Numerical and Analytical Methods in Geomechanics*, *27*, 1079–1098. doi:10.1002/nag.313

Tarantino, A. (2007). A possible critical state framework for unsaturated compacted soils (Technical Note). *Géotechnique*, *57*(4), 385–389.

Toorman, A., Wierenga, P., & Hills, R. (1992). Parameter Estimation of Hydraulic Properties From One-Step Outflow Data. *Water Resources Research*, *28*(11), 3021–3028.

Tuller, M., & Or, D. (2003). *Retention of Water in Soil and the Soil Water Characteristic Curve*. *Environmental Engineering* (pp. 1–20).

Van Dam, J. C., Stricker, J. N. M., & Droogers, P. (1990). From One-step to Multi-step. Determination of soil hydraulic functions by outflow experiments. In *Report 7, Agricultural University Wageningen, Netherlands*.

Van Dam, J. C., Stricker, J. N. M., & Droogers, P. (1994). Inverse Method to Determine Soil Hydraulic Functions from Multistep Outflow Experiments. *Soil Science Society of America Journal*, *58*(3), 647. doi:10.2136/sssaj1994.03615995005800030002x

Van Genuchten, M. T. (1980). A Closed-form Equation for Predicting the Hydraulic Conductivity of Unsaturated Soils. *Soil Science Society of America Journal*, *44*, 892–898. doi:10.2136/sssaj1980.03615995004400050002x

Vanapalli, S. K., Nicotera, M. V., & Sharma, R. S. (2008). Axis Translation and Negative Water Column Techniques for Suction Control. *Geotechnical and Geological Engineering*, *26*, 645–660. doi:10.1007/s10706-008-9206-3

Wang, X., & Benson, C. H. (2004). Leak-Free Pressure Plate Extractor For Measuring the Soil Water Characteristic Curve. *Geotechnical Testing Journal*, *27*(2), 1–10. doi:10.1520/GTJ11392

Watson, K. K. (1966). An Instantaneous Profile Method for Determining the Hydraulic Conductivity of Unsaturated Porous Materials. *Water Resources Research*, *2*(4), 709–715. doi:10.1029/WR002i004p00709

Wendroth, O., Ehlers, W., Hopmans, J. W., Kage, H., Halbertsma, J., & Wösten, J. H. M. (1993). Reevaluation of the Evaporation Method for Determining Hydraulic Functions in Unsaturated Soils. *Soil Science Society of America Journal*, *57*, 1436–1443.

Wildenschild, D., Jensen, K., Hollenbeck, K., Llangasekare, T., Znidarcic, D., Sonnenborg, T., & Butts, M. (1997). A Two-Stage Procedure for Determining Unsaturated Hydraulic Characteristics Using a Syringe Pump and Outflow Observations. *Soil Science Society of America Journal*, *61*(2), 347–359.

Wind, G. P. (1996). Capillary conductivity data estimated by a simple method. In *Water in the Unsaturated Zone, Proceedings of Wageningen Syposium, IASAH,* (pp. 172–176). Gentbrugge, Belgium.

Wong, D., Fredlund, D., Imre, E., & Putz, G. (1989). Evaluation of AGWA-II thermal conductivity sensors for soil suction measurement. *Transportation Research*, 131–143.

Yang, H., Rahardjo, H., Leong, E.-C., & Fredlund, D. G. (2004). Factors affecting drying and wetting soil-water characteristic curves of sandy soils. *Canadian Geotechnical Journal*, *41*, 908–920. doi:10.1139/T04-042

Zornberg, J. G., & McCartney, J. S. (2010). Centrifuge Permeameter for Unsaturated Soils. I: Theoretical Basis and Experimental Developments. *Journal of Geotechnical and Geoenvironmental Engineering*, *136*(8), 1051–1063. doi:10.1061/(ASCE)GT.1943-5606.0000319